ASSESSMENT OF MULTIPLE APPROACHES FOR USING SOIL MOISTURE TO EVALUATE DROUGHT IN THE U.S. GREAT PLAINS

A Dissertation

by

SHANSHUI YUAN

Submitted to the Office of Graduate and Professional Studies of
Texas A&M University
in partial fulfillment of the requirements for the degree of

DOCTOR OF PHILOSOPHY

Chair of Committee,	Steven M. Quiring
Committee Members,	Oliver W. Frauenfeld
	Inci Güneralp
	Vijay P. Singh
Head of Department,	David M. Cairns

December 2016

Major Subject: Geography

ABSTRACT

Drought is a natural phenomenon induced by precipitation deficiency and it impacts economy, environment and society. The drought monitoring tools include direct measurements, such as precipitation, soil moisture and streamflow and indirect estimations, like drought indices and model simulations. The newly developed North American Soil Moisture Database (NASMD) provides quality-controlled soil moisture observations over the entire U.S. to help assess the reliability of these drought monitoring tools. In this dissertation study, we focused on the assessment of drought indices and model simulated soil moisture using in situ data from NASMD.

First, we focused on four soil moisture statistics: percentile, trend, variability and persistence in 0-10 cm and 0-100 cm soil layers. The result reveals that the crop moisture index well represent the soil moisture conditions in the top 100 cm soil layer based on higher correlation, more similar trend, variability and persistence. In the top 10 cm soil layer, no drought index is the most appropriate one for all the statistics. In general, drought indices considering potential evapotranspiration (PET) are more appropriate for representing soil moisture in 0-10 cm soil layer. Then we developed a more realistic Palmer Drought Severity Index (PDSI) using two-source PET model. Based on the comparison with original PDSI and Penman-Monteith based PDSI, we found the choice of PET method would impact the spatial and temporal patterns of drought and the drought severity during extreme drought events. Thirdly, we tested the reduced optimal interpolation (ROI) method to soil moisture in Oklahoma and compared

it with two geo-statistical interpolation methods: the inversed distance weighting (IDW) method and Cokriging method. The ROI method is significantly more accurate than IDW and it also outperforms Cokriging. We demonstrate that ROI can recreate soil moisture at unsampled locations. Last, we assessed the accuracy of soil moisture in Earth system models (ESMs) by using in situ and satellite observations. The results show that models can reproduce the seasonal variability in soil moisture over CONUS but with overestimation in the western U.S. and underestimation in the eastern U.S. There are significant regional and inter-model variations in performance.

ACKNOWLEDGEMENTS

I would like to give my heartfelt thanks and deepest respect to my academic advisor, Dr. Steven Quiring. Since the first day I joined Texas A&M University, he keeps inspiring me with his wisdom, knowledge and professionalism. My appreciation also goes to the members of my committee, Dr. Oliver Frauenfeld, Dr. Inci Guneralp and Dr. Vijay Singh, for their guidance and suggestions throughout the course of this research.

Thanks also go to my friends and colleagues in the Climate Science Lab. Studying and playing together with them make my time at Texas A&M University a great experience. I also want to extend my gratitude to all the faculty and staff in the Department of Geography for their kind help.

Finally, I want to express the most special thanks to my wife and parents. As amazing family members, they bring me tremendous love and support.

CONTRIBUTORS AND FUNDING SOURCES

Contributors

Part 1, faculty committee recognition

This work was supervised by a dissertation committee consisting of Professor Steven Quiring [advisor], Professor Oliver Frauenfeld and Professor Inci Guneralp of the Department of Geography and Professor Vijay Singh of the Department of Biological and Agricultural Engineering.

Part 2, student/advisor contributions

All work for the dissertation was completed by the student, under the advisement of Steven Quiring of the Department of Geography.

Funding Sources

This work was made possible in part by the National Science Foundation CARRER Award under Grant Number AGS-1056796. Its contents are solely the responsibility of the authors and do not necessarily represent the official views of the NSF CARRER Program.

NOMENCLATURE

2S	the two-source PET model
AET	Actual Evapotranspiration
CAFEC	climatically appropriate for existing conditions
CCM	Community Climate Model
CHRM	Climate High-Resolution Model
CMI	Crop Moisture Index
CMIP5	Coupled Model Intercomparison Project Phase 5
CPC	Climate Prediction Center
DAR	Daily Average Replacement
ECV	Essential Climate Variable
EDI	Effective Drought Index
EOF	Empirical Orthogonal Function
ESM	earth system model
GCM	general circulation model
GLACE	Global Land-Atmosphere Coupling Experiment
MAE	mean absolute error
NARR	NCEP North American Regional Reanalysis
NASMD	North American Soil Moisture Database
NLDAS-2	Phase 2 of the North American Land Data Assimilation System
IDW	Inversed Distance Weighting

PM	Penman-Monteith equation
PDSI	Palmer Drought Severity Index
PET	potential evapotranspiration
RCM	regional climate model
ROI	Reduced Optimal Interpolation
SPEI	Standardized Precipitation Evapotranspiration Index
SPI	Standardized Precipitation Index
TH	Thornthwaite equation
VIC	Variable Infiltration Capacity
VWC	volumetric water content

TABLE OF CONTENTS

Page

LIST OF FIGURES

Page

LIST OF TABLES

Page

CHAPTER I

INTRODUCTION

1.1 Introduction

Drought is a naturally recurring feature of the climate system that is characterized by a prolonged deficiency of precipitation (Dai, 2011a). Drought affects society, environment and economy and causes large losses. Quantitative information on the duration, severity and spatial extent of drought events can help monitor and predict drought conditions (Rhee et al., 2008). Accurate information is important for decision-makers to develop better mitigation adaptation strategies (Yuan et al., 2016).

Soil moisture is a critical variable for drought monitoring (Anderson et al., 2012) and prediction (Ford et al., 2015a). Although there are relatively few direct measurements of soil moisture (Hartmann et al., 2013), it is very useful for assessing drought duration and intensity (Seneviratne et al., 2010). The application of in situ measured soil moisture is limited by its spatial and temporal coverage. The North American Soil Moisture Database, NASMD (Quiring et al., 2016), aims to collect the densest possible network of in situ soil moisture in North America. The NASMD has data from ~1800 soil moisture stations in the U.S. This is much less than the number of precipitation site (more than 10,000 in the U.S. based on the National Weather Service Cooperative Observer Program). Soil moisture observations also have a much shorter period of record than other meteorological observations. The longest record of in situ soil moisture in U.S. only extend back to the 1990s (e.g., Soil Climate Analysis

Network), while temperature and precipitation records start from late 19th century (Menne et al., 2009). Because of the limited spatial and temporal coverage of soil moisture, it is necessary to find other ways of representing observed soil moisture. These so-called soil moisture proxy variables are useful because they can help fill the spatial and temporal gaps in observed soil moisture. They can also help for provide insights on future changes in soil moisture under a changing climate.

This doctoral research will use soil moisture observations to evaluate which drought monitoring tools/indices are most appropriate for representing soil moisture conditions. It will also develop better methods to more realistically measure and monitor drought conditions. This dissertation will address two main research questions: 1) How accurate are current drought indices for representing soil water conditions? 2) How accurate are simulations of future drought conditions? Four objectives are required to answer the research questions:

1) Identify the drought index that best represents soil moisture;

2) Develop a more physically-realistic drought index and validate it using observed soil moisture;

3) Identify the best methodology for estimating observed soil moisture at unsampled locations.

4) Evaluate the accuracy of soil moisture simulations in the Earth System Models that are part of CMIP5.

1.2 Background

Due to lack of direct measurements of drought impacts, there is no uniform method to characterize drought conditions. Many different drought indices have been used to monitor drought (Heim, 2002;Quiring, 2009). The drought indices that are commonly used to monitor drought conditions include: Palmer Drought Severity Index (PDSI) introduced by Palmer (1965), Standardized Precipitation Index (SPI) introduced by McKee et al. (1993), Standardized Precipitation Evapotranspiration Index (SPEI) introduced by Vicente-Serrano et al. (2009), and Effective Drought Index (EDI) introduced by Byun and Wilhite (1999). Each drought index has advantages and disadvantages and therefore it may not accurately represent drought conditions at every location or for every type of drought (Vicente-Serrano et al., 2010).

Previous studies have evaluated the performance of drought indices using different observations in different regions. For example, Keyantash and Dracup (2002) assessed seven meteorological drought indices using observed precipitation, streamflow and computed soil moisture. They found that the SPI ranked highly in terms of robustness, sophistication and extendibility. Morid et al. (2006) compared seven drought indices in Iran and found that there was significant variability in terms of their ability to accurately detect drought onset and to represent the spatial and temporal patterns of drought. Jain et al. (2015) evaluated six drought indices in India and found that the time scale and location of interest had a significant influence on the performance of the drought indices and that there was not a single best index for all locations and time scales. McEvoy et al. (2012) evaluated two multi-scalar drought indices, SPI and SPEI

using temperature percentile, reservoir elevation and streamflow, in Nevada and California at time scales ranging from 1 to 72 months. They found that the SPEI performed slightly better than SPI when compared to summer stream flow. Vicente-Serrano et al. (2010) also compared a multi-scalar drought index (SPEI) with two different versions of the PDSI and found that the PDSI provides information on medium-term or long-term drought conditions in most regions. However, among previous evaluation studies, there are very rare studies using in situ soil moisture to evaluate drought indices.

Soil moisture is not only a variable that reflects drought conditions, but also a factor that causes drought. Previous studies have identified three main reasons that cause drought. First, large-scale atmospheric circulation patterns, which are associated with sea surface temperature anomalies, are an important remote forcing that can cause drought to occur (Hoerling and Kumar, 2002;Trenberth and Guillemot, 1996). Second, local land-atmosphere interactions influence rainfall variability and can either trigger drought initiation or contribute to drought intensification (Guo et al., 2011). Finally, random variability ("noise") within the climate system can also contribute to drought occurrence (Hoerling et al., 2014;Kumar et al., 2013). Among the three reasons, the local effect of land-atmosphere interactions is closely associated with soil moisture (Seneviratne et al., 2010).

Soil moisture plays an important role in land-atmosphere interactions by affecting energy and water fluxes (Eltahir, 1998;Seneviratne et al., 2010). Both the water balance and the energy balance are coupled through evapotranspiration and it is strongly

influenced by soil moisture in the water limited regimes (Teuling et al., 2009;Seneviratne et al., 2006). A positive (negative) soil moisture anomaly increases (decreases) the evapotranspiration, cools (warms) the land surface and alters patterns of moisture and atmosphere circulations (Eltahir, 1998;Namias, 1991).

Due to lack of available observed soil moisture, numerical simulations based on land surface models and General Circulation Models (GCMs) are commonly used to evaluation soil moisture-climate interactions. For soil moisture-temperature interactions, Durre et al. (2000) used a simple water balance model to evaluate the dependence of summertime daily maximum temperature on antecedent soil moisture. Brabson et al. (2005) used HadCM3 to examine the relationship of soil moisture to extreme temperatures in Britain and found longer spells of extreme temperature are associated with extended periods of low soil moisture. Fischer et al. (2007) found soil moisture-temperature interactions increased the duration of heat waves in the Climate High-Resolution Model (CHRM). Soil moisture-temperature feedbacks in plains, mountain and coastal regions, were examined by Stéfanon et al. (2014). Similarly, a large number of GCMs (Kim and Wang, 2007;Meng, 2009;Oglesby, 1991;Koster et al., 2004;Seneviratne et al., 2013) and regional climate models (RCMs) (Bosilovich and Sun, 1999;Paegle et al., 1996;Wei and Dirmeyer, 2012) have been used to study interactions between soil moisture and precipitation. Most of these studies support a positive feedback between soil moisture and precipitation. Positive feedback means that anomalies in soil moisture lead to accordant anomalies in precipitation, which can then enhance the soil moisture anomalies. Oglesby and Erickson (1989) imposed desert-like

initial soil moisture over an extensive area of North America using the Community Climate Model (CCM1). They found that soil moisture reductions in July prolonged and/or amplified drought over North America, and moisture advection from the Gulf of Mexico played an important role in determining the areas where the reduced soil moisture persisted. Bosilovich and Sun (1999) found that simulations of the 1993 flood became much less severe when initial soil moisture was reduced in two 1-month integrations starting from 1 June and 1 July by using the Purdue Regional Model (PRM). In addition, Bosilovich and Schubert (2002) suggested strong precipitation recycling (a direct pathway through which soil moisture influences precipitation) over the Mississippi River basin during summer. Kim and Wang (2007) investigated the impact of anomalous soil moisture conditions on subsequent precipitation over North America through a series of numerical experiments. They showed that the impact of spring soil moisture anomalies is not evident until early summer. Meng and Quiring (2010) conducted a series of numerical experiments to evaluate the influence of spring soil moisture anomalies on summer precipitation variations in the U.S. Great Plains. Their results showed that the timing of soil moisture anomalies is an important factor that influences soil moisture-precipitation interactions. Model simulated soil moisture-climate interactions contribute a lot to our understanding, but since GCMs have large uncertainties (Flato et al., 2013), multi-model ensembles are commonly used to evaluate soil moisture-climate interactions. The Global Land-Atmosphere Coupling Experiment (GLACE) (Guo and Dirmeyer, 2006;Koster et al., 2006;Koster et al., 2004) investigated soil moisture-climate interactions using a 12-GCM ensemble. The second phase of this

experiment began in 2011 (Koster et al., 2010) and its experimental design were conducted in the context of CMIP5 in 2013 (Seneviratne et al., 2013). The GLACE identified the regions with strong soil moisture-climate coupling strength at global scale. The experiment showed consistent signals of soil moisture-precipitation interactions with soil moisture-temperature interactions. However, they also found the changes of initial soil moisture will affect temperature mean and extremes more strongly than precipitation.

The number of observation data based soil moisture-climate interactions studies are relatively limited. Globally, FLUXNET measurements showed similar spatial distribution of soil moisture-temperature coupling strength from model simulations (Teuling et al., 2009). Taylor et al. (2012a) demonstrated afternoon rain preferentially falls over dry soil based on top 5-cm satellite observed soil moisture. Regionally, Mahmood et al. (2012) found weaker association between soil moisture and precipitation than between soil moisture and maximum surface temperature. In situ soil moisture is found to strongly impact air temperature in the upper quantile of the percent hot days distribution in Oklahoma (Ford and Quiring, 2014b). Ford et al. (2015c) found convective precipitation in Oklahoma preferentially over dry soils. More negative feedback of soil moisture is found based on observations. Therefore, to close the disagreement between model and observation studies, more work on verifying model simulated soil moisture-climate interactions using multi-source based observations is necessary.

The relatively short period of record and sparse spatial coverage of in situ soil moisture make drought evaluation and land-atmosphere interactions studies challenging. Therefore, in some previous studies, the SPI has been used as a proxy of surface moisture deficits to characterize the impacts on warm temperature (Hirschi et al., 2011;Mueller and Seneviratne, 2012;Ford et al., 2016). Even though, there has not yet been a comprehensive assessment of which drought indices are most appropriate for representing soil moisture conditions. These drought indices are important because they can be calculated with readily available data (temperature and precipitation) and therefore they will although soil moisture proxies to be developed to fill in the spatial and temporal gaps in observed soil moisture. The first objective of this dissertation is to provide a comprehensive evaluation of these drought indices and to determine which drought indices are most strongly associated with soil moisture conditions (Chapter 2). Existing drought indices have limitations as soil moisture proxies because they are not physically-based and do not include all of the relevant processes that influence soil moisture. Therefore, another avenue of research (Chapter 3) in this dissertation is to develop an improved version of the PDSI that will explicitly account for ET from multiple sources. An additional challenge faced when using in situ soil moisture is the lack of spatial coverage. Therefore, this dissertation evaluates two-commonly used approaches for estimating soil moisture at unsampled locations and compares it to an approach that has not previously been applied to soil moisture (Chapter 4). Finally, we are not only interested in variations in soil moisture conditions in the past, but how those conditions may change in the future. Therefore, the final objective of this dissertation

(Chapter 5) will use observed soil moisture measurements, both in situ and satellite, to evaluate the accuracy of soil moisture simulations in the CMIP5 models. The results of this analysis will be useful for identifying which ESMs are most appropriate for assessing future changes in drought conditions and for evaluating how the strength and nature of land-atmosphere interactions may change in the future in the U.S. Great Plains.

1.3 Study Area

The U.S. Great Plains lie between the Mississippi River and the Rocky Mountains in the United States, covering North Dakota, South Dakota, Nebraska, Kansas and parts of Oklahoma, Texas, New Mexico, Colorado, Wyoming and Montana. In this doctoral research, the study region is the U.S. Great Plains which is defined as Texas, Oklahoma, Kansas, Nebraska and South Dakota (Figure 1.1).

The climate of the U.S. Great Plains is characterized by a strong north – south temperature gradient and a strong east – west precipitation gradient (Karl et al., 2009;Meng, 2009). While there are 70 to 90 days with over 32 °C in the south, only 10 to 20 days are above 32 °C in the north (Karl et al., 2009). Annual precipitation ranges from less than 200 mm in the west to over 1100 mm in the east of GP, but large season-to-season and year-to-year fluctuations are frequent and July and August are often hot and dry (Miller et al., 2002;Padbury et al., 2002;Meng, 2009). The region is periodically subjected to extended periods of drought; high winds in the region may then generate dust storms. The U.S. Great Plains is one of three areas in the world (the central Great

Plains of North America, the Sahel, equatorial Africa and India) that have the strongest land-atmosphere coupling strength (Koster et al., 2004).

Over 70% of the U.S. Great Plains' region is used for agriculture. Annual agricultural production is more than $41.5 billion dollars. Droughts (such as 1930s Dust Bowl, 1988 drought (Namias, 1991) and 2010 – 2013 droughts (Wang et al., 2014) have affected agriculture in this region, caused numerous agricultural and economic losses. Therefore, drought is the main limiting factor for agricultural production in the U.S. Great Plains.

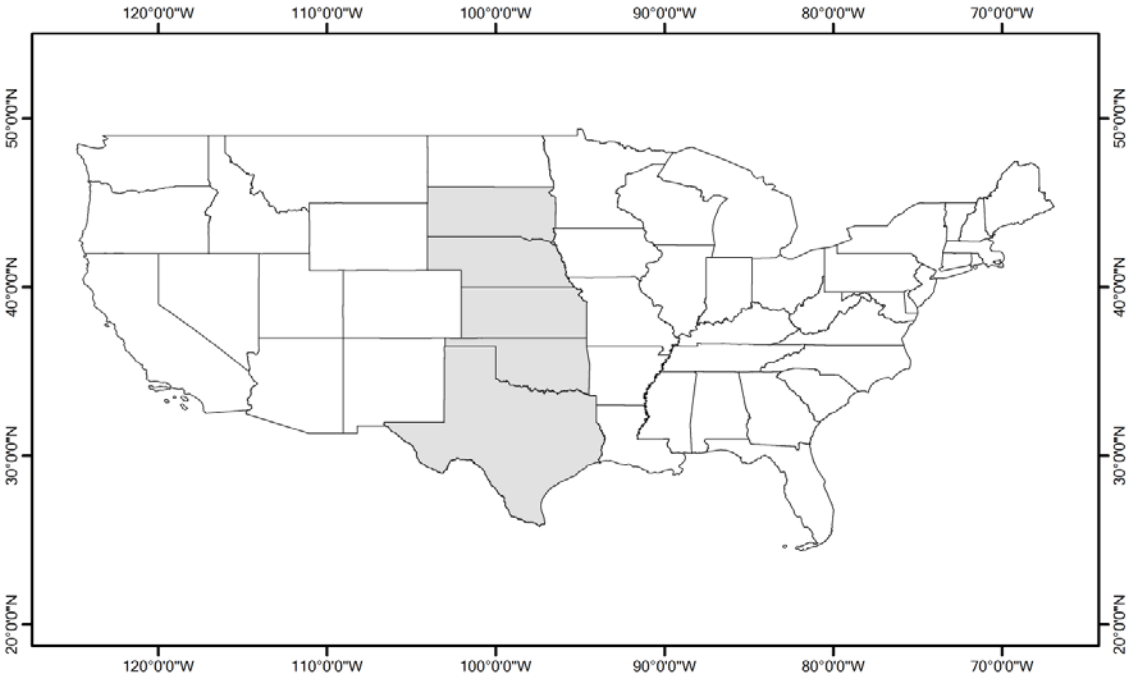

Figure 1. 1. U.S. Great Plains study region

CHAPTER II

EVALUATION OF DROUGHT INDICES AS SOIL MOISTURE PROXIES

2.1 Introduction

Drought is a recurring climate phenomena characterized by below-normal precipitation over an extended period of months, years, or even decades (Dai, 2011a). Drought can have a major influence on organisms, ecosystems, economy, and society (Heim, 2002). Globally, droughts cause billions of dollars in damage and affect millions of people each year (Dai, 2011a). However, it is difficult to define and monitor drought, and there are many different definitions and indices for measuring drought.

Drought indices are commonly used to monitoring drought conditions because there are few high-quality and long-term direct measures of drought (Hartmann et al., 2013). The development and application of these indices goes back to the beginning of twentieth century (Heim, 2002). A large number of drought indices exist, each having a variety of data input requirements and each providing a somewhat different measure of drought. Some of the indices that are commonly used include the following: Palmer Drought Severity Index (PDSI) and Moisture Anomaly Index (Z index) (Palmer, 1965), Standardized Precipitation Index (McKee et al., 1993), percent normal, satellite-based measures of vegetation health (Quiring and Ganesh, 2010), and indices that are based on soil moisture such as the Standardized Soil Moisture Index and the Multivariate Standardized Drought Index (Hao and AghaKouchak, 2013).

Soil moisture is a direct measure of drought (Hartmann et al., 2013) and its feedback to climate may cause prolonged drought events. Soil moisture is documented to influences temperature and precipitation on sub-daily (Ford et al., 2015b) to seasonal scales (Meng, 2009). The impact of soil moisture on climate occurs via influencing surface energy balance and water transfer (Seneviratne et al., 2010). Previous studies commonly found negative soil moisture anomalies would limit the evapotranspiration so that to increase the near-surface air temperature (Teuling et al., 2010;Guo and Dirmeyer, 2013). However, more complicated soil moisture-precipitation feedback mechanisms are discussed based on different approaches. Positive feedback shows that dry soil would limit evapotranspiration, leading to less moisture enters into atmosphere, which may cause less precipitation (Koster et al., 2004). On the contrast, negative feedback demonstrates that reduced evapotranspiration would increase near-surface air temperature and then strengthen the convective process. As a result, higher possibility of convective precipitation may occur over dryer soil (Ford et al., 2015c). Hence, soil moisture is a critical variable to evaluate and predict drought and associated extreme climatic events, such as heat waves.

Soil moisture and drought indices are able to reflect moisture deficits over land surface. Several previous studies used the drought index SPI as soil moisture proxy to investigate land-atmosphere interactions. Hirschi et al. (2011) applied quantile regression method to show the relations between SPI and summer hot extremes in the southeastern Europe. The results showed the intensification of hot extremes over drier soil conditions. Ford et al. (2016) also used SPI to express the soil moisture deficits and

identified the long-term variability of soil moisture-maximum temperature coupling over contiguous U.S. They pointed out the coupling strength varies over time and is affected by SST anomalies.

Since previous studies have used drought index as soil moisture proxies and lack of studies focused on comprehensive evaluation of different drought indices using soil moisture, it is necessary to do inter-comparison of multiple drought indices with soil moisture. This chapter will evaluate different drought indices for approximating soil moisture in land-atmosphere interaction studies.

2.2 Data and Methods

2.2.1 Long-term (1980 – 2012) Soil Moisture

Long-term soil moisture is derived from Phase 2 of the North American Land Data Assimilation System (NLDAS-2; http://ldas.gsfc.nasa.gov/nldas/). Hourly soil moisture is simulated by four land surface models: Mosaic, Noah, Sacramento (SAC) and Variable Infiltration Capacity (VIC). Each model showed different biases relative to in situ soil moisture (Xia et al., 2015b). In general, Noah and VIC are wetter than the observations while Mosaic and SAC are drier than the observations. We calculate the four-model ensemble to reduce the biases induced by each individual model. Hourly soil moisture is averaged to daily then to weekly. We used soil moisture content in 0 – 10 cm and 0 – 100 cm to represent water content in surface and deep soil layer. All the NLDAS-2 data are with 1/8 spatial resolution.

2.2.2 Short-term (2003 – 2012) Soil Moisture

Besides simulated soil moisture from NLDAS, weekly in situ soil moisture is added for short-term (2003 – 2012) evaluation. Daily soil moisture data were obtained from North American Soil Moisture Database (http://soilmoisture.tamu.edu/). The North American Soil Moisture Database archives data from a variety of national and state networks (Quiring et al., 2016). Data from 132 stations are used in this study (Figure 2.1). These stations are collected from four observational networks (AmeriFlux, Oklahoma Mesonet, West Texas Mesonet and Soil Climate Analysis Network), as shown in Table 2.1. In this study, any stations with short periods of missing data (< 10 days) are infilled using the daily average replacement (DAR) method (Ford and Quiring, 2014a). Soil moisture measurements at different depths are used to estimate the volumetric water content (VWC) in the top 10 cm and top 100 cm of the soil column. For example, the VWC measured at 5 cm is assumed to represent the VWC in 0 – 10 cm soil layer. When there are multiple soil moisture sensors within the top 100 cm, the measurements are combined using a depth-weighted average. Daily soil moisture measurements are then averaged to a weekly value. The in situ measurements are also aggregated spatially to facilitate comparison with the drought indices. We use a simple spatial average to aggregate all of the stations within each 0.125° × 0.125° grid cell. Then all of the grid cells with stations in them are averaged to produce a regional or national dataset for comparing the in situ and modelled soil moisture. Although this spatial average method is not the optimal technique to reduce sampling errors (Crow et al., 2012), it is simple and has been widely used in previous evaluations studies (Robock

et al., 2003;Albergel et al., 2012a;Xia et al., 2015b). This approach reduces some of the bias associated with the point-versus-grid scale mismatch.

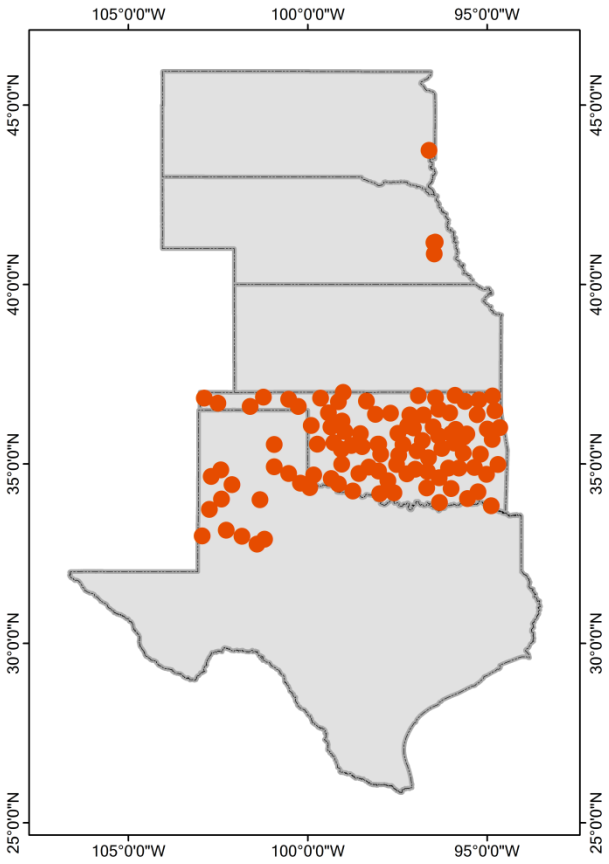

Figure 2. 1. Spatial distribution of in situ soil moisture measurements

Table 2. 1. List of observational networks in this chapter.

Network	Number of Sites (Used in this dissertation)	Reference
AmeriFlux	3	(Baldocchi et al., 2001)
Oklahoma Mesonet	104	(Scott et al., 2013)
Soil Climate Analysis Network	7	(Schaefer et al., 2007)
West Texas Mesonet	18	(Schroeder et al., 2005)

2.2.3 Soil Moisture Trend, Variance and Persistence

The drought indices will be evaluated based on their ability to accurately represent four soil moisture characteristics: percentile, trend, variance and persistence. The soil moisture percentile is calculated using the cumulative distribution function (CDF) of the soil moisture measurements and the drought indices. The degree of similarity between the soil moisture and drought index percentiles is evaluated using the correlation coefficient. Significance tests are done using the 95% confidence level. The soil moisture trend is calculated based on the spatially-averaged mean annual percentile for both the drought indices and the soil moisture observations. The inter-annual and intra-annual variance of drought indices and soil moisture are represented using standard deviation. The standard deviation of i^{th} week from all the years is shown for the inter-annual variance of i^{th} week. The standard deviation of all the weeks in one year is shown as intra-annual variance of that year. The persistence is based on the lagged autocorrelation of weekly time series. For each grid cell or station site, lagged autocorrelation is calculated from lagged 1 week to 12 weeks. Robock et al. (1995)

found that a linear fit does not change significantly after $\ln(r)$ drops below -1. The time, that r takes to drop below $1/e$, is persistence.

2.2.4 Meteorological Data

Gridded meteorological data, including precipitation and temperature, are necessary to calculate the drought indices. These data are also obtained from NLDAS-2. NLDAS-2 precipitation data are derived from NOAA Climate Prediction Center (CPC) gauge-based precipitation data. This data set is adjusted by Parameter-elevation Regressions on Independent Slopes Model. Temperature data for NLDAS-2 are derived from the analysis fields of the NCEP North American Regional Reanalysis (NARR). Original data from NLDAS-2 are hourly data with 0.125° × 0.125° spatial resolution. For estimating weekly PET, precipitation data are accumulated from hourly to weekly values; temperature data are averaged to weekly values.

2.2.5 Drought Indices

Four drought indices are evaluated in this chapter. The Standardized Precipitation Index (SPI) and the Standardized Precipitation and Evapotranspiration Index (SPEI) are based on the probability distribution. The SPI is calculated by standardizing the probability of precipitation, while the SPEI standardizes the difference between precipitation and potential evapotranspiration. In this chapter, we used Gamma distribution while calculating SPI and SPEI. The Crop Moisture Index (CMI) and Palmer

Z Index (Z index) are branches of Palmer Drought Severity Index (PDSI). These two indices are designed for relative short time scale.

Except for SPI, the PET is necessary to calculate SPEI, CMI and Z index. In this chapter, the PET is calculated by the Thornthwaite equation. The Thornthwaite equation is a function of monthly air temperature, latitude, and month.

$$PET = 16\left(\frac{10T}{I}\right)^{a} \tag{2.1}$$

where T is monthly averaged temperature, I is the heat index, and a is estimated by an I-related third-order polynomial. Heat index I is a function of T:

$$I = \sum_{i=1}^{12}\left(\frac{T}{5}\right)^{1.51} \tag{2.2}$$

2.3 Results

2.3.1 Percentile Comparison

Figure 2.2 and 2.3 show the relationship between the spatially-averaged soil moisture percentiles and drought-index based percentiles during 1980 – 2012 and 2003 – 2012, respectively. For 1980 – 2012, the relationship between SPI, SPEI and Z index in the 0 – 100 cm soil layer is weaker and more random than in the 0 – 10 cm soil layer. Hence, SPI, SPEI and Z index have higher correlation with 0 – 10 cm soil moisture (r = 0.58, 0.65 and 0.63) than with 0 – 100 cm soil moisture (r = 0.36, 0.37 and 0.52). The only exception is CMI. Figure 2.2e shows that the relationship in the higher percentiles

of CMI and soil moisture in 0 – 10 cm soil layer is more scattered. As a result, the correlation for 0 – 100 cm soil layer (r = 0.8) is higher than 0 – 10 cm soil layer (r = 0.71). Among the four drought indices, CMI has the highest correlation with soil moisture, followed by the Z index. The correlation between SPI and soil moisture is similar to the correlation between SPEI and soil moisture.

A similar analysis was conducted using in situ soil moisture from 2003 – 2012 (Figure 2.3). The results are consistent with the comparisons done using the model-simulated soil moisture. Generally, the relationships between SPI, SPEI and Z index and soil moisture in 0 – 100 cm soil layer are weaker. CMI is highly correlated with soil moisture percentiles in both layers, especially in the 0 – 100 cm. This agrees with the model-simulated results.

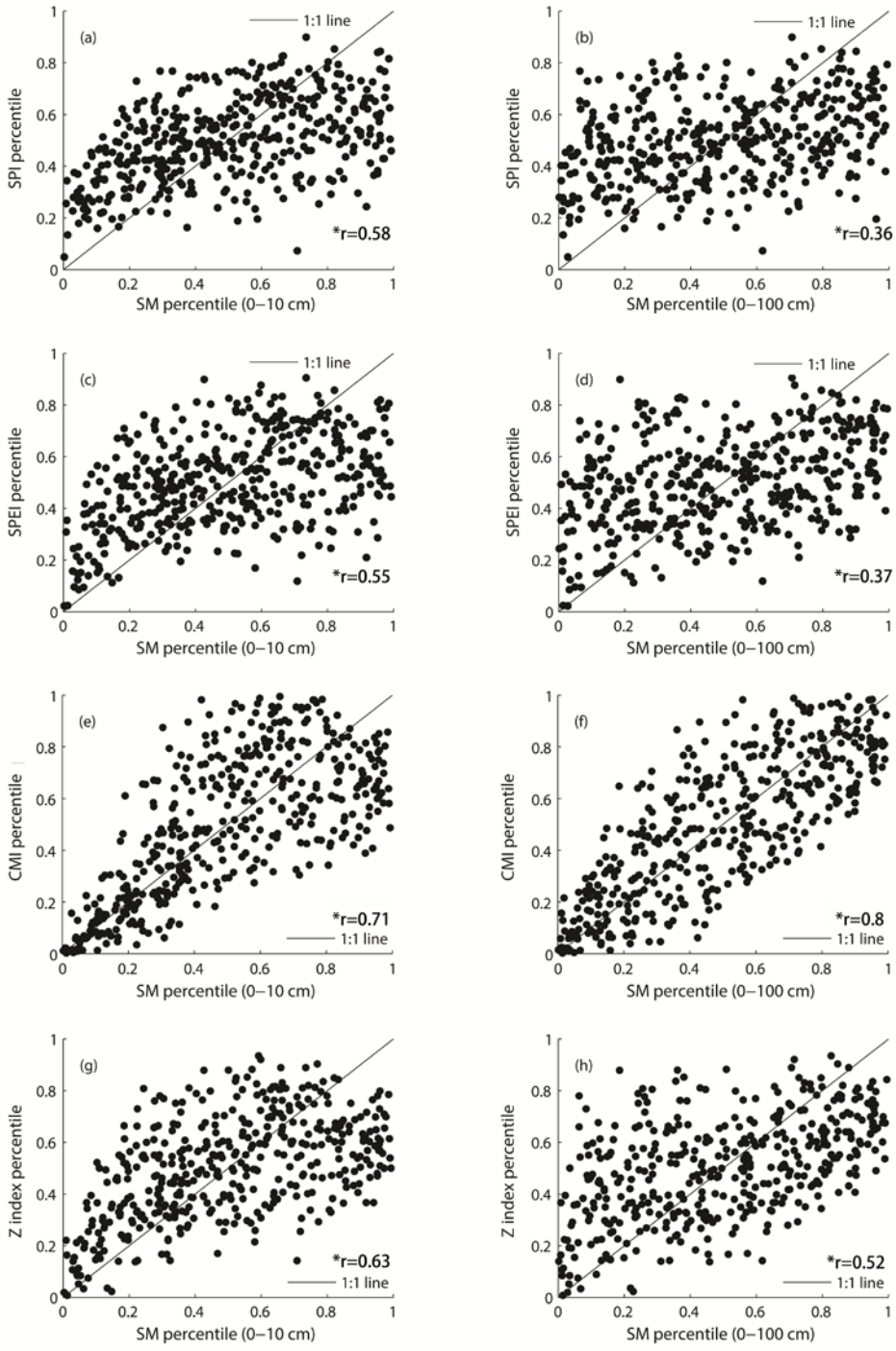

Figure 2. 2. Scatter plots of spatially-averaged NLDAS soil moisture percentiles and (a), (b) SPI, (c), (d) SPEI, (e), (f) CMI and (g), (h) Z index. Left panel: 0 – 10 cm, right panel: 0 – 100 cm, 1980 – 2012.

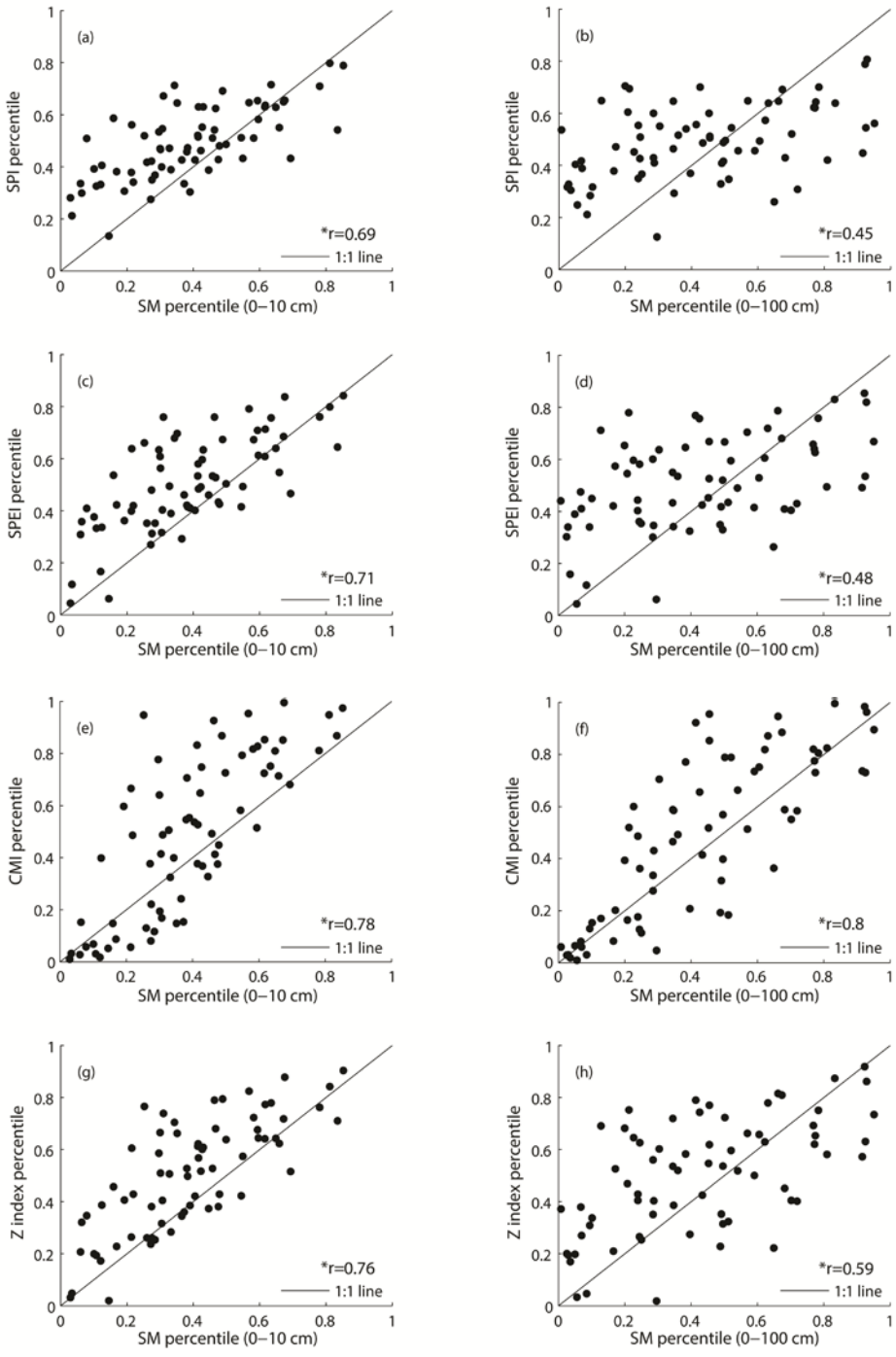

Figure 2. 3. Scatter plots of spatially-averaged in situ soil moisture percentiles and (a), (b) SPI, (c), (d) SPEI, (e), (f) CMI and (g), (h) Z index. Left panel: 0 – 10 cm, right panel: 0 – 100 cm, 2003 – 2012.

2.3.2 Spatial Pattern of Correlation

Figure 2.4 shows the spatial pattern of correlations over the U.S. Great Plains from 1980 to 2012. SPI and SPEI have a similar spatial pattern of correlations in the 0 – 10 cm soil layer (Figure 2.4a and b). In western Oklahoma, northern Texas, parts of central Texas and along the Texas coast, the correlations are relatively higher ($r > 0.7$). In the rest area, the SPI and SPEI are moderately correlated ($r = 0.4 – 0.7$) with soil moisture. High correlations ($r > 0.7$) between CMI and 0 – 10 cm soil moisture (Figure 2.4c) are found over most part of the U.S. Great Plains, except in western and most southern Texas ($r = 0.4 – 0.7$). The area with high correlations ($r > 0.7$) of Z index, as shown in Figure 2.4d is larger than that of SPI and SPEI but smaller than that of CMI. In 0 – 100 cm soil layer, the correlations between SPI, SPEI and soil moisture (Figure 2.4e and f) in northern Great Plains are lower ($r < 0.4$) than in southern Great Plains ($r = 0.4 – 0.7$). The correlations in this layer are lower than in 0 – 10 cm soil layer. The area (Figure 2.4g) with high correlations ($r > 0.7$) between CMI and 0 – 100 cm soil moisture still covers most parts of the U.S. Great Plains, except western Texas and central Nebraska. As shown in Figure 2.4h, over the entire South Dakota, Nebraska, Kansas, eastern Oklahoma, western and northeastern Texas, Z index is moderately correlated with soil moisture ($r = 0.4 – 0.7$) while in western Oklahoma, northcentral and southeastern Texas, Z index is highly correlated with soil moisture ($r > 0.7$). In general, drought indices are more highly correlated with soil moisture in 0 – 10 cm layer than in 0 – 100 cm. In both soil layers, CMI is highly correlated with soil moisture over larger area than the other three indices.

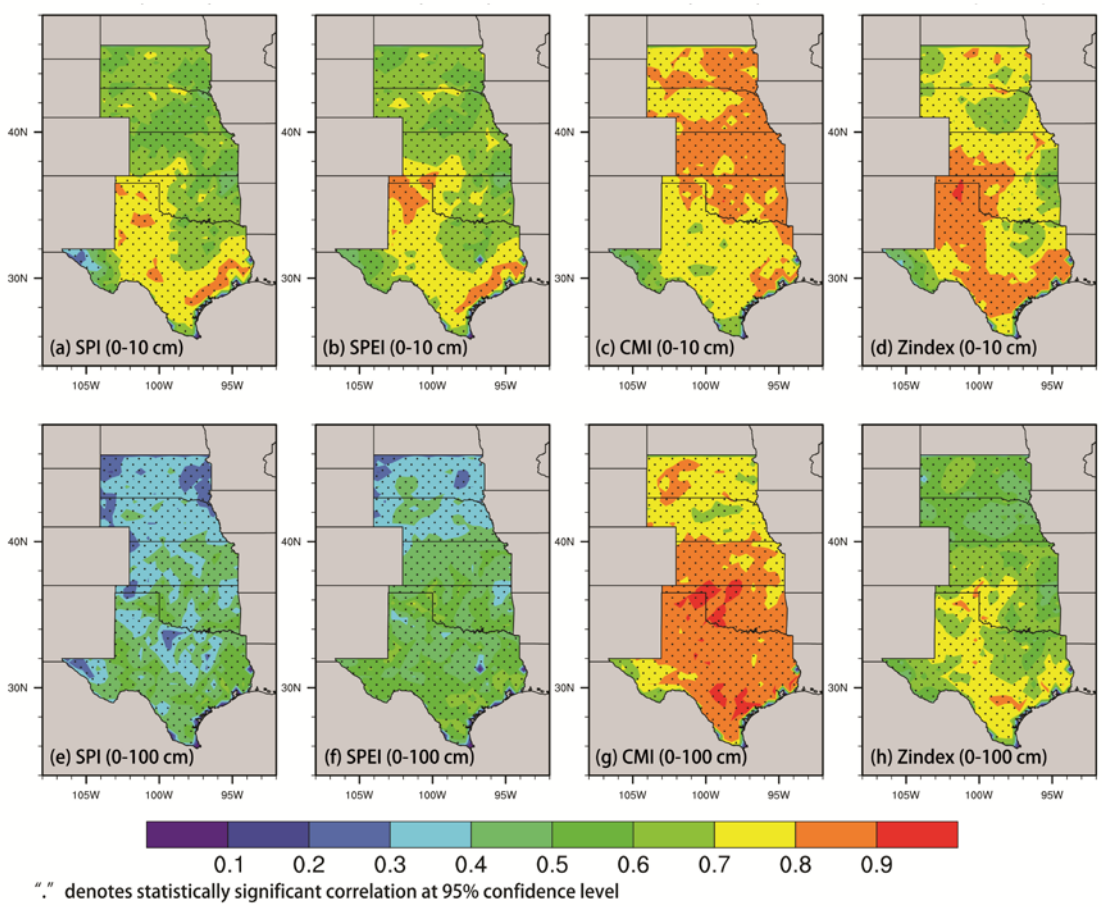

Figure 2. 4. Spatial pattern of correlations in the U.S. Great Plains between NLDAS-2 soil moisture in the 0 – 10 cm and 0 – 100 cm soil layers and 4 drought indices (SPI, SPEI, CMI and Z-index) from 1980 to 2012.

Figure 2.5 shows the correlation between in situ soil moisture and four drought indices at each station from 2003 to 2012. SPI shows high ($r > 0.7$) and low ($r < 0.4$) correlations with soil moisture in 0 – 10 cm layer (Figure 2.5a) at 10 and 9 stations, respectively. In the same layer, SPEI, CMI and Z index show high correlations with soil moisture at 11, 41 and 29 stations, respectively (Figure 2.5b, c and d). The stations with

high correlations for CMI are located in southcentral Oklahoma while for Z index, the high correlation sites are concentrated in eastern Oklahoma. In 0 – 100 cm soil layer, several stations in northwest Texas show very low correlations ($r < 0.2$) between SPI, SPEI and Z index and soil moisture (Figure 2.5e, f and h). In this layer, CMI shows substantially higher correlation than the other drought indices (Figure 2.5g). At 33 out of 75 sites, CMI is highly correlated with soil moisture, while the numbers of sites with high correlation for SPI, SPEI and Z index is 0, 0 and 4.

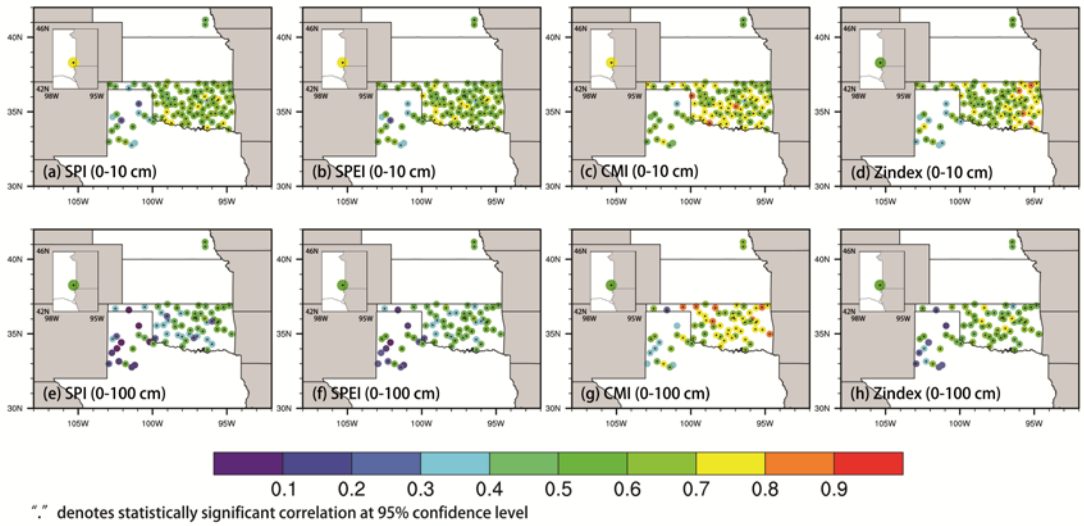

Figure 2. 5. Correlations between in situ soil moisture in the 0 – 10 cm and 0 – 100 cm soil layers and 4 drought indices (SPI, SPEI, CMI and Z index) from 2003 to 2012 at sites in the U.S. Great Plains.

2.3.3 Trend Analysis

Global drought trends are a matter of significant debate in the literature. Dai (2011a) pointed out under climate change, the drought severity is increasing. However,

Sheffield et al. (2012) found there is no significant change of drought in the past 60 years by comparing different forcing data and potential evapotranspiration models. This section evaluates the trends in the mean annual drought indices and soil moisture percentiles in the U.S. Great Plains (Figure 2.6). In both the 0 – 10 cm and 0 – 100 cm layer, all of the drought indices show statistically significant decreases from 1980 to 2012, except SPI. This indicates that there is generally a drying trend in the U.S. Great Plains. The SPI indicates a different trend because it does not account for temperature changes and evapotranspiration. Therefore, the difference between the SPI and other drought indices can be used to demonstrate that much of the drying trend is due to an increase in temperatures in the region (and therefore more evaporative demand) as opposed to a decrease in precipitation (less supply). Warmer temperatures tend to enhance evapotranspiration and this in turn leads to lower soil moisture and drier conditions in the U.S. Great Plains. As shown in Figure 2.6a, there are statistically significant decreases in soil moisture in both layers. The drying trend is stronger in the 0 – 10 cm soil layer (-0.0021 $year^{-1}$) than in the 0 – 100 cm soil layer (-0.0014 $year^{-1}$). When comparing these trends to the SPEI, CMI and Z index, it is apparent that these drought indices tend to overestimate the drying trend in the U.S. Great Plains. This may result from the use of the Thornthwaite equation to estimate Potential Evapotranspiration (PET) because it is solely based on the temperature and therefore may overestimate PET. We will test the impact of using more physically-based approaches for calculating PET in the next chapter.

All the drought indices and soil moisture indicate a significant drying trend from 2003 to 2012 (Figure 2.6b). The drying trend of SPI (-0.0079 $year^{-1}$) is weaker than SPEI (-0.0111 $year^{-1}$), CMI (-0.0166 $year^{-1}$) and Z index (-0.0196 $year^{-1}$). This is consistent with the results based on 1980 – 2012 data. The drying trends of drought indices and soil moisture are much stronger in the last 10 years. This is likely due to internal climate variability, but a specific attribution of the causes of this drying is beyond the scope of this study.

The percentiles of observed soil moisture in the 0 – 100 cm soil layer during 2003 to 2012 changes more dramatically (-0.0148 $year^{-1}$) than the observed soil moisture in the 0 – 10 cm soil layer (-0.0089 $year^{-1}$). The drying trend of 0 – 10 cm soil is closer to SPI (-0.0079 $year^{-1}$) while the trend of 0 – 100 cm soil moisture is more similar with CMI (-0.0166 $year^{-1}$). This could demonstrate that surface soil moisture is more sensitive to precipitation than deep soil moisture.

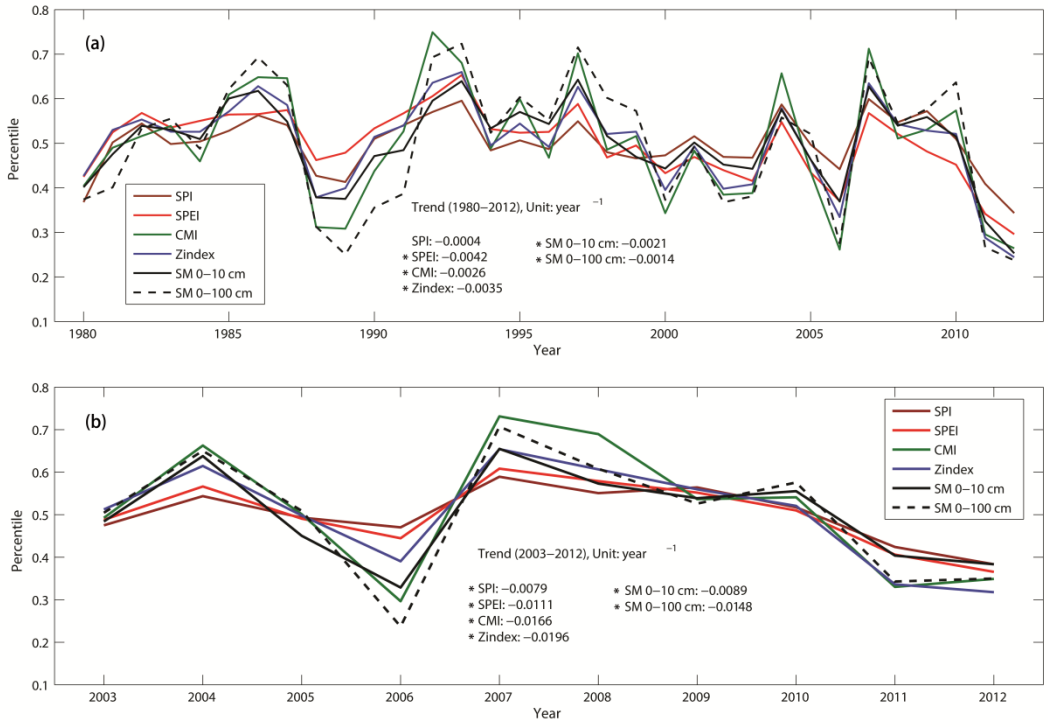

Figure 2. 6. Time series of spatially-averaged mean annual SPI (brown), SPEI (red), CMI (green), Z index (blue), soil moisture in 0 – 10 cm soil layer (black solid) and soil moisture in 0 – 100 cm soil layer (black dashed) over the U.S. Great Plains. (a) NLDAS-2 soil moisture from 1980 to 2012, (b) in situ soil moisture from 2003 to 2012.

2.3.4 Inter-annual Variability of Drought Indices and Soil Moisture

Inter-annual variability in the drought indices and soil moisture are evaluated using the standard deviation. It is calculated on a weekly basis from 1980 to 2012 (Figure 2.7a). The standard deviation of soil moisture in 0 – 100 cm (black dash line) is lower than that of soil moisture in 0 – 10 cm (black solid line) all over the year. Among the four drought indices, Z index (blue solid line) shows the greatest variability. The peak of inter-annual variability of CMI (green solid line) is found in summer. The

seasonal patterns of inter-annual variabilities of CMI and soil moisture in 0 – 100 cm layer are similar: increasing from the beginning of year till summer and then decreasing till the end of year. The seasonal patterns of inter-annual variabilities of SPI (red solid line), SPEI (brown solid line), Z index and soil moisture in 0 – 10 cm layer are similar which show greater variability in the late spring and summer, less variability in the fall. For the time period from 2003 to 2012 (Figure 2.7b), the standard deviation of Z index is overall larger than the other drought indices, as well as soil moisture throughout the year. The variability of soil moisture in 0 – 100 cm is consistently lower. Summer is commonly indicated as the season with higher inter-annual variability by all the indices and soil moisture. Especially for CMI, the standard deviation keeps low in winter and then increases rapidly till summer. The change ranges from 0.1 to 0.44, which is bigger than SPI (0.25 – 0.34), SPEI (0.23 – 0.38), Z index (0.28 – 0.42) and soil moisture in 0 – 10 cm (0.19 – 0.32) and in 0 – 100 cm (0.13 – 0.33).

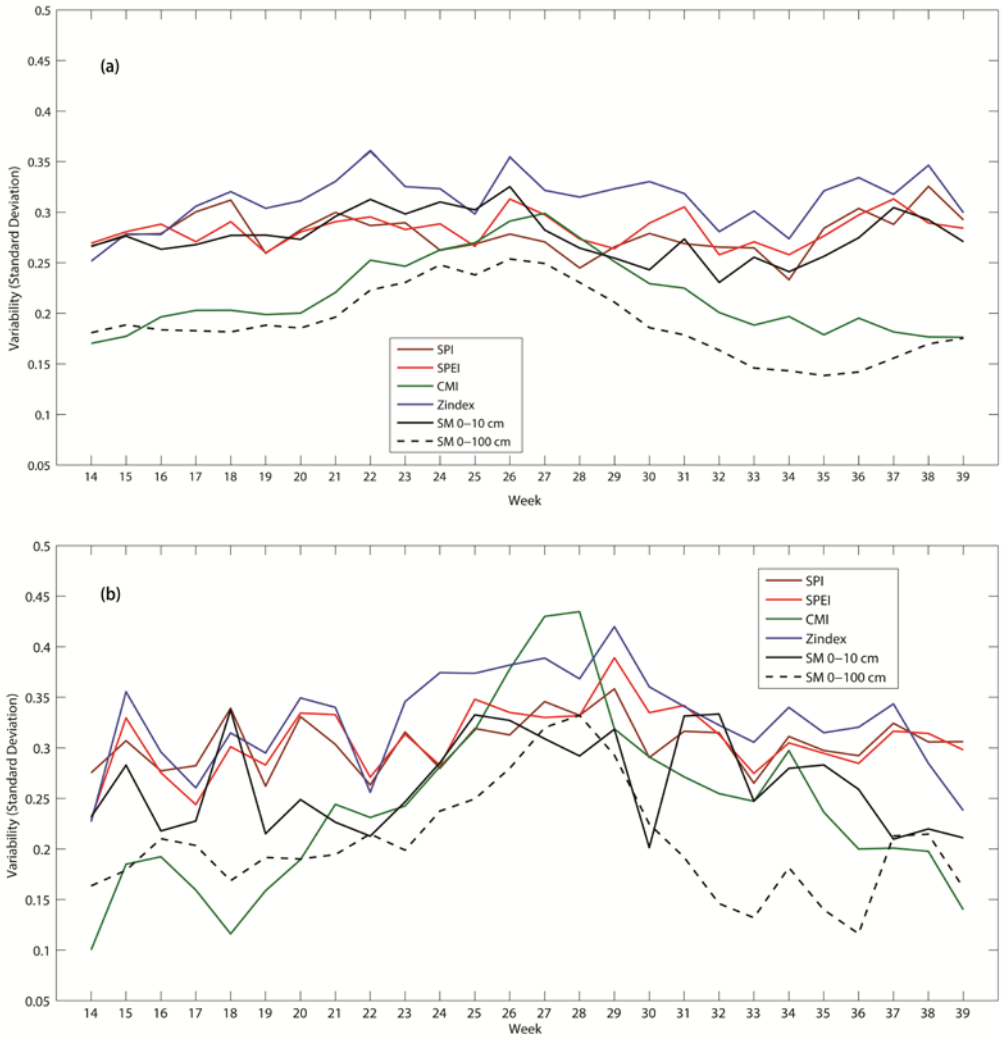

Figure 2. 7. Inter-annual variability of SPI (brown), SPEI (red), CMI (green), Z index (blue), soil moisture in 0 – 10 cm soil layer (black solid) and soil moisture in 0 – 100 cm soil layer (black dashed) over the U.S. Great Plains (a) NLDAS-2 soil moisture from 1980 to 2012, (b) in situ soil moisture from 2003 to 2012.

2.3.5 Intra-annual Variability of Drought Indices and Soil Moisture

We also assess the intra-annual variance of each index and soil moisture by calculating the standard deviation of all the weeks in each year. The histograms of the

standard deviations are shown in Figure 2.8a – f and Figure 2.9a – f for 1980 – 2012 and 2003 – 2012, respectively. As shown in Figure 2.8c, the standard deviation of CMI is more evenly distributed than the other three drought indices This is similar to the standard deviation of soil moisture in the 0 – 100 cm soil layer (Figure 2.8f). The shape of histogram of soil moisture in 0 – 10 cm layer (Figure 2.8e) is most similar to the SPEI (Figure 2.8b). We also compare the multi-year averaged standard deviation of each drought index with soil moisture. Based on Figure 2.8, multi-year averaged standard deviation of SPI (0.263) is slightly smaller than soil moisture in 0 – 10 cm (0.268) while Z index is slightly larger (0.272). The mean standard deviation of CMI (0.245) is the closest to soil moisture in 0 – 100 cm (0.240).

The histogram of intra-annual variabilities of CMI from 2003 to 2012 (0.18 – 0.32) ranges wider than the other three indices (SPI: 0.24 – 0.30, SPEI: 0.24 – 0.30 and Z index: 0.26 – 0.32). Compared with soil moisture in 0 – 10 cm layer (0.20 – 0.28) and in 0 – 100 cm layer (0.18 – 0.30), the range is more similar to the later one. On the contrary, the mean standard deviation of CMI (0.253) is closer to the mean standard deviation of 0 – 10 cm soil moisture (0.239). Relative to the mean standard deviation of soil moisture (0 – 10 cm: 0.239, 0 – 100 cm: 0.225), SPI (0.271), SPEI (0.269) and Z index (0.281) all show larger difference than CMI (0.239).

We also calculate the difference of intra-annual variability between drought indices and soil moisture in each layer. We compare the differences and select one drought index with largest difference and one with smallest difference for each year. Then we count how many times each drought index is selected as the most different

drought index with soil moisture (blue bar) or the least different drought index with soil moisture (brown bar). The result based on the differences between drought indices and NLDAS-2 soil moisture from 1980 to 2012 is shown in Figure 2.8g (0 – 10 cm) and h (0 – 100 cm). The result based on the differences between drought indices and in situ soil moisture from 2003 to 2012 is shown in Figure 2.9 g (0 – 10 cm) and h (0 – 100 cm). From 1980 to 2012, SPEI is most frequently (14 years) selected as the drought index with the least different intra-annual variability with 0 – 10 cm soil moisture, followed by CMI and SPI (8 years) and then Z index (3 years). During the same period, Z index is selected as the drought index with the most different intra-annual variability with 0 – 10 cm soil moisture in 11 years, followed by CMI in 10 years, SPI in 8 years and SPEI in 4 years. In 0 – 100 cm soil layer, CMI is most frequently (14 years) identified as the drought index with most similar intra-annual variability with NLDAS-2 soil moisture while Z index is most frequently (14 years) identified as drought index with least similar intra-annual variability. Relative to in situ 0 – 10 cm soil moisture from 2003 to 2012, SPEI (5 years) and Z index (5 years) is most frequently selected as the drought index with the least and most different intra-annual variability, respectively. In 0 – 100 cm soil layer, CMI is selected in 5 years because of its closest intra-annual variability to soil moisture. The Z index has the most different intra-annual variability in 5 years. The statistical results based on simulated and observed soil moisture are consistent with each other.

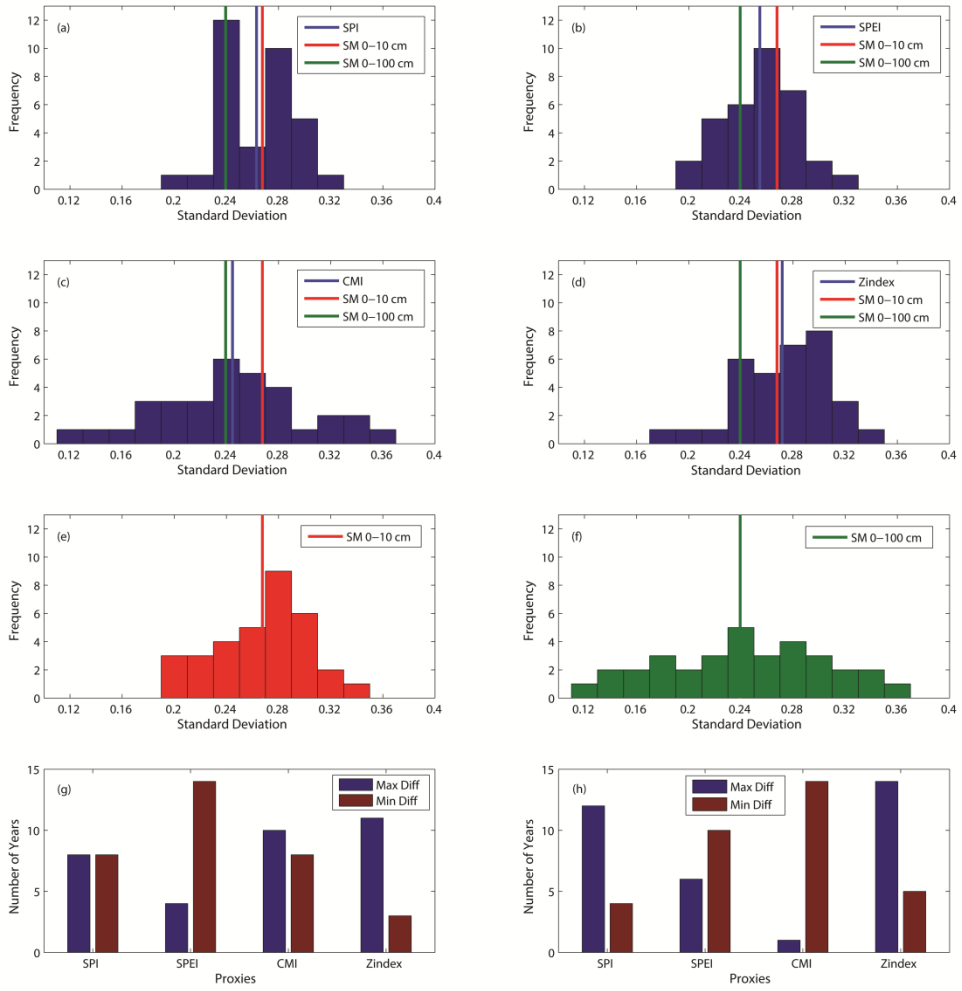

Figure 2. 8. Histograms of intra-annual variability of (a) SPI, (b) SPEI, (c) CMI, (d) Z index, (e) soil moisture in 0 – 10 cm soil layer and (f) soil moisture in 0 – 100 cm soil layer over the U.S. Great Plains from 1980 to 2012 and frequency of minimum difference year (brown bar) and maximum difference year (blue bar) relative to (g) soil moisture in 0 – 10 cm soil layer and (h) soil moisture in 0 – 100 cm soil layer.

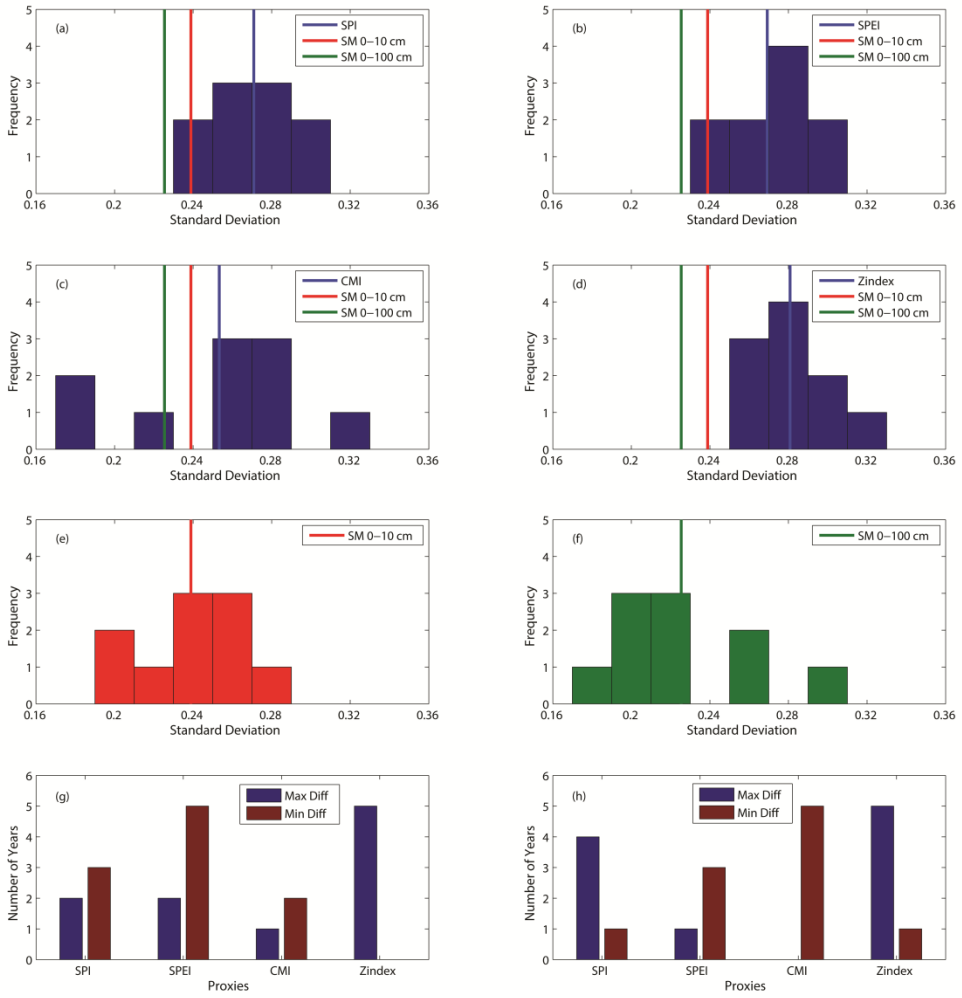

Figure 2. 9. Same as Figure 2.8, but for 2003 – 2012 using in situ soil moisture.

2.3.6 Persistence of Drought and Soil Moisture

The impacts of soil moisture on the climate system can last for months. This is known as soil moisture persistence, or memory (Wu and Dickinson 2004). In this section, we characterize the persistence of drought indices and soil moisture. Figure 2.10 shows the persistence of drought indices and soil moisture in warm season (April to September)

based on the lagged autocorrelation. Based on both long-term average (Figure 2.10a) and short-term average (Figure 2.10b), CMI and 0 – 100 cm soil moisture have substantially longer persistence. In Figure 2.10a, in April and May, the persistence of CMI and 0 – 100 cm soil moisture are as long as 12 weeks. The persistence of CMI starts to decrease after May while the persistence of 0 – 100 cm soil moisture keeps 12-week persistence till June. From July to September, the persistence of CMI decreases faster than 0 – 100 cm soil moisture. In contrast, the persistence of 0 – 10 cm soil moisture, SPI, SPEI and Z index are fairly stable. SPI shows shortest persistence (less than 2 weeks). The persistence of 0 – 10 cm soil moisture is longer than Z index, SPEI and SPI but much shorter than CMI and 0 – 100 cm soil moisture. In Figure 2.10b, consistent results are illustrated. CMI and 0 – 100 cm soil moisture have longest persistence. However, the persistence of 0 – 10 cm soil moisture, Z index and SPEI are more fluctuant. The longest persistence of 0 – 10 cm soil moisture and Z index reach to 7 weeks in June and 5 weeks in July respectively.

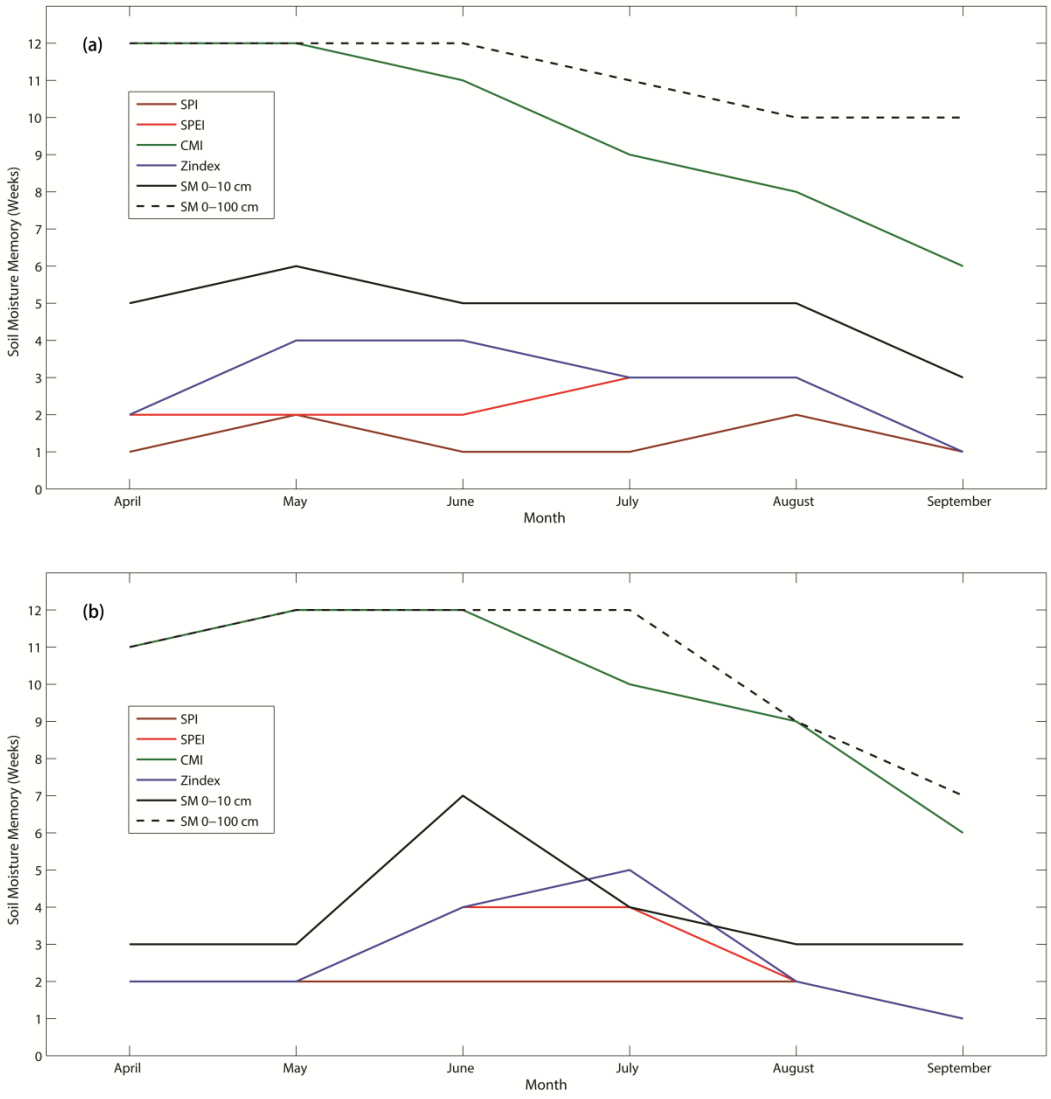

Figure 2. 10. Spatially-averaged persistence of SPI (brown), SPEI (red), CMI (green), Z index (blue), soil moisture in 0 – 10 cm soil layer (black solid) and soil moisture in 0 – 100 cm soil layer (black dashed) over the U.S. Great Plains (a) from 1980 to 2012, (b) from 2003 to 2012.

Figure 2.11 shows the spatial patterns of persistence of drought indices and soil moisture in different months based on 1980 – 2012 data. The persistence of SPI is

consistently shorter than 2 weeks over the entire U.S. Great Plains during the entire warm season. The persistence of SPEI is also short (< 3 weeks) over the most U.S. Great Plains during warm season. The regions with relative longer persistence (> 3 weeks) of SPEI shift from west Texas to southwest Texas and then to central Texas from April to August. The persistence of CMI is much higher than SPI and SPEI all over the U.S. Great Plains. In April, the persistence of CMI stays long (> 12 weeks) in the western Great Plains, while in southeast Oklahoma, the persistence value is relative shorter (~4 weeks). The long persistence stays in western South Dakota and Nebraska and most Texas in May. The region with long persistence of CMI keeps reducing in June. Only in small parts of western South Dakota and Nebraska and central Texas, the persistence of CMI is still longer than 10 weeks. From July to September, the persistence of CMI is moderately long (4 – 10 weeks) over most U.S. Great Plains except in eastern Kansas, where the persistence is still longer than 10 weeks. The Z index persistence is also short in April and September (< 4 weeks). However, in May, June and July, the "hot spot" of long persistence (> 10 weeks) of Z index is found in Texas. In August, the area of the "hot spot" shrinks and locates in western Texas. The persistence of soil moisture in 0 – 10 cm soil layer (~5 weeks) is shorter than that of soil moisture in 0 – 100 cm soil layer (~10 weeks). The higher persistence of 0 – 10 cm soil moisture is found over the boundary between Nebraska and Kansas. This region extends to South Dakota and Nebraska in June and July. The spatial pattern of persistence of 0 – 100 cm soil moisture does not change a lot from April to September. Over the boundary between Nebraska and Kansas, South Dakota and western Texas, the persistence (> 12 weeks) is much

longer than in other regions (< 10 weeks). Overall, the persistence of CMI and soil moisture in 0 – 100 cm soil layer is longer than other drought indices and soil moisture in 0 – 10 cm soil layer.

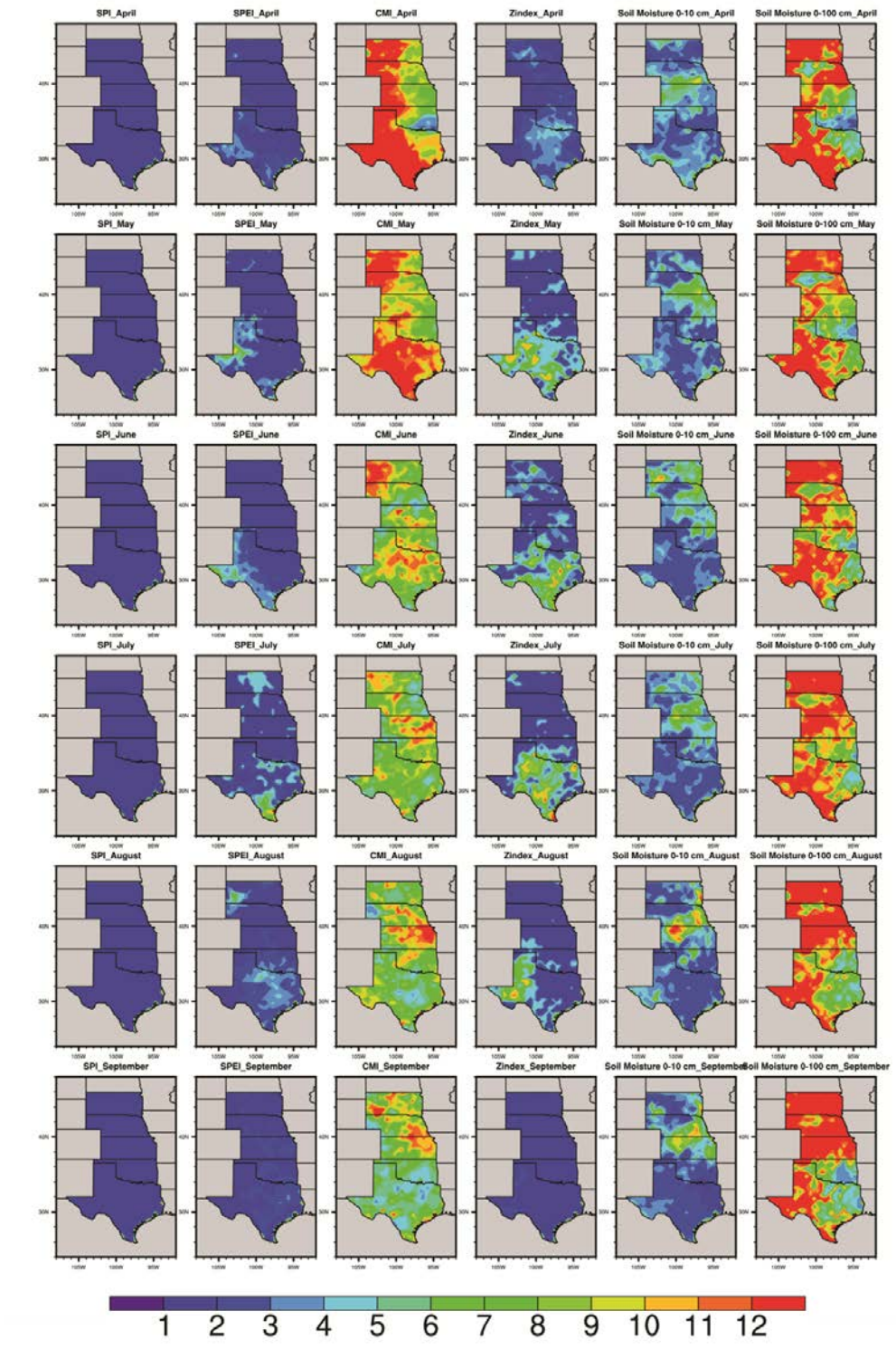

Figure 2. 11. Spatial pattern of persistence of drought indices and NLDAS-2 soil moisture in warm season (April to September) from 1980 to 2012.

2.4 Conclusions

Drought indices and soil moisture are both useful sources of information for drought monitoring. Soil moisture observations can be used to improve the development and application of drought indices. Drought indices can be used as soil moisture proxies to describe surface moisture conditions. In this chapter, we evaluated four short-term drought indices using two independent soil moisture data sources: model simulations and in situ observations. The evaluation compared how four factors (percentile, trend, variability and persistence) are represented in the drought indices and soil moisture observations.

Our results show that soil moisture percentiles in the 0 – 10 cm soil layer are more highly correlated with SPI, SPEI and Z index percentiles than soil moisture in 0 – 100 cm while CMI is more highly correlated with soil moisture percentiles in the 0 – 100 cm soil layer than the near-surface layer. Spatially, the highest correlation between soil moisture (0 – 100 cm) and drought indices occurs in the southern Great Plains regardless of the choice of drought indices. Soil moisture percentiles in the 0 – 10 cm soil layer are highly correlated with SPI, SPEI and Z index in Texas.

A statistically significant drying trend from 1980 to 2012 is found in all the drought indices that account for PET. However, this trend is stronger than shown by the observed soil moisture. We will focus on assessing the impacts of the methodology used for calculating PET in the following chapter. As a result of increasing temperatures, the drying trend is more pronounced in the last 10 years.

We did not find good agreement regarding inter-annual variability between the drought indices and observed soil moisture (0 – 10 cm). However, the inter-annual variability of CMI does agree well with the 0 – 100 cm soil moisture. SPEI is the most appropriate index for capturing the intra-annual variability in the 0 – 10 cm soil based on distribution, mean standard deviation and frequency of minimum difference. While CMI is the most appropriate index for capturing the intra-annual variability in the 0 – 100 cm soil moisture.

Among the four drought indices, CMI has the longest persistence, followed by Z index, SPEI and SPI. The persistence of 0 – 100 cm soil moisture is similar to CMI but it decrease slower than CMI from April to September. The persistence of 0 – 10 cm soil moisture is shorter than that of CMI and 0 – 100 cm soil moisture but longer than that of other three indices. Spatially, all the drought indices and soil moisture in 0 – 100 cm soil moisture commonly indicate there is longer persistence in Texas while soil moisture in 0 – 10 cm show longer persistence between Nebraska and Kansas.

In summary, CMI is the best index for representing soil moisture conditions in the top 100 cm based on the percentile, trend, variability and persistence because it was designed for measuring agriculture drought and moisture available for crops. Although SPI was used in previous studies to investigate land-atmosphere interactions, however due to the results of this study, we do not recommend using SPI to represent soil moisture condition because it is designed for meteorological drought and ignores the influence of ET. The three drought indices (SPEI, CMI and Z index) using PET in their calculations also show different performances and may over-estimate drought trends.

This leads to further questions on how to calculate PET. Therefore, this issue will be addressed in the next chapter.

CHAPTER III

DROUGHT FROM 1980 TO 2012: A SENSITIVITY STUDY OF USING DIFFERENT METHODS FOR ESTIMATING POTENTIAL EVAPOTRANSPIRATION IN THE PALMER DROUGHT SEVERITY INDEX[*]

3.1 Introduction

Drought indices are an important tool that can be used to evaluate the timing, duration, and intensity of drought. Over 100 drought indices have been developed since the beginning of twentieth century (Heim, 2002). Previous review articles, such as Quiring (2009) have described many of the most commonly used drought indices and evaluated their strengths and weaknesses, while Mishra and Singh (2010) and Zargar et al. (2011) provide comprehensive reviews of nearly 100 drought indices.

Given the range in derivations and the different responses of these drought indices, not all are suitable for monitoring agricultural, meteorological, or hydrological drought conditions (Quiring and Papakryiakou, 2003). Here we have chosen to focus on the Palmer Drought Severity Index (PDSI) because it is the most widely used drought index in the U.S. to monitor droughts (Dai, 2011b; Heim, 2002). The PDSI has been used in long-term analyses of drought variability and to detect changes in drought

---

[*] This chapter is reprinted with permission from "Drought in the U.S. Great Plains (1980-2012): A sensitivity study using three different methods for estimating potential evapotranspiration in the Palmer Drought Severity Index" by Shanshui Yuan and Steven Quiring, 2014. Journal of Geophysical Research-Atmospheres: 19, 10,996–11,010, doi: 10.1002/2014JD021970, Copyright 2014 by John Wiley and Sons.

characteristics during the last 100 years (Dai, 2011a, 2012; Sheffield et al., 2012). It has also been used to examine how climate change may influence drought frequency, severity, and duration (Burke and Brown, 2008; Dai, 2012; Rind et al., 1990; Sheffield and Wood, 2008).

The original PDSI was published in 1965 by W. Palmer (Palmer, 1965). It considers antecedent precipitation, moisture supply, and moisture demand using a simple two-layer bucket-type water balance model. The PDSI classifies moisture conditions into 11 categories, as shown in Table 3.1. Traditionally, the PET calculated in the PDSI is based on the Thornthwaite equation. This is a temperature-dependent method of estimating PET that is not very accurate in energy-controlled regions (Alley, 1984; Hobbins et al., 2008; Mishra and Singh, 2010). Although Guttman (1991) demonstrated that precipitation is the most important factor that controls the PDSI, replacing the Thornthwaite equation with a more physically based PET method should strengthen the ability of the PDSI to accurately depict drought conditions (van der Schrier et al., 2011). A number of previous studies have used the Penman-Monteith equation, which considers wind speed, humidity, and radiation, to calculate PDSI (Burke et al., 2006; Dai, 2011a; Sheffield et al., 2012; van der Schrier et al., 2011, 2006a, 2006b). Dai (2011a) found that using the Penman-Monteith equation for calculating PET did not have a significant influence on global drought patterns, and this was confirmed by van der Schrier et al. (2011). They agreed the lack of sensitivity of PET estimates is due to Palmer's "climatically appropriate for existing conditions" (CAFEC) coefficients which normalize the PET values using the long-term climatology. However, Sheffield et al. (2012)

demonstrated using the Penman-Monteith-based PDSI resulted in fewer observed changes in global drought characteristics during the last 60 years as compared to the original PDSI. Global drought trends are still a matter of debate. Dai (2011a) found a significant global drying trend based on using the PDSI with the Penman-Monteith equation for estimating PET. However, Sheffield et al. (2012) applied a similar approach and concluded that the drying trend found by (Dai, 2011a) is overestimated. Damberg and AghaKouchak (2014) confirmed the results of Sheffield et al. (2012) by using the Standardized Precipitation Index to examine global trends in moisture conditions.

Table 3. 1. Categories of drought conditions for PDSI by Palmer (1965)

PDSI	Classification	PDSI	Classification
Larger than 4.0	Extremely wet	smaller than -4.0	Extremely dry
3.0 – 4.0	Severely wet	-4.0 – -3.0	Severely dry
2.0 – 3.0	Moderately wet	-3.0 – -2.0	Moderately dry
1.0 – 2.0	Slightly wet	-2.0 – -1.0	Slightly dry
0.5 – 1.0	Incipient wet spell	-1.0 – -0.5	Incipient dry spell
-0.5 – 0.5		Near normal	

Although the Penman-Monteith equation is a physically based approach, it uses a "big leaf" assumption that is most suitable for regions that have complete canopy cover or bare soil (Stannard, 1993). The two-source PET model considers radiation balances at the canopy level and soil surface separately (Shuttleworth and Wallace, 1985). This

improvement helps PET models more accurately describe areas with sparse vegetation. However, there have been few studies applying the two-source model for calculating PDSI. Liu et al. (2009) analyzed the drought response to land cover land use changes in North China. Xu et al. (2012) applied the two-source model based PDSI to assess the response of vegetation to drought in the same region.

The aim of this chapter is to improve the PDSI by replacing the Thornthwaite equation with the physically based two-source model and to compare the two-source PDSI with the Penman-Monteith PDSI and the original PDSI. Drought trends in the U.S. Great Plains (Texas, Oklahoma, Kansas, Nebraska, and South Dakota) from 1980 to 2012 will be evaluated using all three versions of the PDSI.

3.2 Data and Methods

3.2.1 Meteorological Data

Gridded meteorological data, including precipitation, maximum temperature, mean temperature, minimum temperature, wind speed, air pressure, downward long-wave radiation, and downward shortwave radiation, are necessary to drive PET models. These data are obtained from NLDAS-2 (Xia et al., 2012). NLDAS provides reliable initial states for the atmosphere, ocean, and land surface (Mitchell et al., 2004). Hourly NLDAS meteorological forcing data (1/8°) are downscaled from the NARR which is with 32 km spatial resolution and 3 h temporal resolution. NLDAS-2 precipitation data are derived from NOAA CPC gauge-based precipitation data. This data set is adjusted

by Parameter-elevation Regressions on Independent Slopes Model. NLDAS-2 downward shortwave radiation data are improved through applying a bias-correction algorithm to the NARR surface downward shortwave radiation. For estimating daily PET, precipitation and radiation data are accumulated from hourly to daily values; the other forcing data are averaged to daily values.

3.2.2 Land Surface Parameters

Land surface information is also critical for calculating the two-source PDSI. Elevation, vegetation classifications, and their corresponding parameters are obtained from NLDAS-2. The original source of the elevation data is the GTOPO30 database (Verdin and Greenlee, 1996). The vegetation data set is based on the global 1 km University of Maryland vegetation classification (Hansen et al., 2000). The frequency of each vegetation type in each 1/8° grid is the weighting factor that is used to rescale vegetation parameters from 1 km resolution to 1/8° resolution.

Soil moisture is a direct measure of drought impact (Robock et al., 2000). In this study, the correlation between observed soil moisture and different PDSI values are used to evaluate the performance of different PDSIs. Observed soil moisture over the U.S. Great Plains from 2005 to 2012 is obtained from the North American Soil Moisture Database (http://soilmoisture.tamu.edu). A total of 142 stations from five different networks (South Dakota Automated Weather Network, Automated Weather Data Network, Atmospheric Radiation Measurement, Oklahoma Mesonet, and West Texas Mesonet) are used in this analysis. Observed soil moisture is converted from volumetric

water content (VWC) at the various sensor depths to VWC in the top 1m of the soil. This VWC value is compared to the different forms of PDSI evaluated in this study.

3.2.3 PET Models

Potential evapotranspiration influences the water balance in the PDSI by acting as a threshold in calculating actual evapotranspiration (AET). If precipitation is greater than PET, AET equals to PET, while if precipitation is less than PET, AET is contributed by PET together with soil water storage. In this study, we used three approaches to estimate PET: the Thornthwaite equation (TH), the Penman-Monteith equation (PM), and the two-source PET model (2S). In the original PDSI (Palmer, 1965), the TH (Thornthwaite, 1948) is used to calculate PET by building a function of monthly air temperature, latitude, and month, as shown in eq. 2.1 (last chapter).

The Penman-Monteith equation (PM) is a physically based method that is widely used for estimating PET. Compared with the TH, the PM requires more variables and can more realistically simulate PET (van der Schrier et al., 2011). The PM creates a reference land cover and assumes that both energy and mass fluxes occur at the reference height. The Food and Agricultural Organization (FAO) defines the PM as

$$PET = \frac{0.408\Delta\left(R_n - G\right) + \gamma \frac{900}{T+273} U_2 \left(e_a - e_d\right)}{\Delta + \gamma\left(1 + 0.34U_2\right)} \tag{3.1}$$

where R_n is net radiation, Δ is slope of the vapor pressure curve, G is soil heat flux, U_2 is wind speed, $e_a - e_d$ is vapor pressure deficit, and γ is psychometric constant.

The two-source PET model (2S), also known as the Shuttleworth-Wallace model, is an improvement over the PM because the PM assumes both heat fluxes and mass fluxes happen at the hypothetical reference height, which is covered by a single uniform big leaf. This assumption is rarely valid over a large area or a sparse vegetation covered region. The 2S identifies two independent heat sources: canopy surface and soil surface. At each heat source, there exists corresponding radiation balance and aerodynamic principles.

As shown in Figure 3.1 (Zhou et al., 2006), the 2S model considers five land surface resistances: aerodynamic resistance between canopy source and reference level (r_a^a), aerodynamic resistance between soil surface and canopy source (r_a^s), bulk boundary-layer resistance of canopy (r_a^c), bulk stomatic resistance of the canopy (r_s^c) and soil surface resistance (r_s^s) when soil moisture is at field capacity. r_a^c and r_s^c restrict the water vapor being out from the leaf stomata; r_s^s and r_a^s control the water movement from soil surface. Total PET consists of: transpiration (ET_c), interception evaporation (ET_i) and soil evaporation (ET_s). These three components can be calculated as follows:

$$ET_c = \frac{\Delta R_{nc} + \dfrac{\rho C_p D_0}{r_a^c}}{\lambda\left[\Delta + \gamma\left(\dfrac{r_s^c}{r_a^c}\right)\right]}\left(1 - W_{fr}\right) \tag{3.2}$$

$$ET_i = \frac{\Delta R_{nc} + \dfrac{\rho C_p D_0}{r_a^c}}{\lambda\left(\Delta + \gamma\right)} W_{fr} \tag{3.3}$$

$$ET_s = \frac{\Delta(R_{ns} - G) + \frac{\rho C_p D_0}{r_a^s}}{\lambda\left[\Delta + \gamma\left(1 + \frac{r_s^s}{r_a^s}\right)\right]} \quad (3.4)$$

Where Δ is slope of saturation vapor pressure curve, R_{nc} and R_{ns} mean net radiation is absorbed by canopy and soil, respectively, G is the substrate soil heat flux, ρ is mean air density, C_p is air specific heat, γ is the psychrometric constant, λ is the latent heat of vaporization, W_{fr} is wetted fraction of the canopy and D_0 is the water vapor deficit at the source height. More detail on the equations for calculating the above variables are described by Mo et al. (2004).

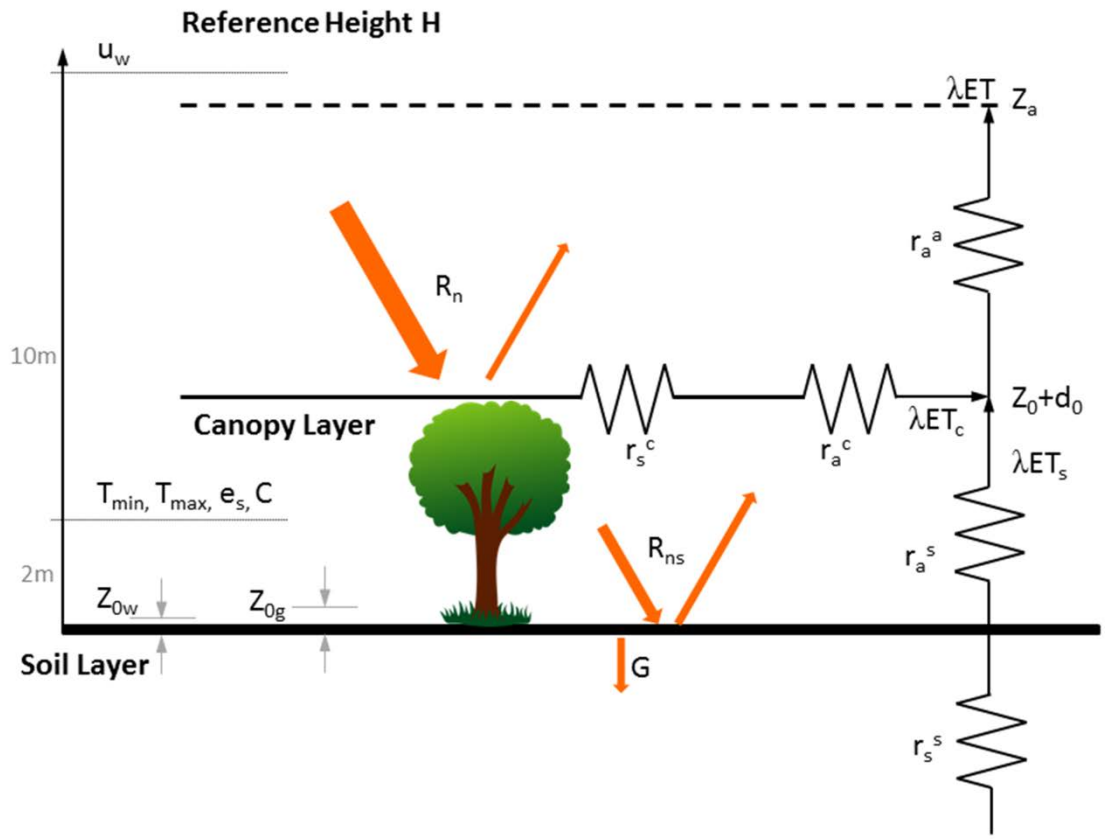

Figure 3. 1. Schematic diagram of the two-source evapotranspiration model (Zhou et al., 2006).

3.2.4 PDSI

The Palmer Drought Severity Index (PDSI) uses a water balance model with two soil layers to evaluate moisture supply and demand (Palmer, 1965). The water balance model is governed by evapotranspiration (ET), recharge to soils (R), runoff (RO), water loss to the soil layers (L), and the potential values of PET, PR, PRO, and PL. The inputs for calculating the PDSI are precipitation (P) and temperature (T). Palmer (1965) introduced “climatically appropriate for existing conditions” (CAFEC) value to represent

the needed amount of each water flux to maintain a normal water condition. The CAFEC precipitation is calculated by eq 3.5.

$$\widehat{P} = \alpha_i PE + \beta_i PR + \lambda_i PRO - \delta_i L \tag{3.5}$$

In eq 3.5, α_i, β_i, λ_i and δ_i are water-balance coefficients, which equal to $\frac{\overline{ET_i}}{\overline{PET_i}}$, $\frac{\overline{R_i}}{\overline{PR_i}}$, $\frac{\overline{RO_i}}{\overline{PRO_i}}$ and $\frac{\overline{L_i}}{\overline{PL_i}}$, respectively. The bar indicates that these values are calculated based on multi-year mean values for each month.

The moisture anomaly index (Z index) is calculated as $\left(P - \widehat{P}\right)K$, where P is the actual precipitation and K is a climatic characteristic coefficient. For the central U.S., K can be calculated by eq 3.6 and 3.7.

$$K = \frac{17.67}{\sum_{i=1}^{12} \overline{D}_i K_i'} K_i' \tag{3.6}$$

$$K_i' = 1.5 \log_{10}\left(\frac{\frac{\overline{PE_i} + \overline{R_i} + \overline{RO_i}}{\overline{P_i} + \overline{L_i}} + 2.8}{\overline{D}_i} \right) + 0.5 \tag{3.7}$$

where D is "moisture departure", represented by $P - \widehat{P}$. Finally, the PDSI value is determined by $X_t = 0.897 X_{t-1} + Z_t/3$.

3.3 Results

3.3.1 Comparison of PET Values

PET is a key factor in calculating the PDSI. The original PDSI calculates PET using TH, which estimates PET as a function of day length, latitude, and temperature. The PM-based PET is more physically realistic, combining the energy balance and mass transfer approaches. The 2S further improves on PM by treating the soil surface and canopy layer as two independent heat sources.

Comparison of the area-averaged annual PET calculated using the TH, PM, and 2S approaches (Figure 3.2) shows that there are substantial differences among them. The TH-based mean annual PET is the smallest and the 2S is the largest. Mean annual TH-based PET for the U.S. Great Plains is 859.8 $mmyr^{-1}$, which is less than the PM-based PET (1971.9 $mmyr^{-1}$) and the 2S-based PET (2035.6 $mmyr^{-1}$). The TH-based PET has the largest trend in annual values from 1980 to 2012 (2.33 $mmyr^{-1}$), followed by the 2S-based PET (1.89 $mmyr^{-1}$) and the PM-based PET (0.98 $mmyr^{-1}$). This increasing trend in annual TH-estimated PET occurs because TH is strongly controlled by air temperature. As shown in Figure 3.2, the mean annual 2-m air temperature from NLDAS-2 over the U.S. Great Plains increased by ~1°C between 1980 and 2012.

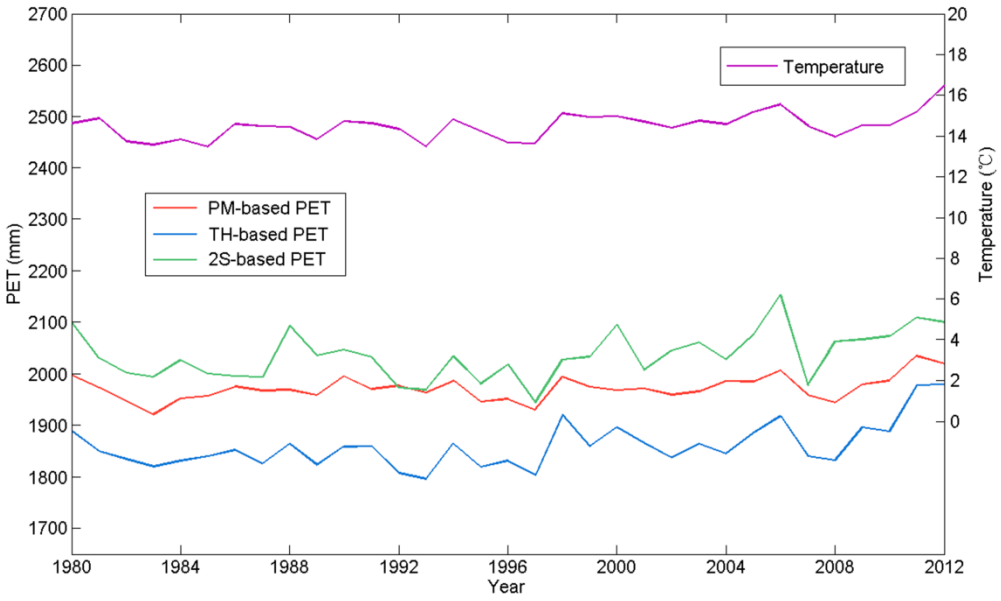

Figure 3. 2. Time series of area-averaged annual PET calculated by the TH (blue), the PM (red), and the 2S (green) and NLDAS-2 2m air temperature (purple) over the U.S. Great Plains from 1980 to 2012.

Figure 3.3 shows the intra-annual variability of PET values. The PM and 2S PET estimates are similar. The 2S-based PET is generally higher than the PM-based PET, except during June and September. The peak in PM and 2S PET occurs in July, while the peak in TH PET is in August. In July – September, in contrast to the rest of year, TH PET is higher than the other two PET estimates. In the 2S model, transpiration is generally the dominant source of annual PET (Figure 3.4). It accounts for 52% of total annual PET. Transpiration is the largest component of PET between May and September. Soil evaporation is the largest component during the rest of the year. The largest values of transpiration and interception evaporation occur in July, which corresponds to the

peak in leaf area index (LAI) (not shown). Soil evaporation reaches its highest value in June due to the combination of energy and moisture availability.

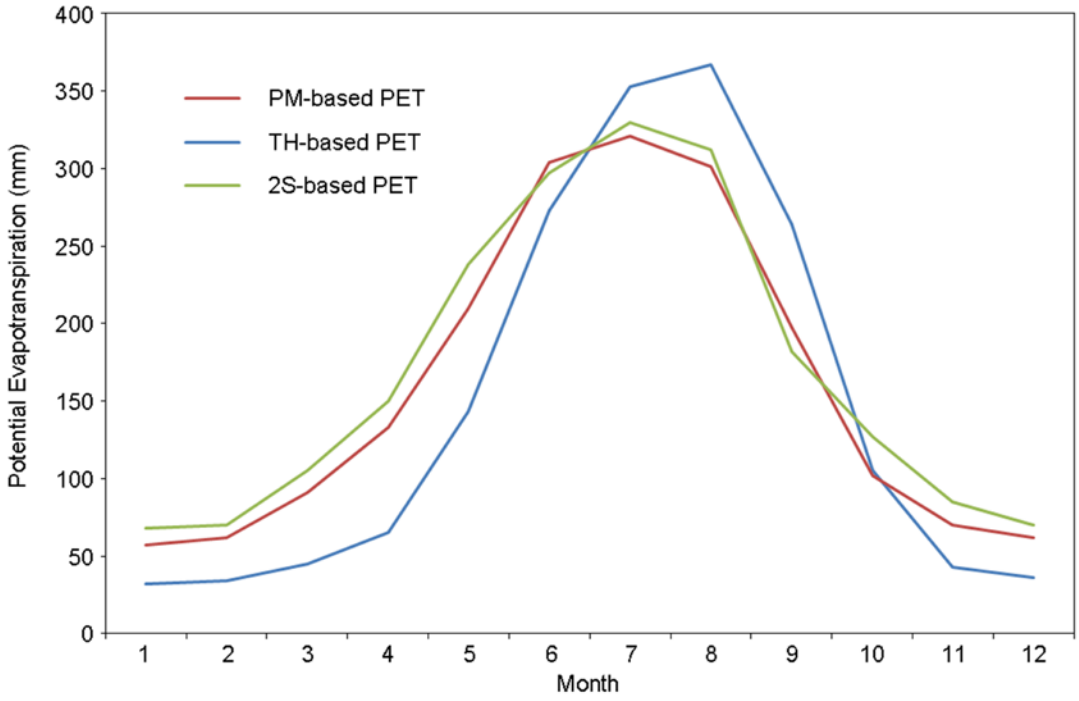

Figure 3. 3. Seasonal pattern of area-averaged PET estimated by the TH (blue), the PM (red), and the 2S (green) over the U.S. Great Plains.

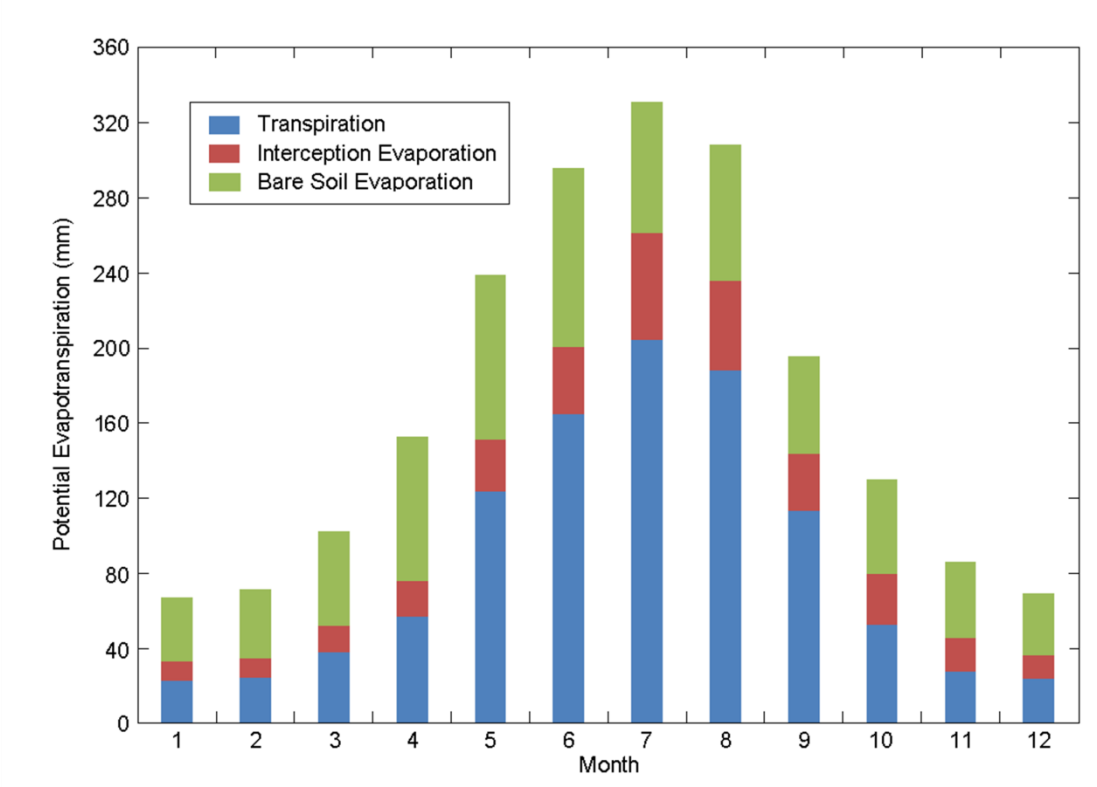

Figure 3. 4. Seasonal pattern of three components of total PET (calculated by the 2S model): canopy transpiration (blue), interception evaporation (red), and bare soil evaporation (green) over the U.S. Great Plains.

3.3.2 Comparison of PDSI Values

Three different versions of the PDSI were calculated using TH, PM, and 2S-based PET. All of the other input variables (e.g., precipitation data) needed to calculate the PDSI were held constant. Wells et al. (2004) developed a self-calibrated version of the PDSI that automatically calibrates the parameters in the PDSI rather than using the empirical constants proposed by Palmer (1965). This is supposed to provide a better representation of local climate conditions. In this study, we chose to use the empirical

constants provided by Palmer (1965), because they were developed using data from the U.S. Great Plains.

Overall, the TH, PM and 2S PDSI values are relatively similar (Figure 3.5), despite the differences in PET. However, there are substantial differences in the PDSI values in some instances. For example, in October 1983 the PM-based PDSI is smaller than the TH and 2S PDSI. While in December 1986, the 2S PDSI was drier than the TH and PM. Figure 3.6 (upper) shows the differences between the PM-based and TH-based PDSI, while Figure 3.6 (lower) shows the differences between the PM-based and 2S-based PDSI. During most months before 1998, the PM-based PDSI is drier than the TH-based PDSI. After 1998, the TH-based PDSI are generally drier than the PM-based PDSI.

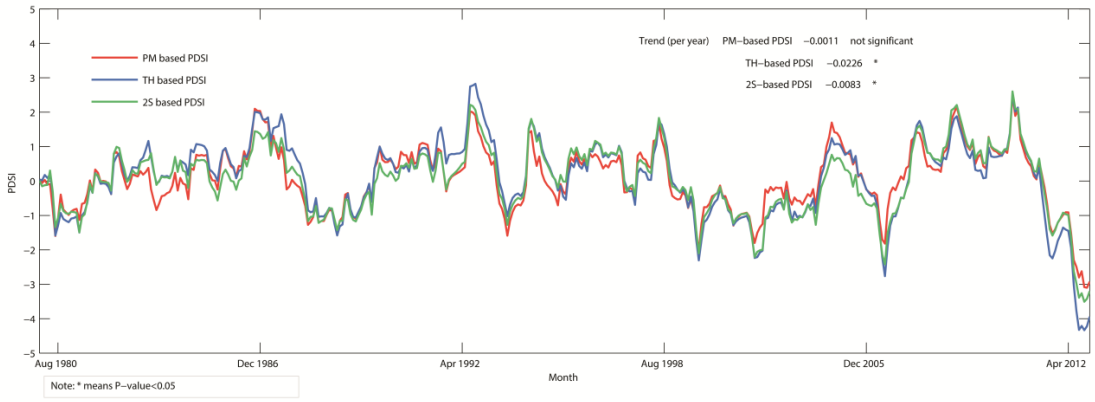

Figure 3. 5. Time series of area-averaged monthly PDSI calculated by the TH (blue), the PM (red), and the 2S (green) over the U.S. Great Plains from 1980 to 2012.

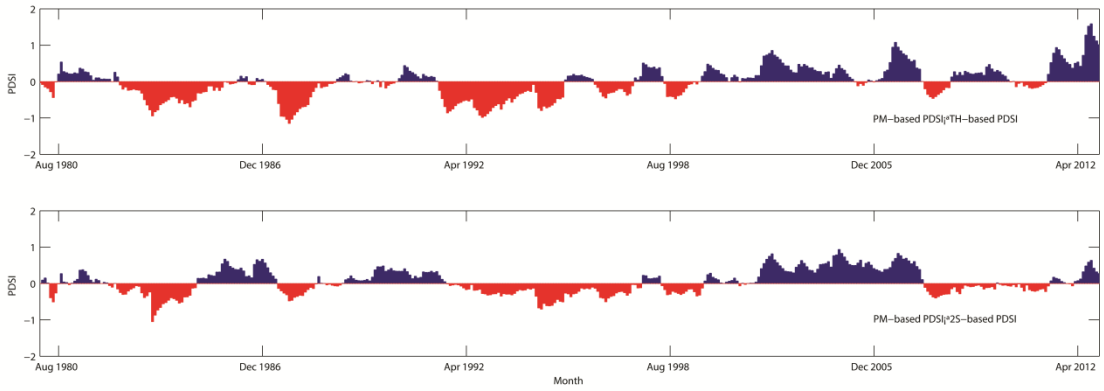

Figure 3. 6. Differences (top) between the PM-based PDSI and the TH-based PDSI and (bottom) between the PM-based PDSI and the 2S-based PDSI over the U.S. Great Plains from 1980 to 2012.

There is significant inter-decadal variability in moisture conditions in the Great Plains, but little long-term trend (Figure 3.5). Linear functions were fit to all the PDSI time series (based on the mean annual PDSI value to remove seasonal impacts). The Mann-Kendall trend test was applied to test significance. The Mann-Kendall test requires serially independent data (Yue et al., 2002). We tested the lag-1 correlations of the mean annual PDSI and found that the correlations are not statistically significant (r^2 = 0.08, not significant) and therefore it meets the assumptions of the Mann-Kendall test. There are slight decreasing (drier) trends based on all three PDSIs and the TH-based PDSI has the strongest negative trend (-0.0226 $year^{-1}$). Both the TH-based PDSI and the 2S-based PDSI pass the Mann-Kendall trend test with 95% confidence interval.

Spatial distributions of drought trends (1980 to 2012) are summarized in Figure 3.7. The three versions of the PDSI generally show a consistent spatial pattern of drying

and wetting trends in the Great Plains. There are small positive trends in PDSI values (wetter conditions) in most of South Dakota, Nebraska and Kansas. There are negative trends in PDSI vales (drier conditions) in most of Oklahoma, except the northeast corner. Texas features a mixture of wetting and drying trends. However, the magnitude of the drying/wetting trends over some regions varies based on the different PDSI methods. The trends in South Dakota, Nebraska, Kansas and Oklahoma are robust because all three approaches show similar spatial patterns. In central Texas, there is a discrepancy between the TH-based PDSI and the other two PDSI methods. A closer examination of the spatial pattern of the locations with statistically significant trends in PDSI reveals that the TH-based and PM-based PDSI tend to be more spatially contiguous than the 2S-based PDSI (Figure 3.7). That is, the locations with statistically significant positive and negative trends for the TH-based and PM-based PDSI are clustered together. This makes sense because these patterns are being determined solely by trends in weather conditions. The seemingly more random pattern in the locations of the statistically significant positive and negative trends for the 2S-based PDSI is due to the fact that these patterns are determined both by trends in weather conditions as well as variations in vegetation (land cover). Grid cells that are located right next to each will experience similar temperature and precipitation conditions, but may have different dominant vegetation. Therefore, the PET estimate in the 2S-based PDSI may be quite different in adjacent grid cells and so the spatial patterns of the 2S-based PDSI will be less spatially coherent than the TH-based and PM-based PDSI.

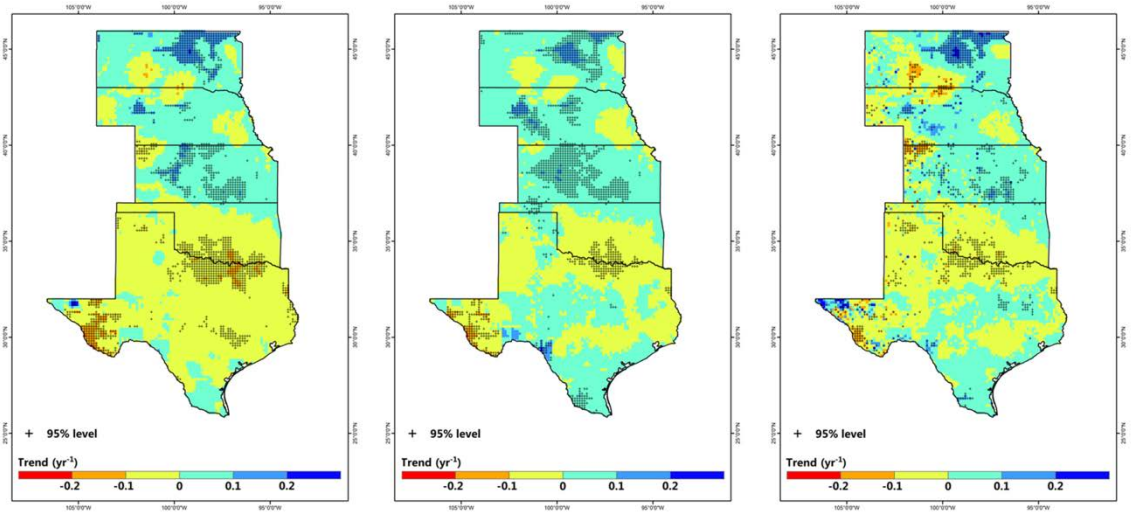

Figure 3. 7. Spatial pattern of trends in the PDSI estimated by (left) the TH, (middle) the PM, and (right) the 2S. Statistically significant trends at the 95% level are indicated by a cross.

The Mann Kendall test based on the mean annual PDSI showed that there are statistically significant (p value = 0.05) drying/wetting trends in ~15% of the U.S. Great Plains (16.2% based on the TH; 11.8% based on the PM; 15.2% based on the 2S). Figure 3.8 shows the spatial pattern of differences between the 2S-based PDSI and the other two PDSI methods. Compared with the PM-based PDSI, the 2S-based PDSI shows significantly drier conditions in northern South Dakota, western Nebraska, parts of Kansas, western Oklahoma and northern/western Texas. The stronger wetting trends are concentrated in northeastern South Dakota, eastern Nebraska, eastern Kansas, northeastern Oklahoma and eastern/western Texas. The 2S-based PDSI and the TH-based PDSI show significant disagreement over broader regions of the U.S. Great Plains. The TH-based PDSI has drier trends in southern and eastern parts of Texas and southern

Oklahoma, and wetter trends in western South Dakota, western Nebraska, and northwestern Kansas.

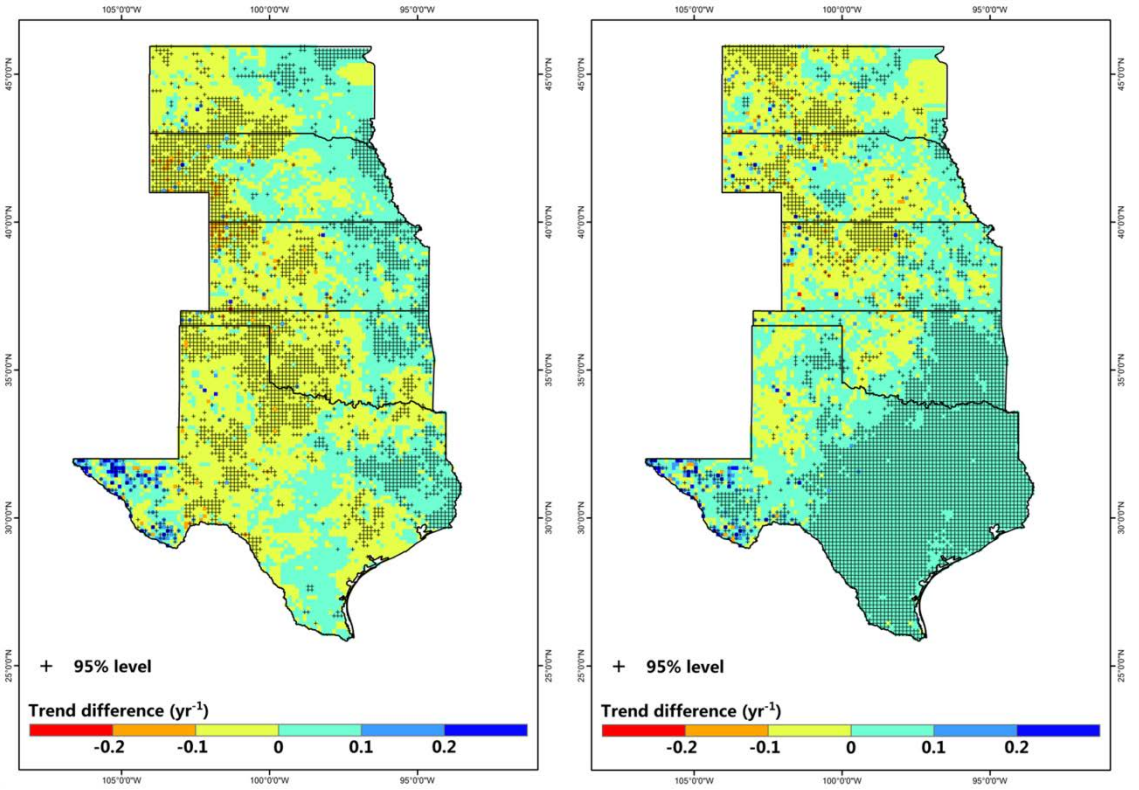

Figure 3. 8. Difference of trends in the PDSI (left) between the 2S and the PM, (right) between the 2S and the TH. Statistically significant trends at the 95% level are indicated by a cross.

It appears that the spatial patterns of differences correspond, to some extent, with land cover type (Figure 3.9). Over regions dominated by croplands and closed shrub lands, the 2S-based PDSI indicates drier conditions than the PM-based PDSI. Over wooded grassland, the 2S-based PDSI tends to be wetter than the TH-based PDSI. Since

the TH-based PDSI includes no vegetation information, the PM-based PDSI considers land cover as a default parameterization at a reference height (“big leaf” assumption) and the 2S-based PDSI treats land cover as two independent sources (soil and canopy), the impact of land cover on the spatial distribution of PDSI trend differences cannot be ignored.

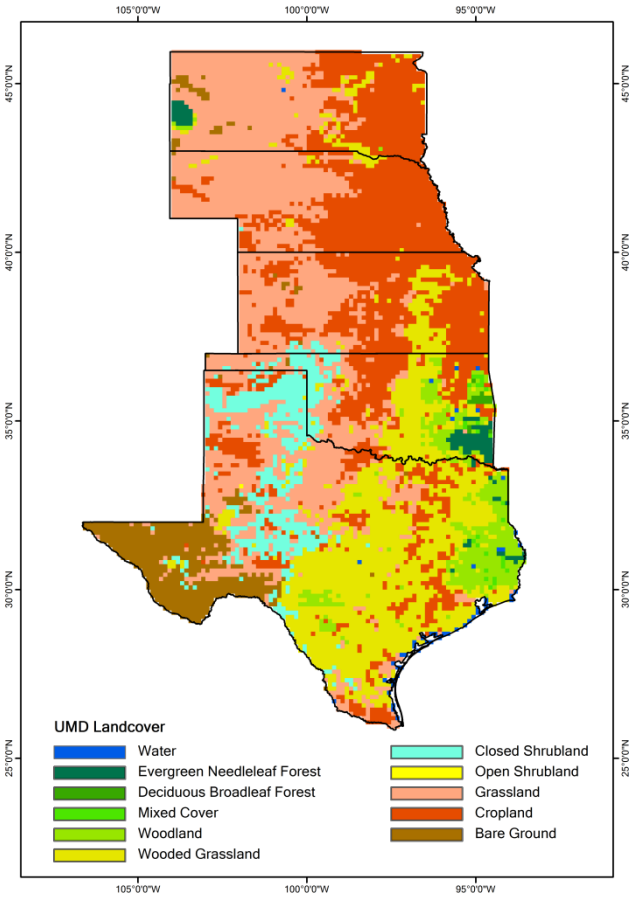

Figure 3. 9. Spatial distribution of land cover type over the U.S. Great Plains.

To further identify the influence of land cover on PDSI estimation, we performed land cover sensitivity experiments in the U.S. Great Plains using the 2S-based PDSI. The six principal land covers are grassland (31.5%), cropland (28.8%), wooded grassland (20.9%), closed shrubland (6.2%), bare ground (6.0%) and woodland (4.4%). In each experiment, one of these 6 dominant land cover types was set as the only land cover for the entire U.S. Great Plains. All the experiments, except the one driven by wooded grassland (0.023 year^{-1}), show a drying trend (Figure 3.10). Over bare ground, the most significant drying trend (-0.0168 year^{-1}) occurs because bare ground has a direct impact on water and energy exchanges. For example, bare ground does not redistribute precipitation and solar radiation into two different layers in the 2S model (i.e., there is no canopy interception).

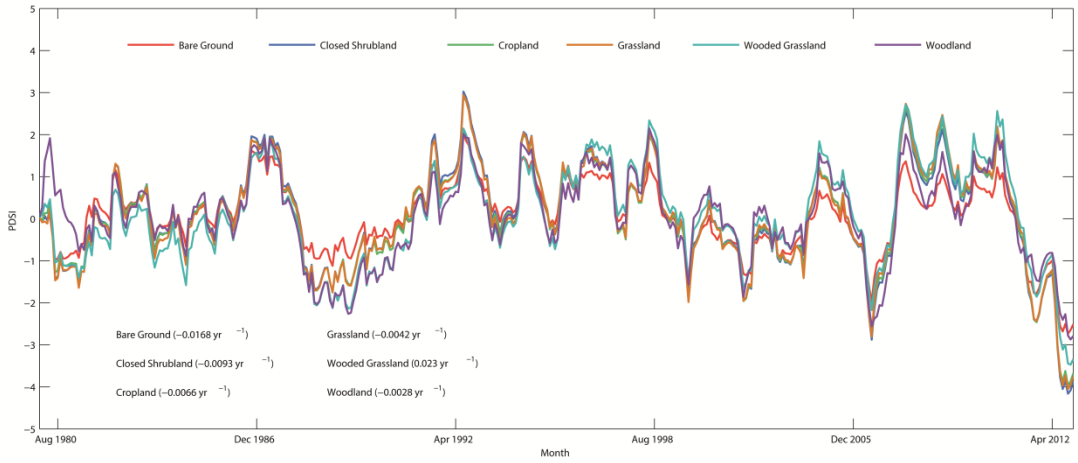

Figure 3. 10. Time series of area-averaged monthly 2S-based PDSI driven by six land cover types: bare ground (red), cropland (green), wooded grassland (azure blue), closed shrubland (Prussian blue), grassland (yellow), and woodland (purple) over the U.S. Great Plains from 1980 to 2012.

The spatial patterns of PDSI trends (Table 3.2) are similar over grassland (Figure 3.11 left), cropland (not shown) and closed shrubland (not shown). Wooded grassland (Figure 3.11 middle) and woodland (not shown) also have similar spatial patterns of PDSI trends. However, wooded grassland has more areas with statistically significant wetter trends (17.2%) as compared with grassland (10.3%). Over bare ground (Figure 3.11 right) there is less spatial coherence in the location of the regions with statistically significant trends. It appears that the PET models are most sensitive to bare ground. Previous studies have showed that PET is strongly influenced by LAI (Zhou et al., 2006;Yuan et al., 2008). As a result of the differences in seasonal patterns of LAI for different land covers and how this corresponds to trends in climate conditions (e.g., monthly temperature and precipitation), this can influence the monthly PDSI and impact the PDSI trends.

Table 3. 2. Fraction of area with drying/wetting trend covered by different land covers

	Drying	**Significant Drying**	**Wetting**	**Significant Wetting**
Grassland	55.70%	7.90%	44.30%	4.60%
Cropland	56.50%	7.90%	43.50%	4.50%
Closed Shrubland	58.80%	9.00%	41.20%	4.60%
Wooded Grassland	34.70%	1.50%	65.30%	17.20%
Woodland	35.80%	2.70%	64.20%	10.30%
Bare Ground	61.50%	14.10%	38.50%	5.70%

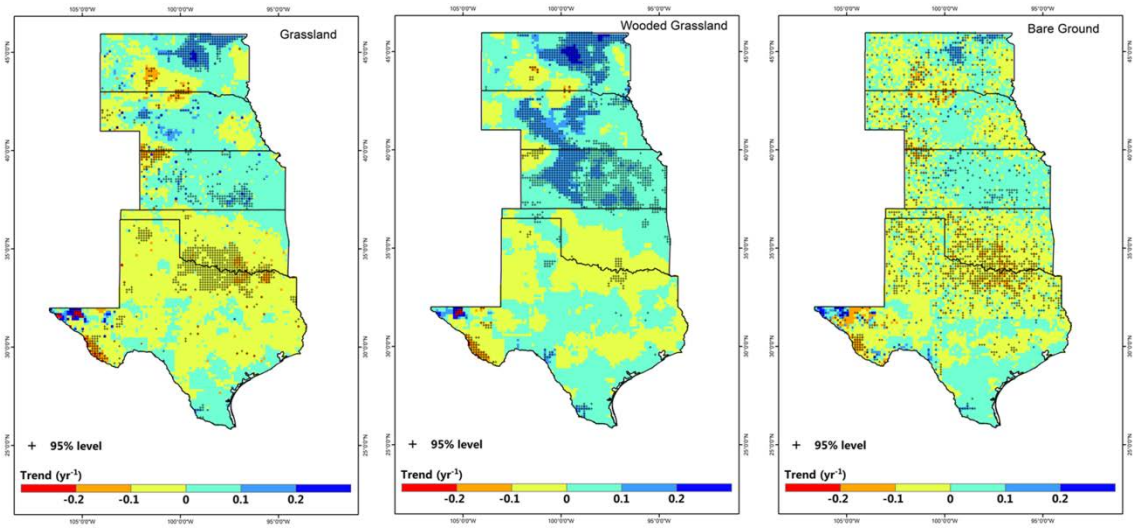

Figure 3. 11. Spatial pattern of trends of the 2S-based PDSI driven by (left) grassland, (middle) wooded grassland, and (right) bare ground over the U.S. Great Plains.

3.3.3 Comparison with Observed Soil Moisture

The three PDSI methods were evaluated using observed soil moisture data. Monthly Z-index values were correlated with observed monthly soil moisture (top 1 m of the soil) at 142 stations in South Dakota, Nebraska, Kansas, Oklahoma and Texas. The May to October PDSI and monthly soil moisture anomalies were compared at each location and the correlation coefficients are shown in Table 3.3. All three versions of the PDSI have moderately strong correlations (~0.5) with soil moisture in South Dakota, Nebraska, Kansas and Oklahoma. In Texas, correlations are lower (~0.3). Theoretically, the 2S-based PET model is the most physically-based. However, according to the correlation analysis, the performance of the 2S-based PDSI is significantly better than

the TH-based PDSI, but it is not significantly better than the PM-based PDSI, especially in Nebraska, Oklahoma and Texas.

Table 3. 3. Correlation analyses (r) of PDSI Z-Index and observed soil moisture

r	South Dakota	Nebraska	Kansas	Oklahoma	Texas
TH-based	0.50 (3/9)	0.40 (6/40)	0.43 (1/8)	0.41 (4/47)	0.29 (15/38)
PM-based	0.50 (2/9)	0.50 (1/40)	0.48 (1/8)	0.51 (3/47)	0.33 (12/38)
2S-based	0.50 (2/9)	0.53 (2/40)	0.48 (1/8)	0.52 (2/47)	0.39 (5/38)

() means number of stations with statistically significant correlations/total number of stations

3.3.4 Evaluation of Drought Severity

As discussed above, all three versions of the PDSI show that there is an overall tendency towards drier conditions in the U.S. Great Plains between 1980 and 2012. The use of different methods for estimating PET leads to the slight differences in the magnitude of the drying trends. The TH-based PDSI has the strongest trend and the PM-based PDSI has the weakest trend. The percentage of the U.S. Great Plains area under drought conditions (PDSI < -3.0) is shown in Figure 3.12. There has been a notable increase in the area under drought since 2000. Before 2000, the largest percentage of dry area was less than 40%, after 2000, both the frequency and the coverage of droughts over the U.S. Great Plains increase dramatically. Although there are only small

differences between the 3 methods in the overall drought trends for the U.S. Great Plains, there are larger differences when comparing the area under drought. These differences are especially notable during severe drought events. The TH-based PDSI indicates a greater area under drought conditions than the other two approaches. The differences between the three are especially pronounced in 2006, 2011 and 2012. In 2006 and 2011, the area under drought as estimated by the TH-based PDSI is twice as large as the area estimated by the PM-based PDSI. In 2012, the differences among the three versions of PDSI exceed 15% of the area of the U.S. Great Plains. Extreme droughts in the U.S. Great Plains are always associated with extreme high temperature. Therefore, the TH-based PDSI estimates the particularly large drought area. PET from soil is more sensitive to temperature than from canopy, the 2S-based PDSI estimates larger drought area than the PM-based PDSI.

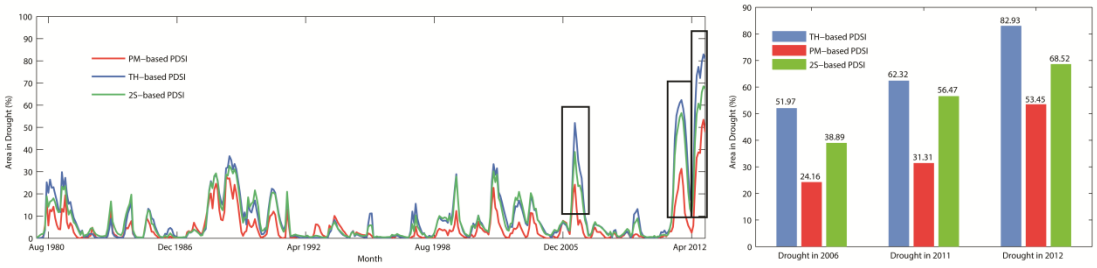

Figure 3. 12. Time series of the percentage of area in drought (left) estimated by the TH (blue), the PM (red), and the 2S (green) from 1980 to 2012. Area in droughts in 2006, 2011, and 2012 (right) estimated by the TH (blue), the PM (red), and the 2S (green).

3.3.5 Comparison with Previous Studies

Previous research conducted by Dai (Dai et al., 2004;Dai, 2011b) used a global PDSI dataset to evaluate drought trends. We compared our PDSI analysis with Dai's results (Dai, 2011b, a) and found that our results are consistent with the temporal patterns shown in Dai (2011b) (Figure 3.13). However, Dai's PDSI is more variable than ours. That is, Dai's PDSI shows higher values during wet periods and lower values during dry periods. This is likely due to the differences in the length of record and CAFEC coefficients. Both Dai's TH-based PDSI and PM-based PDSI have statistically significant ($P < 0.05$) decreasing trends. Although Dai's TH-based PDSI is only available till 2005, and therefore does not include the droughts in 2006, 2011 and 2012, their drying trend (-0.0351 $year^{-1}$) is larger than the trend in our TH-based PDSI (-0.0226 $year^{-1}$). Dai's PM-based PDSI (-0.0192 $year^{-1}$) also shows a stronger drying trend than both our PM-based PDSI (-0.0011 $year^{-1}$, not significant) and 2S-based PDSI (-0.0083 $year^{-1}$, $P < 0.05$). These differences are likely because Dai's used different climatic forcing data (Sheffield et al., 2012), a longer period for calculating climatological normals and a different PDSI parameterization. Hence, our results generally agree with Dai's and show that there is a drying trend in the U.S. Great Plains.

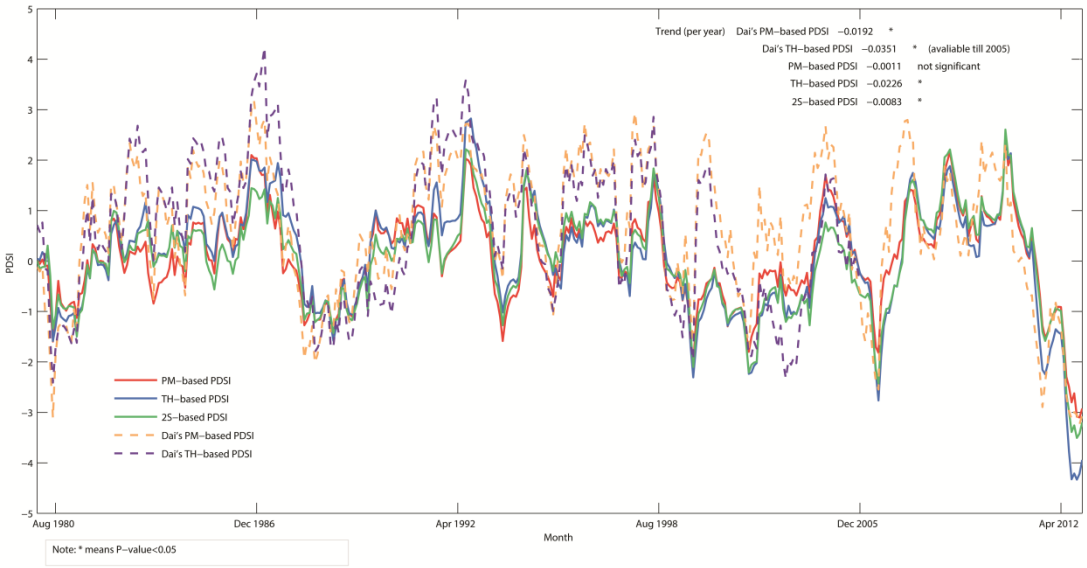

Figure 3. 13. Similar with Figure 3. 5. Added Dai's TH-based PDSI (yellow dashed line) from 1980 to 2005 and Dai's PM-based PDSI (purple dashed line) from 1980 to 2012.

3.4 Discussion and Conclusions

This chapter evaluated the sensitivity of the PDSI using three different methods for estimating PET. Our results demonstrated that there are large differences in mean annual PET over the U.S. Great Plains. The differences are reflected in both annual PET values and long-term (33 years) trends. The temperature-based TH may not be the best approach to estimate PET because it is overly dependent on temperature. Previous studies have shown that temperature is not the only factor that influences PET (or even the most important factor). For example, solar radiation (Roderick and Farquhar, 2002), wind speed (McVicar et al., 2012) and water vapor pressure deficit (Wang et al., 2012) have been shown to influence PET more than temperature. The TH approach does not

account for these factors. In addition, the empirical function used in the TH equation may not reflect the true nature of the relationship between temperature and PET. Wang et al. (2012) found that the trend in PET is not consistent with the increasing trends in temperature (Trenberth, 1990;Kutepov et al., 2006;Hao and AghaKouchak, 2013). More physically-based approaches such as the PM and the 2S address some of the shortcomings in the TH. Both of these methods estimate higher PET values, less interannual variability in PET and less pronounced drying trends. The PM treats the vegetation canopy as a "big leaf", but ignores the bare soil evaporation. The 2S-based PET includes bare soil evaporation and has a higher mean annual PET than the PM. Due to the sensitivity of TH to temperature, the intra-annual variations in the TH-based PET are greater than the other two methods.

Seasonal patterns of PET values indicate that canopy transpiration dominates the intra-annual variations in PET. Seasonal variations in transpiration are strongly controlled by the canopy growth stages, as well as incoming shortwave radiation (Mo et al., 2004). Over the U.S. Great Plains, there is substantial variation in vegetation types (Figure 3.9). Based on the monthly LAI, 92% of the U.S. Great Plains region has maximum LAI in July. In winter, soil evaporation plays a critical role in total PET.

The PDSI is not very sensitive to differences among the PET values estimated by TH, PM and 2S. Moisture supply (precipitation) is the single most important factor that influences the PDSI in the U.S. Great Plains. Water supply, rather than energy supply plays the most critical role in producing AET. Hence, although replacing the TH with the PM or the 2S can provide better estimates of PET, there is limited impact and benefit

if these PET values are being used to calculate the PDSI. Correlation between the three versions of PDSI and observed top 1-m soil moisture also demonstrated that PDSI values are relatively insensitive to PET because the correlations for all 3 methods were very similar.

IPCC AR5 (Hartmann et al., 2013) indicates that there is disagreement among global drought assessments after mid-1980s (Dai, 2011b;van der Schrier et al., 2013;Sheffield et al., 2012). There are a number of reasons for these discrepancies. One reason is that a number of these studies have been based on using a version of the PDSI that relies on TH-based PET. Since the TH is overly dependent on the temperature, the TH-based PET has a significant drying trend which corresponds to the significant positive trend of temperature. Another reason for the discrepancies is the use of different calibration periods. The calibration period for Dai (2011b) was 1950 – 1979, while Sheffield et al. (2012) and van der Schrier et al. (2013) used 1950 – 2008 as their calibration period. This resulted in a drier PDSI from 1980 onwards. A third reason for disagreement among global drought assessments is the use of different forcing data. For example, Sheffield et al. (2012) used CRU TS 3.0 precipitation data, while Dai (2011b) used the GPCP product from 1979 to 2008 and CPC-Chen before 1979. The CRU precipitation product is wetter than others (Hartmann et al., 2013), and this contributes to a reduction in drought severity.

This chapter addresses how using different versions of the PDSI can influence drought trends. Our results show some evidence that the U.S. Great Plains has experienced a drying trend between 1980 and 2012. However, the more physically-based

approaches (the PM and the 2S) show a weaker drying trend than the temperature-based approach (the TH). Though the reported trend in this study ends in 2012 (a year with extreme drought), our sensitivity analysis (not shown) shows that this does not unduly bias the slope of the trend line. We selected 5 different PDSI values for 2013 (PDSI = 0, -1, -2, -3 and -4), ranging from normal to extreme drought. If moisture conditions had been near-normal in 2013, this would slightly reduce the reported drying trend. Drought conditions in 2013 were present throughout much of the study region and therefore the trends reported in this study are considered to be robust.

Sheffield et al. (2012) suggest that the TH overestimates the drying trend because the temperature-based PET model cannot capture the influence of radiation, wind speed, humidity and vapor pressure deficit (Roderick et al., 2007). The 2S accounts for some of these factors and it simulates the soil surface as independent source. The surface resistance of soil is more sensitive to the environment than the canopy resistance (Stannard, 1993). Therefore, distinguishing bare soil evaporation from total PET is important and produces a stronger drying trend than using the PM.

Previous studies show increasing trends in global drought (Dai, 2012;Sheffield et al., 2012). However, the IPCC AR5 (Hartmann et al., 2013) concluded, with a high degree of confidence, that the frequency and intensity of drought in central North American has decreased since the 1950s. Our results show similar trend in South Dakota, Nebraska and Kansas. Damberg and AghaKouchak (2014) also highlighted southwest United States and Texas experience a significant drying trend. Our study is generally consistent with this study. The spatial patterns of drying and wetting in the U.S. Great

Plains are fairly consistent between the three versions of PDSI. Large parts of South Dakota, Nebraska and Kansas show wetting trends in all three versions of the PDSI. In Oklahoma and Texas, there is a mixture of drying and wetting trends. There are some differences in the trends between the three methods and the locations of these differences are coincident with differences in land. It is unclear how significant the causal link with land cover is, but land cover has been confirmed as a factor that influences PDSI calculation. This highlights the need for future work to investigate the relationships between land cover and drought trends.

In summary, this study confirms that PDSI is relatively insensitive to the PET methods used (Dai, 2011b;van der Schrier et al., 2011;Sheffield et al., 2012;Guttman, 1991). However, the use of different PET methods can influence the spatial and temporal patterns of drought and can be important for determining drought severity during major drought events (e.g., 2012 central Great Plains drought).

CHAPTER IV

COMPARISON OF THREE METHODS OF INTERPOLATING SOIL MOISTURE IN OKLAHOMA*

4.1 Introduction

Soil moisture plays a critical role in hydrology, agriculture, ecology and climate. Spatial variability of soil moisture impacts runoff response to precipitation (Berg and Mulroy, 2006), drought (Houborg et al., 2012), land-atmosphere interactions (Seneviratne et al., 2010), and the carbon cycle (Falloon et al., 2011). Therefore, spatially continuous soil moisture surfaces are useful for many applications. However, in situ soil moisture measurements are typically not dense enough to capture the spatial variability of soil moisture at the regional scale (10^4 to 10^7 km^2) (Robock et al., 2000). Alternatively, satellite remote-sensing, such as the Soil Moisture and Ocean Salinity (SMOS) mission (Kerr et al., 2001), NASA's Aquarius (Le Vine et al., 2007) and Soil Moisture Active-Passive (SMAP) missions (Brown et al., 2013), can provide spatially continuous soil moisture estimates. Of course, the satellite-based approaches also have limitations; they typically only measure water in the top few centimeters of the soil (Crow et al., 2012) and the spatial resolution is relatively coarse (Vereecken et al., 2007). Collow et al. (2012) evaluated the accuracy of SMOS-derived soil moisture with in situ

* This chapter is reprinted with permission from "Comparison of three methods of interpolating soil moisture in Oklahoma" by Shanshui Yuan and Steven Quiring, 2016. International Journal of Climatology (in press), doi: 10.1002/joc.4754, Copyright 2016 by John Wiley and Sons.

measurements in the United States Great Plains. They concluded that the lack of uniform soil moisture measurements makes evaluating SMOS difficult and therefore additional stations are needed to provide a more robust evaluation of satellite-derived soil moisture. There are significant scaling issues involved in comparing in situ soil moisture measurements (a point) to satellite-derived soil moisture (50 km pixel) and most in situ networks are not sufficiently dense to adequately resolve soil moisture variability within each satellite pixel. Model simulation is another method of estimating spatially continuous soil moisture. Pellenq et al. (2003) coupled a simple Soil Vegetation Atmosphere Transfer model with TOPMODEL and estimated soil moisture in the Williams River catchment, Australia. Meng and Quiring (2008) evaluated the accuracy of soil moisture simulations from the Variable Infiltration Capacity (VIC), Decision Support System for Agrotechnology Transfer (DSSAT), and Climatic Water Budget (CWB) models using Soil Climate Analysis Network data. Though numerical models are commonly applied for soil moisture-related research (Baudena et al., 2008;Koster et al., 2004;Zehe and Blöschl, 2004), the reliability of model-simulated soil moisture varies significantly over time and space, as well as from model to model. Xia et al. (2015b) evaluated the accuracy of the soil moisture simulations from the four land surface models of the North-American Land Data Assimilation System Project Phase 2 (NLDAS-2) using in situ data from hundreds of sites in Alabama, Colorado, Michigan, Nebraska, Oklahoma, West Texas and Utah. They demonstrated that the four NLDAS-2 models were able to accurately capture seasonal variations in soil moisture variations in all three soil layers in most states. However, there were some systematic biases in the

simulated soil moisture values. Noah and VIC were systematically wetter than the observations, while Mosaic and SAC were systematically drier than the observations. Xia et al. (2015b) concluded that this may be due to errors in model-simulated evapotranspiration. Generally, evaluations of model-simulated soil moisture demonstrate that the models can accurately simulate variations in soil moisture, but have difficulty getting the absolute magnitude correct (Downer and Ogden, 2003;Meng and Quiring, 2008). Given the limitations of both model-derived and satellite-derived soil moisture, it is useful to generate gridded soil moisture from in situ observations. There are a large number of activities that are reliant on gridded soil moisture data, these include: operational drought monitoring (Lawrimore et al., 2002), calibrating/validating satellites and land surface models (Robock et al., 2003;Xia et al., 2015b;Dirmeyer et al., 2016;Ford et al., 2014) and documenting how soil moisture influences the climate system on seasonal to interannual time scales (Khong et al., 2015;Ford and Quiring, 2014a;Ford et al., 2015a).

Spatial interpolation of in situ soil moisture is challenging because there are many factors that influence how soil moisture varies at regional scales including soil properties, topography, vegetation/land cover/land use and climate (Crow et al., 2012). Heterogeneity of soil properties influences all components of soil water balance and therefore has a direct impact on soil moisture. Rodriguez-Iturbe et al. (1995) found soil properties affect soil moisture distribution because of their influence on infiltration. Famiglietti et al. (1998) and Vereecken et al. (2007) concluded that soil hydraulic conductivities and porosity jointly influence the variability in surface soil moisture.

Routing processes that are affected by topography also influence near-surface soil moisture. Numerous studies have demonstrated that soil moisture is generally lower at locations that are further upslope (Champagne et al., 2010;de Rosnay et al., 2009;Mohanty et al., 2000b). Land cover also plays an important role in determining soil moisture through modifying infiltration and evapotranspiration. Mohanty et al. (2000a) found that vegetation dynamics had a significant impact on intra-seasonal spatial patterns of soil moisture, which is consistent with other studies (Jacobs et al., 2004;Vinnikov et al., 1996). Isham et al. (2005) used a stochastic rainfall model and to demonstrate that the spatial variability of soil moisture is not only controlled by the spatial variability of vegetation, but also by rainfall. Precipitation is the dominant meteorological control of soil moisture (Seneviratne et al., 2010). The relative impact that these factors have on soil moisture varies depending on the spatial scale of analysis. Vinnikov et al. (1999) demonstrated the spatial variability of soil moisture includes two components: large-scale atmospheric forcing and small-scale land surface variability and hydrologic processes. Vinnikov et al. (1999) applied the optimal averaging technique to soil moisture observations. They evaluated the dependence of errors in interpolated soil moisture using this method as a function of station density and grid cell sizes (30 km to 400 km). They found that the errors associated with spatial averaging decrease with an increase in the size of the grid cell or station density. Therefore, accurately interpolating soil moisture observations is a challenging task because of all the factors that influence it and the most appropriate solution will vary depending on the spatial scale of interest.

Previous studies have used a variety of approaches at the field and catchment scales to interpolate soil moisture and to investigate the spatial variability of soil moisture. Perry and Niemann (2008) used inverse distance weighting (IDW) to interpolate soil moisture in the Tarrawarra catchment, Australia. Using this approach they obtained a Nash-Sutcliffe efficiency coefficient of ~0.4. Multiple versions of kriging have also been applied to interpolate soil moisture (Bárdossy and Lehmann, 1998;Baskan et al., 2009). These studies demonstrate that kriging is an accurate interpolation method, but cannot yield physically feasible spatial distribution of soil moisture because it lacks additional physical information such as topography and land cover. Yao et al. (2013) compared four interpolation approaches: ordinary kriging, IDW, linear regression model and hybrid regression kriging in a 2 km^2 catchment in China. They found that distance-based interpolation methods, such as IDW, do not perform well in areas with complex terrain. These studies show that most of the methods used for interpolating soil moisture are not very accurate. It is useful to test other interpolation methods and identify the most appropriate method for accurately interpolating in situ soil moisture measurements.

In this chapter, we evaluate the accuracy of generating soil moisture surfaces. We evaluate three interpolation methods: ROI, ordinary Cokriging (hereafter referred to simply as Cokriging) and IDW. We also evaluate the utility of model-simulated soil moisture. The accuracy of these approaches is evaluated using in situ soil moisture data from 65 stations in Oklahoma.

4.2 Data and Methods

We evaluate three interpolation methods in this study: ROI, Cokriging and IDW. The ROI and Cokriging methods both utilize in situ and model-simulated soil moisture to develop soil moisture surfaces. Model-simulated soil moisture is used to capture the spatial variations/patterns in soil moisture since the model explicitly accounts for variations in land cover, soil type, elevation, and meteorological forcings. IDW is based solely on the in situ observations. It is included in the comparison because it is frequently used for interpolation and it is the simplest and least computationally expensive interpolation method. IDW provides a baseline (low skill method) that is used to show the relative value of employing a more sophisticated approach. These 3 methods are used to interpolate monthly soil moisture to a 0.5 degree grid over Oklahoma. The interpolated surfaces are evaluated using an independent set of in situ measurements.

4.2.1 In Situ Soil Moisture

Daily in situ soil moisture in Oklahoma from 2000 to 2012 were obtained from TAMU North American Soil Moisture Database (soilmoisture.tamu.edu). The North American Soil Moisture Database archives data from a variety of national and state networks, including the Oklahoma Mesonet (Quiring et al., 2015). Data from 65 Oklahoma Mesonet stations are used in this study (Figure 4. 1). In situ soil moisture is measured at four depths (5 cm, 25 cm, 60 cm and 75 cm). We selected these 65 Oklahoma Mesonet stations based on their spatial distribution and amount of missing data. They cover a diverse range of soil and climate regions in Oklahoma. These stations

have a relatively complete time series (> 70% complete) for at least 3 of the measurement depths. The 26 stations (circle) with less than 10% missing data are used for interpolation, while the other 39 stations (triangle) are used for validation (Figure 4. 1). The Daily Average Replacement (DAR) method (Ford and Quiring, 2014a) is used to infill missing data from the 26 stations that are used for interpolation because the ROI method requires temporally continuous data. Soil moisture measurements at different depths are converted to Volumetric Water Content (VWC) in the top 1 m of the soil column. This depth (1 m) is assumed to be greater than the maximum root zone depth in Oklahoma. Therefore, we chose to evaluate the accuracy of the soil moisture interpolations based on the top 1 m. VWC at each depth is assumed to represent average VWC in the corresponding soil layer. For example, the VWC measured at 5 cm is assumed to be the average VWC in 0 – 10 cm soil layer. Then water content in each soil layer is calculated by multiplying VWC with depth of soil layer. The water content in each specific layer is accumulated and finally divided by the soil depth (1 m). Daily soil moisture is then averaged to generate a monthly value and it is used for the comparison of interpolation methods. We chose to focus on the monthly timescale because monthly soil moisture have been previously used in studies investigating climate variability (Huang et al., 1996;Luo et al., 2014), evaluating drought events (Hogg et al., 2013;Dai et al., 2004), and monitoring land surface (Sabater et al., 2008;Biggs et al., 2008) and ecosystem processes (Krishnan et al., 2006). Since the spatial variability of soil moisture is typically greater at daily timescales, we acknowledge that repeating this analysis using daily data may result in larger cross-validation errors for all interpolation methods.

However, the purpose of this paper is to compare the relative accuracy of the interpolation methods. We believe that the results of our analysis are robust and are not dependent on the timescale.

4.2.2 Model-simulated Soil Moisture

This study uses simulated soil moisture from the VIC model (Liang et al., 1994), as provided by the University of Washington Surface Water Monitor (Wang et al., 2009). VIC is forced with observed meteorological data, and it accounts for spatial variations in soil and vegetation. In this study we use the daily soil moisture percentiles for total soil column and these values are averaged to produce a monthly value. VIC output is available at 0.5 degree spatial resolution. Although this is relatively coarse, it is suitable for regional soil moisture studies (Fan and van den Dool, 2004;Hollinger and Isard, 1994). This study will identify the optimum interpolation method for representing regional variations in soil moisture. We acknowledge that the optimum interpolation method may be a function of the spatial scale of analysis, as well as other factors (e.g., topographic complexity), and therefore our results may not be transferable to field-scale soil moisture interpolation. The depth of the soil column that is used in VIC varies from 0.7 m to 1.1 m in Oklahoma, as shown in Figure 4.1. This does not have a significant influence on the results of this study because the soil water content is generally quite stable at 0.7 m to 1.1 m (Wu et al., 2002).

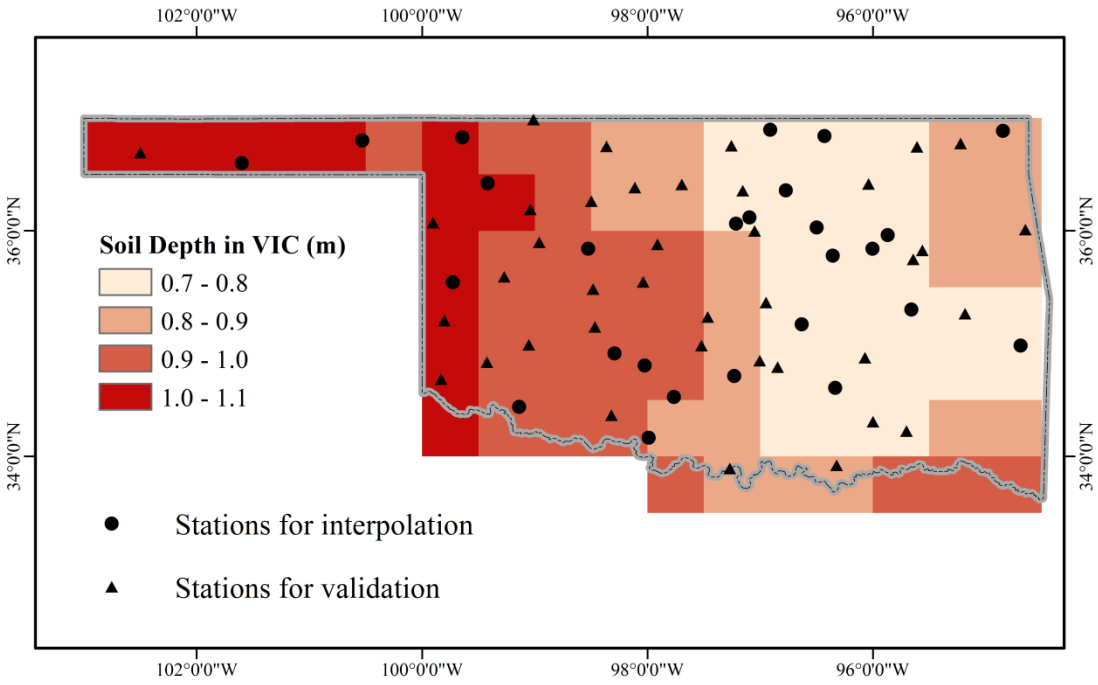

Figure 4. 1. Spatial distribution of in situ stations used in this study, including the stations used for interpolation (circle), the stations used for validation (triangle) and the soil depths in the VIC model.

4.2.3 Reduced Optimal Interpolation, Cokriging and Inverse Distance Weighting

The ROI method was first introduced for constructing gridded sea surface temperature (Kaplan et al., 1998) and sea level pressure fields (Kaplan et al., 2000). As far as we are aware, this is the first time that the ROI method has been applied to soil moisture.

ROI method involves two steps: (1) Empirical Orthogonal Function (EOF) decomposition and (2) estimation of new amplitudes. In the first step, EOF analysis (Preisendorfer and Mobley, 1988) is used to decompose the VIC simulated soil moisture into spatial modes and their related temporal amplitudes as defined in eq. 4.1:

$$\mathbf{SM_M}(x,y,t) = \mathbf{H_M}(x,y)\boldsymbol{\alpha}_\mathbf{M}(t) \tag{4.1}$$

where $\mathbf{SM_M}(x,y,t)$ is a matrix of tempo-spatial signals of soil moisture simulated by the VIC model (each row is a particular grid cell, each column is each month), $\mathbf{H_M}(x,y)$ are the spatial modes and $\boldsymbol{\alpha}_\mathbf{M}(t)$ are the amplitudes over the time period. The EOF n which equals n-th column of $\mathbf{H_M}(x,y)$ multiplied the n-th row of $\boldsymbol{\alpha}_\mathbf{M}(t)$ is a spatial-temporal pattern of soil moisture variability that can explain the percentage of total variance of soil moisture. The smaller n is, the larger percentage can be explained by spatial scale signals and less influenced by noise. In this study, we applied North's rule (North, 1984) to determine the number of EOFs to retain. Therefore, the first 5 EOFs (which account for 96% of the soil moisture variance) were retained for the soil moisture interpolation. We approximate the Oklahoma soil moisture field $\mathbf{SM_R}$ by multiplying the model projected 5-dimentional space of leading EOFs with the in situ optimal estimate of the 5-dimentional vector of temporal amplitudes (eq. 4.2).

$$\mathbf{SM_R}(x,y,t) = \mathbf{H_M}(x,y)\boldsymbol{\alpha}_\mathbf{R}(t) \tag{4.2}$$

The second step is to estimate $\boldsymbol{\alpha}_\mathbf{R}(t)$. The ROI gives the solution for $\boldsymbol{\alpha}_\mathbf{R}(t)$ by minimizing the cost function (eq. 4.3)

$$\mathbf{S}(\alpha_R) = \left(\mathbf{NH_M}\boldsymbol{\alpha}_\mathbf{R} - \mathbf{SM_{In}}^{\mathbf{0}}\right)^T \mathbf{R}^{-1}\left(\mathbf{NH_M}\boldsymbol{\alpha}_\mathbf{R} - \mathbf{SM_{In}}^{\mathbf{0}}\right) + \boldsymbol{\alpha}_\mathbf{R}{}^T \boldsymbol{\Lambda}^{-1}\boldsymbol{\alpha}_\mathbf{R} \quad (4.3)$$

where $\mathbf{N}$ is a projection matrix to transfer the full grid representation of soil moisture field $\mathbf{SM_{In}}$ to the available in situ observations $\mathbf{SM_{In}}^{\mathbf{0}}$. Each element of $\mathbf{N}$ is equal to 1 when and where in situ data are available and 0 otherwise. $\mathbf{R}$ is the error covariance matrix accounting for the observational error (instrument error and sampling error) and representational error (the error due to the truncation of the full set of EOFs to only the first 5 EOFs). $\boldsymbol{\Lambda}$ is a diagonal matrix of the 5 largest eigenvalues of the covariance matrix. A least squares method is applied to find the Optimal Interpolation solutions by minimizing the $\mathbf{S}$ in eq. 4.4 and eq. 4.5:

$$\boldsymbol{\alpha}_\mathbf{R} = \mathbf{k}\mathbf{H_M}{}^T \mathbf{N}^T \mathbf{R}^{-1}\mathbf{SM_{In}}^{\mathbf{0}} \quad (4.4)$$

where

$$\mathbf{k} = \left(\mathbf{H_M}{}^T \mathbf{N}^T \mathbf{R}^{-1}\mathbf{NH_M} + \boldsymbol{\Lambda}^{-1}\right)^{-1} \quad (4.5)$$

Finally, the interpolated soil moisture field over Oklahoma can be estimated by eq. 4.2.

In addition to interpolating soil moisture using the ROI method, we also use the same 26 stations to interpolate soil moisture using the Cokriging method (Isaaks and Srivastava, 1989) and IDW method (Shepard, 1968).

Cokriging utilizes the covariance between main data at the target location and more regionalized the secondary data. In order to keep the comparison fair, in this study, we use the same VIC simulated soil moisture data that are also used as secondary dataset in the ROI method.

$$Z(S_0) = \sum_{i=1}^{n} \lambda_i Z(S_i) + \sum_{i=1}^{n} \beta_i t(S_i) \tag{4.6}$$

Where, $Z(S_i)$ is the measured value at the i_{th} station; λ_i is the weight for the i_{th} station; $Z(S_0)$ is the interpolated value at the target location; n is the number of stations; $t(S_i)$ is the secondary value that is co-located with the $Z(S_i)$; β_i is weight for the $t(S_i)$.

IDW is a weighting algorithm, so the value at the target location is most strongly influenced by the nearest stations. IDW is calculated as follows:

$$Z(S_0) = \sum_{i=1}^{n} \lambda_i Z(S_i) \tag{4.7}$$

$$\lambda_i = \frac{d_i^{-p}}{\sum_{i=1}^{n} d_i^{-p}} \tag{4.8}$$

Where, $Z(S_i)$ is the measured value at the i_{th} station; λ_i is the weight for the i_{th} station; $Z(S_0)$ is the interpolated value at the target location, n is the number of stations, d_i is the distance from the i_{th} station to the target location; p is power parameter, equals to 2. The soil moisture in each grid cell was interpolated using all the 26 stations. The distance weighting was based on the distance from the centroid of the grid cell to each of the stations.

4.2.4 Evaluation of Interpolation Accuracy

The accuracy of the soil moisture surfaces generated using the ROI, Cokriging and IDW methods are evaluated using 39 stations that were not part of the interpolation. To evaluate the performance of these methods, we select the grid cells with stations in them and compare the mean soil moisture in these grid cells with the mean soil moisture from the 39 validation stations. Additionally, we also compare the ROI, Cokriging and IDW interpolations with observations at individual station by calculating the correlation coefficient (r), mean absolute error (MAE) and coefficient of efficiency (E) (Legates and McCabe, 1999). Although the point-versus-grid comparison may not be optimal because of the mismatch in spatial scale, it is a reasonable approach to use in this study since the purpose is to compare the relative performance of the ROI, Cokriging and IDW.

4.3 Results and Discussion

4.3.1 Evaluation of ROI Interpolated Soil Moisture

Figure 4.2a shows the time series of observed (purple), ROI interpolated (red), Cokriging interpolated (blue) and IDW interpolated (green) soil moisture. Based on the spatially averaged time series, all interpolation methods are highly correlated with the observed soil moisture and the correlations are statistically significant ($p < 0.05$). The correlation coefficient (r) for the ROI method is highest (0.92), followed by Cokriging (0.90) and IDW (0.82). The IDW-estimated soil moisture is systematically wetter than the observed soil moisture and it is more variable than ROI and Cokriging, as shown in Figure 4.2b. The plots also show a slight bias towards interpolated soil moisture which means soil moisture interpolated by the Cokriging method tends to be slightly wetter than in situ soil moisture. Overall, there is no systematic bias in the ROI interpolated soil moisture. However, both the ROI method and the Cokriging method overestimate the state-wide VWC in Oklahoma during the dry season. There are two possible reasons for this overestimate. First, VIC has been shown to have a systematic wet bias in summer in previous studies (Xia et al., 2015b). Wang et al. (2009) demonstrated that VIC simulates wetter soils in Oklahoma as compared with the Community Land Model (version 3.5) and Noah. Second, vegetation parameters in VIC are static and therefore the simulated soil moisture may not be representative during extremely dry periods (Ford and Quiring, 2013).

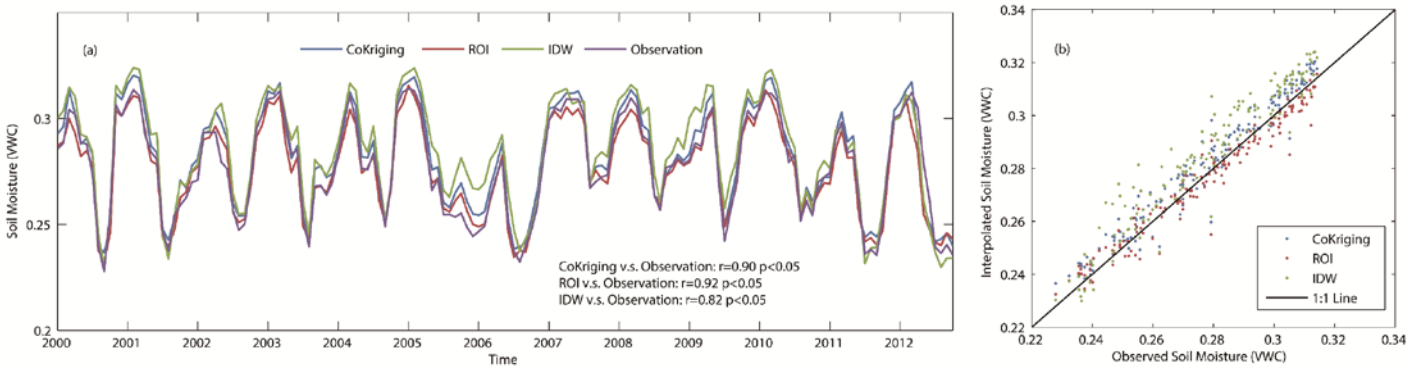

Figure 4. 2. (a) Time series of interpolated monthly soil moisture by ROI (red), IDW (green) and Cokriging (blue) and observed monthly soil moisture (purple). (b) Scatter plot of interpolated versus observed soil moisture.

The ROI method uses the first 5 EOFs of the model-simulated soil moisture to represent the spatial patterns of soil moisture. Using EOFs helps reduce the noise/variability in the station-based soil moisture measurements and therefore improves the interpolation accuracy over IDW which is based solely on station data. Because both ROI and Cokriging utilize model-simulated soil moisture from VIC, our results are somewhat model-dependent. A future study could examine how utilizing different models, such as the Community Land Model or Noah, might influence interpolation accuracy.

Figure 4.3 shows the spatial pattern of multi-year mean monthly soil moisture based on the ROI method. It shows the dry-to-wet moisture gradient from southwest to northeast in Oklahoma. The relatively dry location northwestern corner of the state, matches well with the observed soil moisture. The ROI method accounts for the impact that physical processes, via VIC model, and human factors, such as management and land cover, via the in situ observations, have on the soil moisture patterns. Therefore, theoretically, it should generate more accurate soil moisture interpolations. We quantify the accuracy of the ROI method and compare it with Cokriging and IDW in section 4.3.2.

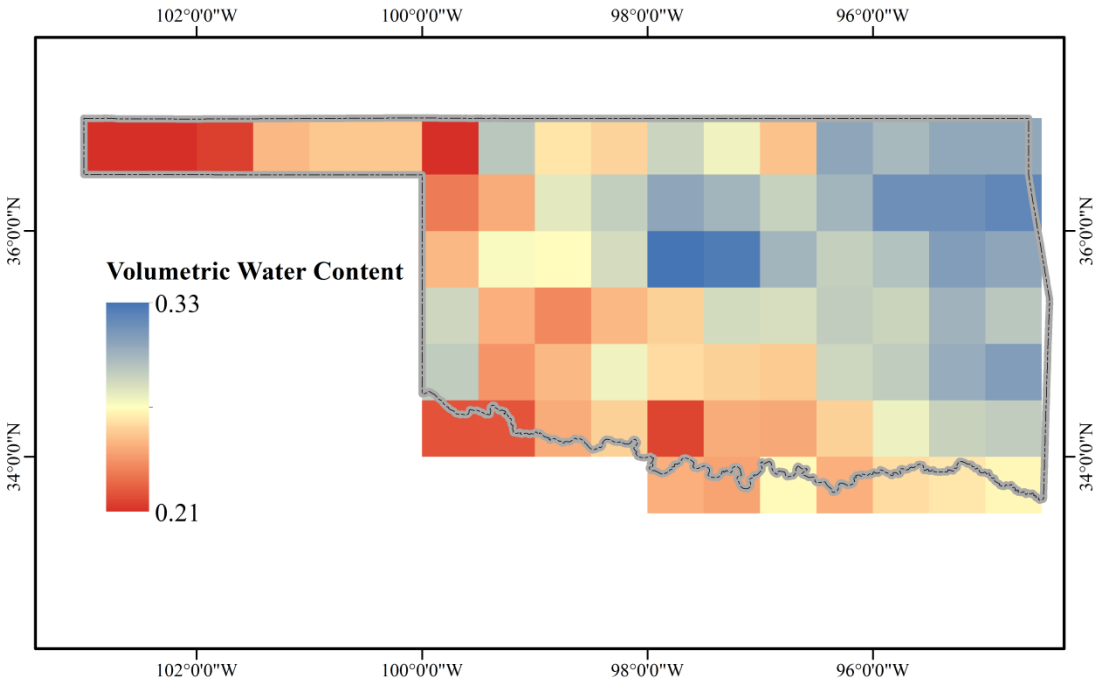

Figure 4. 3. Spatial pattern of multi-year (2000 – 2012) mean monthly soil moisture (VWC) based on the ROI method.

4.3.2 Comparison with IDW Interpolated Soil Moisture

Figure 4.4a, b and c shows the spatial distributions of correlations for the ROI, the Cokriging and the IDW, respectively. The correlation coefficient is calculated using the interpolated and observed time series in each grid cell. Correlation coefficients for the ROI method range from 0.73 to 0.94, they range from 0.63 to 0.94 for the Cokriging, and 0.61 to 0.93 for the IDW. In 39 of 48 grid cells, the ROI method has higher correlations with the observed soil moisture than Cokriging and in 45 of 48 grid cells the ROI method has higher correlations than IDW. The IDW method is quite sensitive to the spatial distribution of stations used in the interpolation. In the three grid cells where the

IDW has higher correlation, there are more stations available for interpolation (> 2) and this increases the accuracy.

To justify why it is necessary to develop interpolation method rather than directly utilizing the model-simulated soil moisture, we show the correlation map based on the VIC simulations in Figure 4.4d. It is interesting to note that, on its own, the VIC-simulated soil moisture is not strongly correlated with the observed soil moisture and at most locations all of the interpolation methods have higher correlations. When the VIC-simulated soil moisture is using as input to the ROI or Cokriging methods, the interpolated soil moisture is more accurate than using a method that solely relies on the observations (i.e., IDW) or model output (i.e., VIC). The low correlation between VIC and observations may also influence the performance of the Cokriging method because higher correlations between secondary and primary data tend to improve the accuracy of Cokriging (Isaaks and Srivastava, 1989).

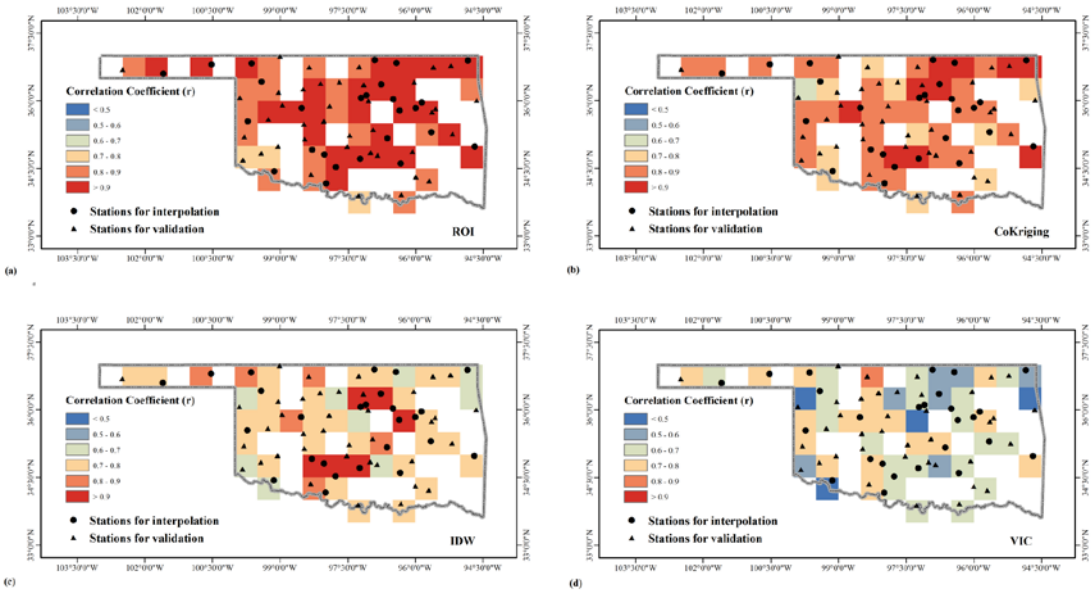

Figure 4. 4. Spatial pattern of correlations between the in situ soil moisture and interpolated/simulated soil moisture based on: (a) ROI, (b) Cokriging, (c) IDW, and (d) VIC.

The accuracy of the interpolation methods are also evaluated at the individual stations. The correlation coefficient (r), mean absolute error (MAE) and coefficient of efficiency (E) are calculated at the 39 stations that were not used in the interpolation. These three statistics show good agreement among the performance of the ROI, the Cokriging and the IDW methods. In terms of correlation, all methods are statistically significant ($p < 0.05$). The station-averaged correlation coefficient for ROI (0.89) is higher than that for Cokriging (0.83) and for IDW (0.78). Similarly, ROI has a higher mean E (0.58) and lower mean MAE (0.02) than Cokriging and IDW. This illustrates that the ROI method is able to accurately represent both the temporal variations in soil moisture and the absolute value. The performance of the Cokriging and the IDW

methods are more variable than ROI for all the three statistics (Figure 4.5). For the ROI method, 36 out of 39 stations have correlations > 0.8 as compared to 29 stations for the Cokriging and 7 for the IDW. The MAE for the ROI method is < 0.03 at all stations. 37 out of 39 stations have the MAE < 0.03 for the Cokriging method and only 14 out of 39 stations have the MAE < 0.03 for the IDW method. For the ROI method, all the stations have positive E, among which, 25 stations are > 0.5. 33 out of 39 stations have positive E and 11 stations are > 0.5 for the Cokriging method. Based on the IDW method, only 19 stations have positive E, and only 7 stations are > 0.5.

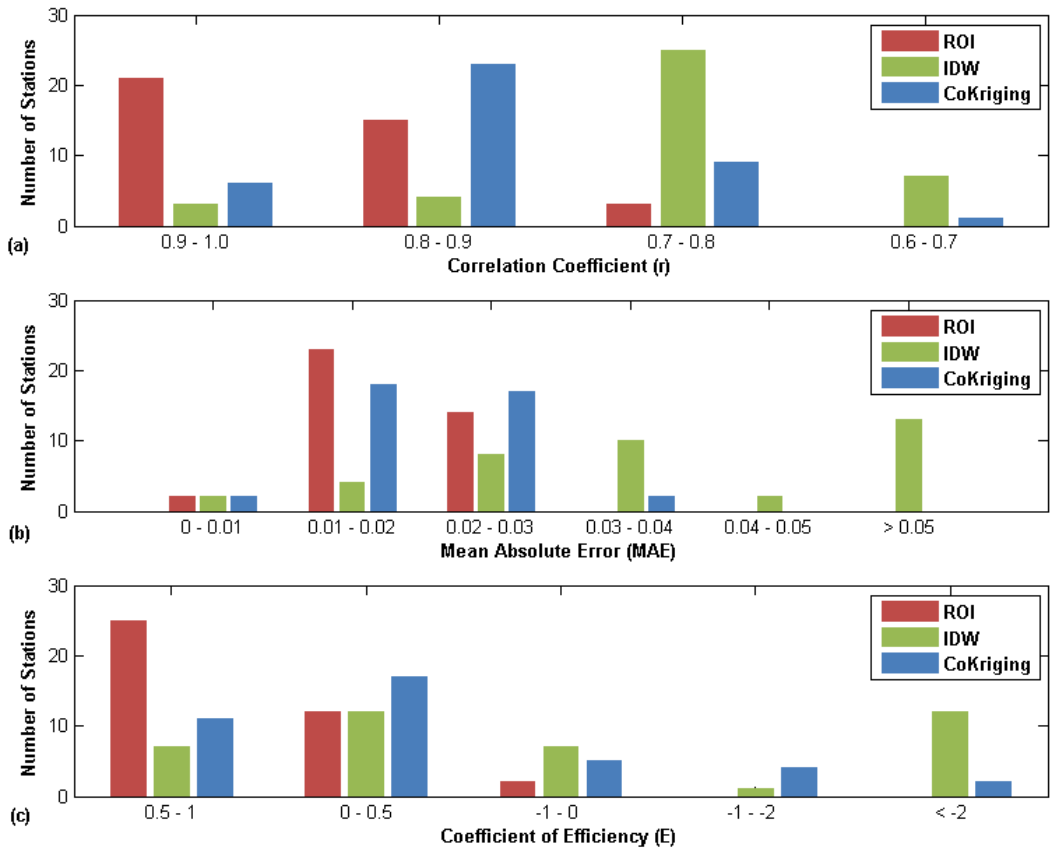

Figure 4. 5. Histograms of performance evaluation statistics (interpolated versus observed): (a) correlation coefficient, (b) mean absolute error, and (c) coefficient of efficiency for all 39 validation sites based on ROI (red), IDW (green) and Cokriging (blue) methods.

The IDW method performs better when there are more stations close to the target location. There is a direct relationship between the number of stations and the accuracy of this method and this relationship is quantified in Section 4.3.3. The ROI and Cokriging methods are less dependent on the number of stations, and the location of the stations used in the interpolation. Although the locations with the best accuracy tend to

be close to the stations used in the interpolation, ROI and Cokriging still perform well at locations that have few stations nearby.

The above analysis focused on the mean performance of each interpolation method over 2000 – 2012. However, it is also important to examine how well each interpolation method does during an extreme event. Therefore, we have chosen to examine the differences between the interpolated and observed soil moisture during a recent severe drought in Oklahoma. Figure 4.6 shows the spatial distribution of difference between interpolated and observed soil moisture under extremely dry conditions associated with the 2011 drought. The interpolation errors vary from +0.03 to -0.06 in August for the ROI method. In comparison the errors vary from +0.06 to -0.09 and +0.05 to -0.09 for the IDW and Cokriging methods, respectively. In September the interpolation errors vary from +0.06 to -0.06 for the ROI method, +0.08 to -0.1 for the IDW method, and +0.07 to -0.09 for the Cokriging methods. In October the interpolation errors vary from +0.07 to -0.06 for the ROI method, +0.08 to -0.11 for the IDW method, and +0.07 to -0.09 for the Cokriging methods. The overall mean error for the ROI method (across all 39 locations) is 0.0005, 0.0008 and 0.001 in August, September and October, respectively. In comparison, the overall mean error for the IDW method (across all 39 locations) is -0.01, -0.02 and -0.01 in August, September and October, respectively. Finally, the overall mean error for the Cokriging method (across all 39 locations) is 0.003, 0.007 and 0.008 in August, September and October, respectively. It appears that for this event, and the others that we analysed (results not shown), the ROI method consistently outperforms IDW and Cokriging, and that the IDW method has the

largest errors. Our results indicate that for this event, both ROI and Cokriging have a wet bias. This is likely because both of the utilize VIC-simulated soil moisture which also has a wet bias for the 2011 drought event. While these two methods do not show a wet or dry bias for the overall results, it is apparent that this may occur for some hydroclimatic events.

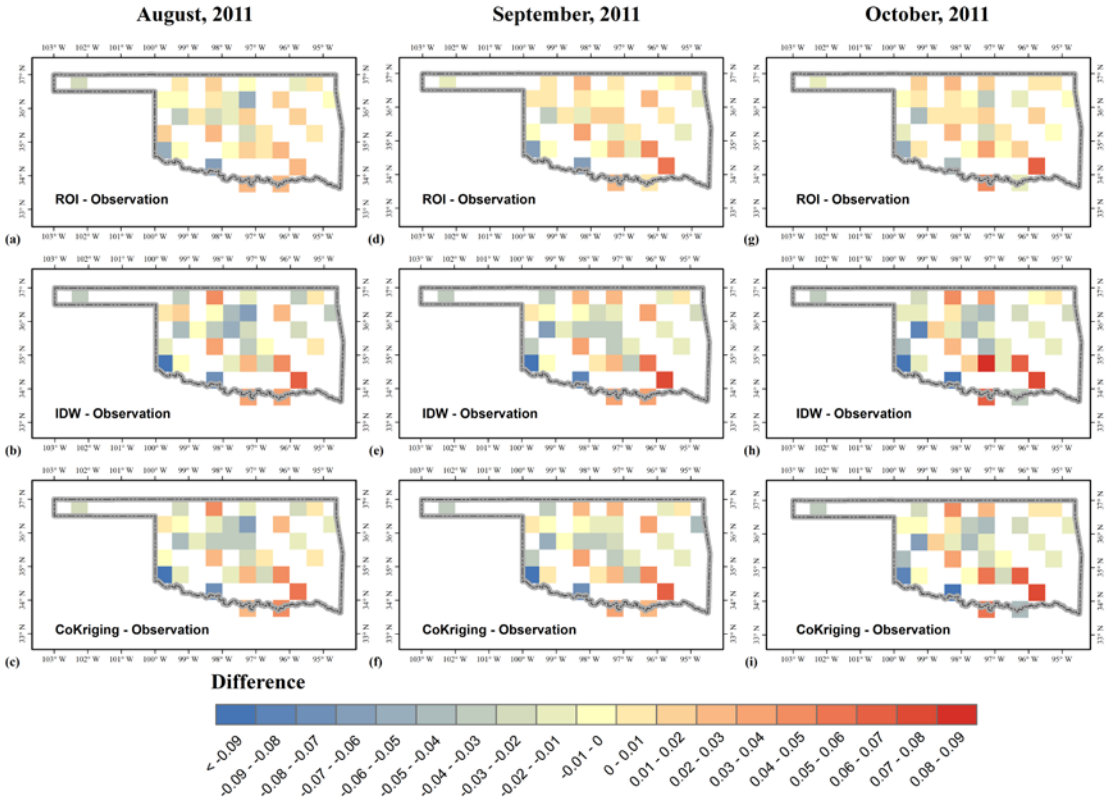

Figure 4. 6. Spatial distribution of differences between interpolated and observed soil moisture (August to October 2011). ROI minus observed soil moisture in August (a), September (d) and October (g). IDW minus observed soil moisture in August (b), September (e) and October (h). Cokriging minus observed soil moisture in August (c), September (f) and October (i).

4.3.3 Sensitivity to Station Density

To develop a better understanding of how the density of stations influences the accuracy of the interpolations, we performed a sensitivity experiment with the ROI, Cokriging and IDW methods. The number of stations that are used for interpolation was varied from 1 to 26. The n stations that are used in each ensemble are selected randomly (with replacement), and the selection process is repeated 1000 times for each ensemble. That is, we randomly select 1 station to use for the interpolation (from the 26 possibilities) and use that station to perform the interpolation. Then, another station is randomly selected and the process is repeated 1000 times. We calculate the correlation (r), mean absolute error (MAE) and coefficient of efficiency (E) for each replicate and then calculate the mean r, MAE and E for each ensemble.

Figure 4.7 shows how the distributions for each statistic vary based on the number of stations used in the interpolation. Although the performance of the ROI method improves at a similar rate as the IDW method, as the number of stations used in the interpolation increase, ROI consistently has higher correlations than IDW. The Cokriging method has consistently higher correlations than the IDW method, but slightly lower correlations than the ROI method. The performance of the Cokriging method improves more slowly as the number of stations used in the interpolation increases, relative to the other two methods. This means that in terms of correlation, both the ROI and IDW method have a similar sensitivity to the number of stations used in the interpolation. The Cokriging method is less sensitive to the number of stations used than the other two methods. The ROI method also has higher E and smaller MAE regardless

of the number of stations used in the interpolation. However, the changes in E and MAE as a function of the number of stations are quite different. Figure 4.7b and c, show that once the number of stations is greater than three, the slopes of E and MAE are quite flat for the ROI and Cokriging methods. This illustrates that these two methods are relatively insensitive to the number stations used for interpolation. Although using more stations does increase the interpolation accuracy (E) and reduce the interpolation error (MAE), the incremental improvements are relatively modest. In comparison, IDW has dramatic changes in both MAE and E when the number of stations is smaller than ten. This demonstrates that the IDW method is relatively sensitive to the number of stations that are used in the interpolation. IDW is not an appropriate method to use for interpolating soil moisture when there are a limited number of stations.

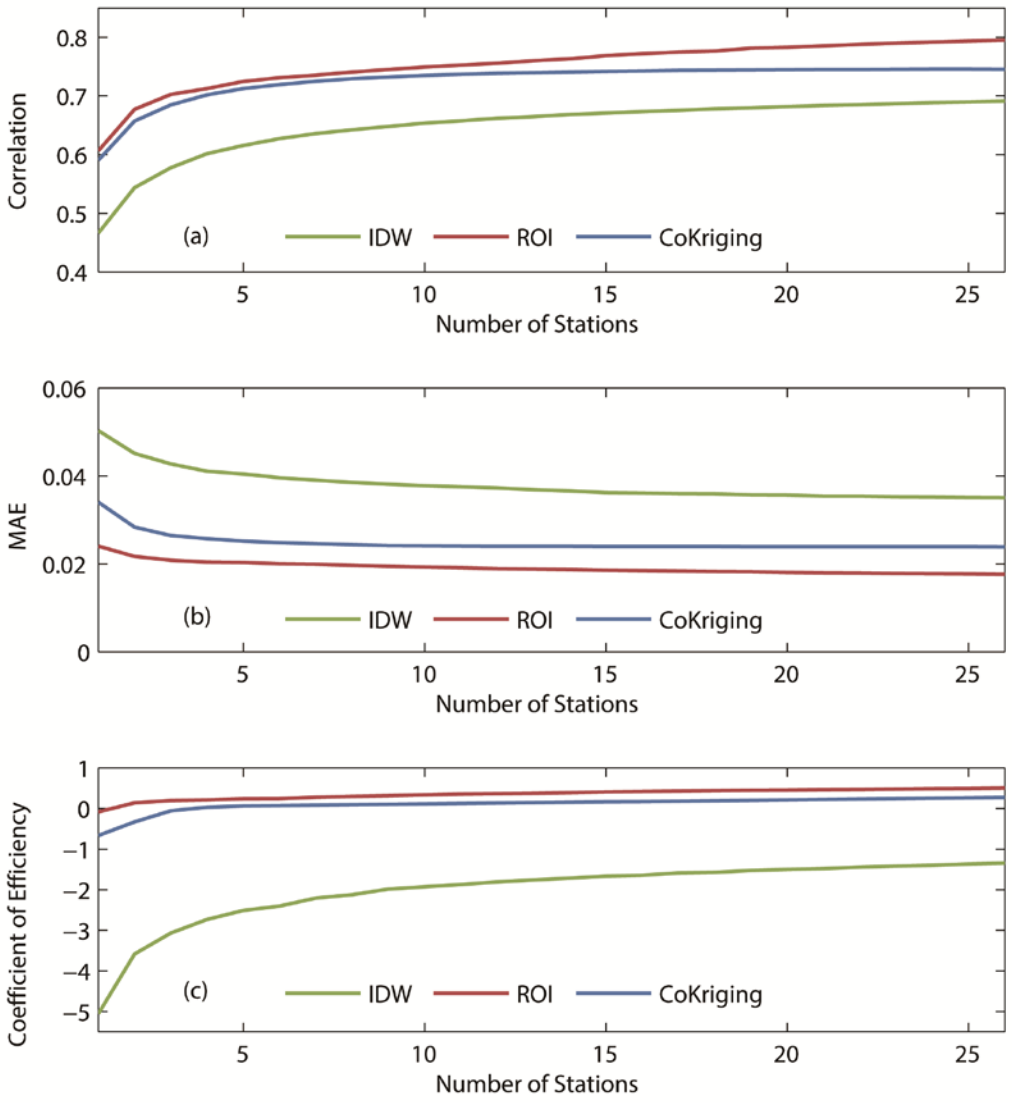

Figure 4. 7. Interpolation accuracy as a function of the number of stations used in the interpolation: (a) correlation coefficient, (b) mean absolute error, and (c) coefficient of efficiency as a function of the number of stations used for IDW, ROI and Cokriging interpolations. Mean results are reported based on 1000 replicates, with n stations (where *n* varies from 1 to 26) being randomly selected for each replicate.

These sensitivity tests demonstrate that the ROI method and the Cokriging method can be successfully employed to interpolate soil moisture in regions where there are relatively few stations.

4.4 Limitations and Conclusions

4.4.1 Limitations

In this study, we compared the accuracy of three interpolation methods in Oklahoma at a 0.5 degree spatial scale and a monthly temporal scale. This spatial resolution (0.5 degree) approximately matches that of current satellite products, such as SMOS (~50 km). Oklahoma is a state that has relatively little topographic complexity and a relatively high density of in situ soil moisture measurements. Therefore, we acknowledge that our results may not be transferable to other geographic regions or spatial scales of analysis (e.g., interpolation of field-scale soil moisture). For example, spatial heterogeneity of soil characteristics may play a more critical role in influencing soil moisture patterns at the field scale.

We used VIC-simulated soil moisture as a secondary data input for two of the interpolation methods that were evaluated in this study. Xia et al. (2015b) showed that the accuracy of model-simulated soil moisture can vary from model to model due to systematic errors in model-simulated evapotranspiration. This study did not evaluate whether our choice of models had a significant impact on the accuracy of the

interpolations. Future research can focus on how the use of different secondary datasets influences the performance of these interpolation methods.

4.4.2 Conclusions

Soil moisture interpolation is challenging because the spatial variability of soil moisture is influenced by many factors, including soil properties, topography, land cover and meteorological conditions. In addition, there are relatively few locations where soil moisture is measured so it is difficult to accurately capture these effects. This study evaluates the utility of the ROI method for interpolating soil moisture data using a relatively sparse network of observations and compares it to the Cokriging and IDW methods.

The spatially averaged state-wide results demonstrate that the ROI, Cokriging and the IDW methods perform reasonably well in Oklahoma. All of these methods had statistically significant correlations with observed soil moisture. However, when evaluating the performance of the three interpolation methods at individual locations, ROI performs better than Cokriging and IDW. One reason is that the ROI method utilizes the first 5 EOFs of model-simulated soil moisture from a physically-based land surface model that accounts for variations in soil properties, elevation, land cover and precipitation. The performance of IDW is strongly influenced by the density and the spatial distribution of in situ data. Our sensitivity tests confirm that the ROI and Cokriging methods can produce reliable estimates of regional soil moisture patterns, even in locations with relatively few stations.

CHAPTER V

EVALUATION OF SOIL MOISTURE IN CMIP5 SIMULATIONS OVER CONTIGUOUS UNITED STATES USING IN SITU AND SATELLITE OBSERVATIONS

5.1 Introduction

Soil moisture plays a critical role in hydrological processes, land-atmosphere interactions and climate variability. Through controlling water mass transfer, soil moisture affects runoff (Penna et al., 2011;Latron and Gallart, 2008;Zhang et al., 2001) and evapotranspiration (Wetzel and Chang, 1987;Vivoni et al., 2008;Detto et al., 2006). Soil moisture also influences the surface energy balance by affecting latent heat and ground fluxes (Ek and Holtslag, 2004;Ford and Quiring, 2014b). Soil moisture is one of the direct measures of drought used to assess future drought conditions in the latest IPCC report (Hartmann et al., 2013). Therefore, accurate soil moisture simulation is useful for many applications.

There are three main types of soil moisture data: in situ observations, remote sensing and model simulations. In situ observations provide point measurements at a variety of depths. The spatial and temporal coverage of in situ observations is quite limited and each in situ network may utilize different instruments and calibration techniques. These factors make it more challenging to use in situ soil moisture, however recent developments have improved the utility of these measurements. For example, the International Soil Moisture Network (ISMN) (Dorigo et al., 2011), which was initiated

in 2010, collects in situ soil moisture from more than 1400 station internationally and provides quality controlled hourly-to-weekly soil moisture data. The North American Soil Moisture Database (NASMD) (Quiring et al., 2016) provides quality controlled daily soil moisture from approximately 1800 stations, most of which are located in the United States. NASMD has been used for validating the North American Land Data Assimilation System (NLDAS) (Xia et al., 2015b, a) and to examine the nature of land-atmosphere interactions (Ford et al., 2015b;Ford et al., 2015c;Wang et al., 2015). There are numerous other studies that use in situ soil moisture from NASMD and ISMN. Ford and Quiring (2014b) used quantile regression to examine the relationship between in situ soil moisture and extreme temperature in Oklahoma. They found the soil moisture anomalies can be used for predicting the percent hot days in the following month. Ford et al. (2015a) found that soil moisture can also be used to predict the onset of flash drought events earlier in Oklahoma. Brocca et al. (2013) found in situ soil moisture can be used to improve daily precipitation estimation at the catchment scale.

Soil moisture observations from satellites remote sensing, such as the Soil Moisture and Ocean Salinity (SMOS) mission (Kerr et al., 2001), NASA's Aquarius (Le Vine et al., 2007) and Soil Moisture Active-Passive (SMAP) missions (Brown et al., 2013) can provide global soil moisture data. Previous studies have shown that satellite-derived soil moisture can accurately capture the annual cycle (Albergel et al., 2012b;Brocca et al., 2011), however, the accuracy of the satellite-derived soil moisture varies significantly both geographically and from product to product (Fang et al., 2016;Wanders et al., 2012). Rötzer et al. (2015) investigated the spatial and temporal

behavior of the SMOS and the MetOp-A Advanced Scatterometer (ASCAT) soil moisture. They demonstrated that SMOS is more strongly affected by temporally invariant factors, such as topography and soil properties, while ASCAT soil moisture is influenced by temporally variant factors, such as precipitation and evaporation. To overcome the limitations of satellite-derived soil moisture estimates, assimilated satellite products have been developed. Renzullo et al. (2014) used the ensemble Kalman filter method to assimilate AMSR-E and ASCAT-derived soil moisture. They found that data assimilation can significantly improve the accuracy of root-zone soil moisture estimates. A merged soil moisture product from active and passive sensors was released by the European Space Agency (ESA) in 2010 (Liu et al., 2011). This is a part of the program on the Global Monitoring of Essential Climate Variables (ECVs), and hereafter it will be referred to as ECV soil moisture. ECV soil moisture has been validated globally (Dorigo et al., 2015) and in regional studies in places such as in China (An et al., 2016) and East Africa (McNally et al., 2016). One of the primary limitations of satellite-based approaches is that they can typically only measure water in the top few centimeters of the soil (Crow et al., 2012).

Model simulation from offline land surface models (Koster et al., 2009) and fully coupled general circulation models (GCMs) (Srinivasan et al., 2000) is another source of spatially continuous soil moisture at variety of depths. However, validation studies have shown that these models can have significant bias. Guo and Dirmeyer (2006) compared 11 land surface models from the Second Global Soil Wetness Project (GSWP-2) and found that although models can reproduce soil moisture anomalies, they do not

accurately simulate the absolute soil water content. (Xia et al., 2015b) evaluated four land surface models within the North-American Land Data Assimilation System Project Phase 2 (NLDAS-2). They concluded that Noah and VIC model are wetter while Mosaic and SAC are drier. Compared with land surface models, coupled GCMs are more commonly used to investigate soil moisture-atmosphere interactions (Seneviratne et al., 2010). Koster et al. (2004) is a benchmark study of soil moisture-temperature and soil moisture-precipitation coupling strength using 12 GCMs in the Global Land-Atmosphere Coupling Experiment (GLACE). They identified three global "hot spots" where one finds strong land-atmosphere coupling. However, they also demonstrated that there are substantial inconsistencies in coupling strength between models. van den Hurk et al. (2010) used realistic soil moisture initializations in the second phase of GLACE (GLACE-2) to improve the forecast skill of summertime temperature and precipitation in Europe.

In 2012, the fifth phase of the Coupled Model Intercomparison Project (CMIP5) was completed to provide a state-of-the-art multi-model dataset for advancing the knowledge of climate variability and climate change (Taylor et al., 2012b). Li et al. (2007) concluded, based on previous versions of the CMIP models, that these models have difficulty accurately simulating the seasonal cycle of soil moisture. They also found that improved simulation of solar radiation and precipitation leads to more accurate soil moisture simulations. Although the CMIP5 models have been used to investigate land-atmosphere interactions (Dirmeyer et al., 2013;Seneviratne et al., 2013;May et al., 2015;Lorenz et al., 2016), to date, there has not been a comprehensive evaluation of the

accuracy of the CMIP5 soil moisture simulations in the United States. Therefore, this paper will address this knowledge gap.

In this chapter, we evaluate CMIP5 soil moisture simulations in two soil layers (0 to 10 cm and 0 to 100 cm) over CONUS using in situ and satellite-derived soil moisture. We evaluate both individual models and the multi-model ensemble mean using in situ soil moisture from 363 sites as well as satellite observations.

5.2 Data and Methods

5.2.1 Subregion Classification

We evaluate the CMIP5 soil moisture simulations over CONUS and in eight regions (Figure 5.1). These regions were defined using a land cover classification from U.S. Geological Survey (Loveland et al., 2000). These regions (dashed boxes in Figure 5.1) were utilized by Notaro et al. (2006) and they have been applied in other land-atmosphere studies (Mei and Wang, 2012;Sanchez-Mejia et al., 2014;Wu and Zhang, 2013). In this study, we made some small adjustments to these regions so that they included more in situ sites (solid boxes in Figure 5.1). The eight regions are: Midwest (MW: 38° – 47.5° N, 94° – 80° W), Northeast (NE: 38° – 47.5° N, 80° – 67° W), Northern Great Plains (NGP: 34.4°– 49° N, 105° – 94° W), Northern Shrubland (NS: 40° – 49° N, 119.4° – 105° W), Northwest (NW: 40° – 49° N, 124° – 119.4° W), Southeast (SE: 30° – 38° N, 92.5° – 75° W), Southern Great Plains (SGP: 25° – 34.4° N, 105° – 94° W) and Southern Shrubland (SS: 30.8° – 40° N, 119.4° – 105° W).

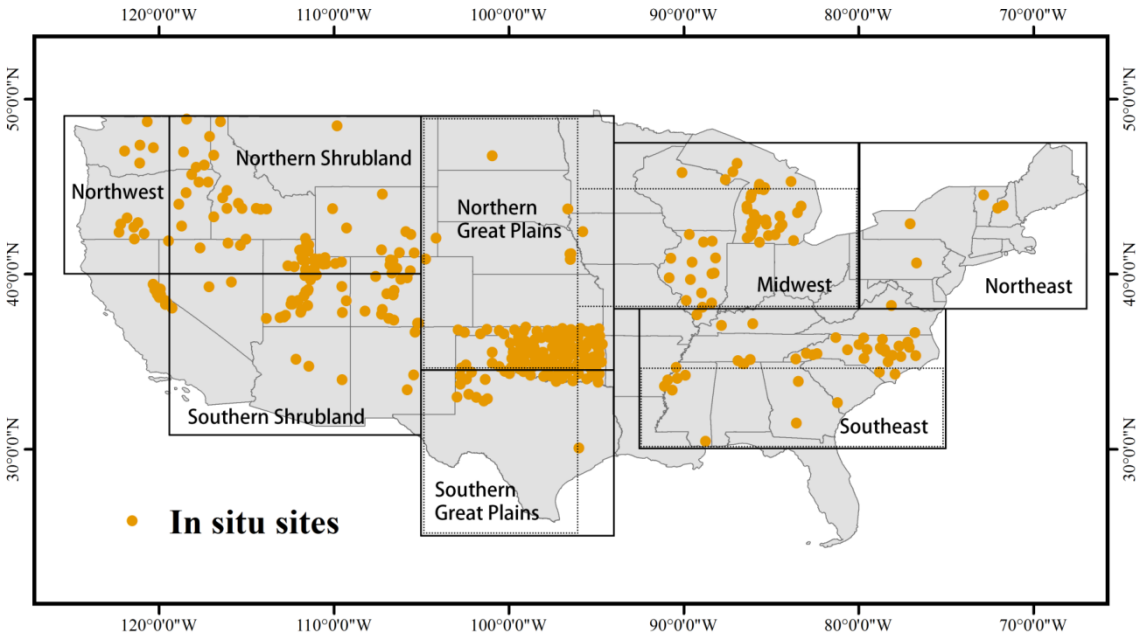

Figure 5. 1. Spatial distribution of in situ sites and map indicating classified subregions.

5.2.2 CMIP5 Models

All the Earth System Models (ESMs) in the CMIP5 archive that have soil moisture data are evaluated in this study. We evaluate monthly near-surface (0 – 10 cm) soil moisture from 17 ESMs and soil column (0 – 100 cm) soil moisture from 14 ESMs that are part of the CMIP5 archive (Table 5.1). Our analysis uses data from 2003 to 2012 because this is the time period with the greater number of in situ observations. Although the CMIP5 experiment ends in 2005, some ESMs, such as BCC-CSM1.1 and CanESM2, have an extended historical simulation through 2012. Therefore, we extend all the model simulations to 2012 by combining the 2006 – 2012 outputs from future emission

scenario: the representative concentration pathways (RCP) 4.5 to the regular historical experiment outputs. RCP 4.5 is a pathway for stabilization of radiative forcing at 4.5 W m^{-2} by 2100 (Thomson et al., 2011). A similar approach was adopted in the IPCC AR5 report (Bindoff et al., 2013). Jones et al. (2013) also used RCP4.5-forced CMIP5 simulations from 2005 to 2010 to investigate near-surface temperature variations. To validate this approach, we compared simulated precipitation based on different RCP scenarios with the Climatic Research Unit (CRU) precipitation in CONUS from 2006 to 2012 (results not shown) and found that the RCP 4.5 simulations closely match the CRU observations.

Table 5. 1. List of 17 CMIP5 models in this study

Model Name	Model Center	Spatial Resolution	Soil Moisture Simulation	
			0 – 10cm	0 – 100 cm
ACCESS1.3	Commonwealth Scientific and Industrial Research Organization (CSIRO) and Bureau of Meteorology (BOM), Australia	145×192	√	√
BCC-CSM1.1	Beijing Climate Center, China Meteorological Administration	64×128	√	√
BNU-ESM	College of Global Change and Earth System Science, Beijing Normal University	64×128	√	√
CanESM2	Canadian Centre for Climate Modelling and Analysis	64×128	√	√
CCSM4	National Center for Atmospheric Research	192×228	√	√
CESM1(CAM5)	Community Earth System Model Contributors	192×228	√	√
CNRM-CM5	Centre National de Recherches Météorologiques and Centre Européen de Recherche et Formation Avancée en Calcul	192×228	√	√

	Scientifique			
CSIRO-MK3.6.0	Commonwealth Scientific and Industrial Research Organization in collaboration with Queensland Climate Change Centre of Excellence	96×192	√	
FGOALS-g2	LASG, Institute of Atmospheric Physics, Chinese Academy of Sciences	60×128	√	√
GFDL-ESM2M	NOAA Geophysical Fluid Dynamics Laboratory	90×144	√	√
GISS-E2-H	NASA Goddard Institute for Space Studies	90×144	√	√
HadGEM2-ES	Met Office Hadley Centre (additional realizations contributed by Instituto Nacional de Pesquisas Espaciais)	145×192	√	√
INM-CM4	Institute for Numerical Mathematics	120×180	√	√
IPSL-CM5A-LR	Institut Pierre-Simon Laplace	96×96	√	
MIROC-ESM	Japan Agency for Marine-Earth Science and Technology, Atmosphere and Ocean Research Institute (The University	64×128	√	√

	of Tokyo) and National Institute for Environmental Studies			
MRI-CGCM3	Meteorological Research Institute	160×320	√	
NorESM1-M	Norwegian Climate Centre	96×144	√	√

5.2.3 In Situ Observations

Daily in situ soil moisture from 2003 to 2012 were obtained from North American Soil Moisture Database (http://soilmoisture.tamu.edu/). The North American Soil Moisture Database archives data from a variety of national and state networks (Quiring et al., 2016). Data from 363 stations are used in this study (Figure 5.1). These stations are collected from eight observational networks, as shown in Table 5.2. Quality-controlled daily soil moisture have been used to validate model simulations in previous studies (Xia et al., 2015c;Dirmeyer et al., 2016). In this study, any stations with short periods of missing data (< 10 days) are infilled using the daily average replacement (DAR) method (Ford and Quiring, 2014a). Soil moisture measurements at different depths are used to estimate the volumetric water content (VWC) in the top 10 cm and top 100 cm of the soil column. For example, the VWC measured at 5 cm is assumed to represent the VWC in 0 – 10 cm soil layer. When there are multiple soil moisture sensors within the top 100 cm, the measurements are combined using a depth-weighted average. Daily soil moisture measurements are then averaged to a monthly value to match the temporal resolution of the ESMs. The in situ measurements are also aggregated spatially to facilitate comparison with the CMIP5 models. We use a simple spatial average to aggregate all of the stations within each 0.25° × 0.25° grid cell. Then all of the grid cells with stations in them are averaged to produce a regional or national dataset for comparing the in situ and modelled soil moisture. Although this spatial average method is not the optimal technique to reduce sampling errors (Crow et al., 2012), it is simple and has been widely used in previous model evaluations (Robock et

al., 2003;Albergel et al., 2012a;Xia et al., 2015b). This approach reduces some of the bias associated with the point-versus-grid scale mismatch. Utilization of this approach over the entire CONUS provides an overview of soil moisture simulations in CMIP5 models. However, we are also interested in spatial variations in model performance. Therefore, we also evaluated model performance after dividing CONUS into eight regions.

Measuring water content in frozen soils is a challenge (Xia et al., 2015c). Therefore, the CONUS analysis only evaluates the CMIP5 simulations during the warm season (April-September). For regional evaluation, we use data from all the months in the three southern regions (Southeast, Southern Great Plains and Southern Shrubland) where frozen soils do not occur. All other regions only use data from the warm season.

Table 5. 2. List of observational networks used in this chapter.

Network	Number of Sites (Used in this dissertation)	Reference
AmeriFlux	4	(Baldocchi et al., 2001)
North Carolina Environment and Climate Observing Network	24	(Pan et al., 2012)
Illinois Climate Network	16	(Hollinger et al., 1994)
Michigan Automated Weather Network	34	(Andresen et al., 2011)
Oklahoma Mesonet	104	(Scott et al., 2013)
Soil Climate Analysis Network	66	(Schaefer et al., 2007)
Snowpack Telemetry	97	(Schaefer and Paetzold, 2001)

West Texas Mesonet	18	(Schroeder et al., 2005)

5.2.4 Satellite Observations

Satellite-derived soil moisture from the soil moisture climate change initiative (CCI) project (http://www.esa-soilmoisture-cci.org/) is used in this study. This project is a part of the European Space Agency Programme on Global Monitoring of Essential Climate Variables (ECV) (Liu et al., 2012). ECV soil moisture is based on active and passive remote sensing data and it has been validated using reanalyses (Albergel et al., 2013a;Albergel et al., 2013b) and in situ observations (Pratola et al., 2014). The spatial resolution of monthly ECV soil moisture is 0.25°. ECV soil moisture is not available during the cold season in the northern United States. Therefore, similar to the in situ observations, only warm season evaluations are undertaken for CONUS and the five northern regions. Data from all months is used in the three southern regions.

5.2.5 Evaluation Metric

Pearson correlation (r), mean absolute error (MAE), and the coefficient of efficiency (E) (Legates and McCabe, 1999) are used to quantify the agreement between observations and model simulations. Taylor's skill score (S) (Taylor, 2001) is also used to measure the ability of individual CMIP5 models to reproduce the climatological soil moisture distribution. The equation of S is shown as following, eq. 5.1:

$$S = \frac{4(1+R)}{\left[\sigma + (1/\sigma)\right]^2 (1+R_0)} \tag{5.1}$$

where R is the correlation between the simulated and observed soil moisture. σ is the ratio of standard deviation of model simulation over standard deviation of observation, and R_0 is the theoretical maximum correlation, equals to 1.

5.3 Results

5.3.1 Evaluation of Model Ensemble over CONUS

Figure 5.2 shows the relationship between the CMIP5 ensemble mean and satellite-derived and in situ soil moisture during the warm season. All three of these datasets were averaged over CONUS. The multi-model ensemble mean is highly correlated with the in situ observations (Figure 5.2a and c). The correlation (r) between the in situ and model-derived soil moisture is 0.92 in the 0 – 10 cm soil layer and it is 0.91 in the 0 – 100 cm soil layer. Both of these correlations are statistically significant ($p < 0.05$). In the 0 – 100 cm soil layer, the CMIP5 soil water content is systematically higher than the in situ observations, especially during drier months (i.e., when soil water content is < 0.25 cm^3 cm^{-3}). Figure 5.2b shows that there is a weaker relationship between the CMIP5 ensemble and ECV soil moisture and the correlation is only 0.65. It appears that the variance of the satellite-derived soil moisture is much less than the CMIP5 ensemble. The ECV soil moisture only varies from ~0.18 to 0.24 cm^3 cm^{-3}, while CMIP5 varies from ~0.16 to 0.27 cm^3 cm^{-3}. Therefore, the ECV soil moisture tends to be systematically greater than CMIP5 during drier months and systematically lower than CMIP5 during wetter months.

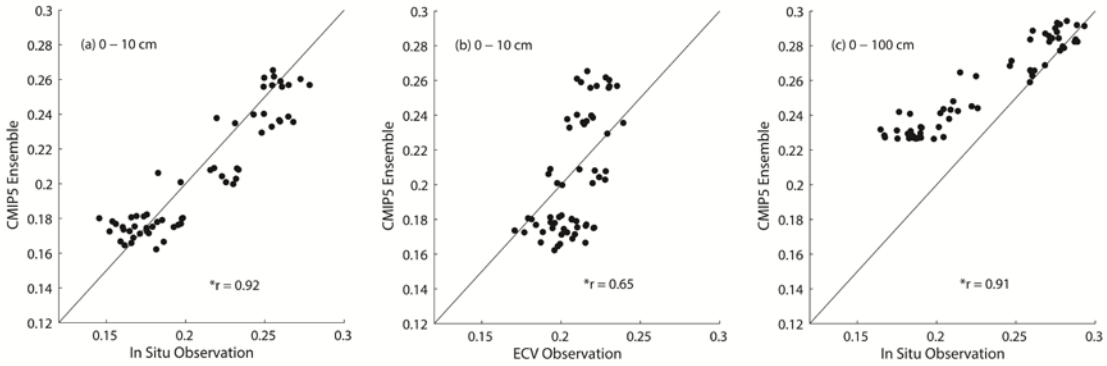

Figure 5. 2. Scatter plots of spatial averaged CMIP5 ensemble with ECV in 0 – 10 cm soil layer (a) with in situ in 0 – 10 cm soil layer (b) and with in situ in 0 – 1 m soil layer (c) during warm season (April to September).

We also examined the mean monthly soil moisture in the 0–10 cm and 0–100 cm soil layers from April to September. Figure 5.3a shows the seasonal cycle in the 0–10 cm soil moisture for the in situ observations, ECV satellite data and CMIP5 models. Although there are substantial inter-model variations among the CMIP5 models, particularly with regards to the absolute soil water content, the CMIP5 ensemble (black line) shows strong agreement with in situ observations (red line). Both show that soil moisture decreases from April until August and then soil moisture recharge begins starting in September. Both the CMIP5 ensemble and the in situ observations have a similar seasonal cycle in terms of both the magnitude and timing. In comparison, the satellite-derived ECV soil moisture (blue line) shows little month to month variability and has a very weak seasonal cycle. Neither the timing nor the magnitude of these variations matches the in situ observations and the CMIP5 ensemble.

Figure 5.3b shows the seasonal cycle in the 0–100 cm soil moisture for the in situ observations and the CMIP5 models. ECV soil moisture data are not shown since satellites are only able to estimate near-surface soil moisture. The seasonal cycle of soil moisture in the 0–100 cm layer is similar to the 0–10 cm layer. Soil water content is highest during the early part of the warm season (April/May) and it declines until reaching a minimum in August. There is general agreement between the in situ observations and CMIP5 ensemble, however there are notable differences in the magnitude of the soil water content. In addition, the dry down shown in the CMIP5 ensemble is less pronounced than in the in situ observations. There are substantial inter-model variations among the CMIP5 models, particularly with regards to the absolute soil water content which is similar to the 0–10 cm soil layer. We will focus on evaluating the performance of individual models in the following sections of the chapter.

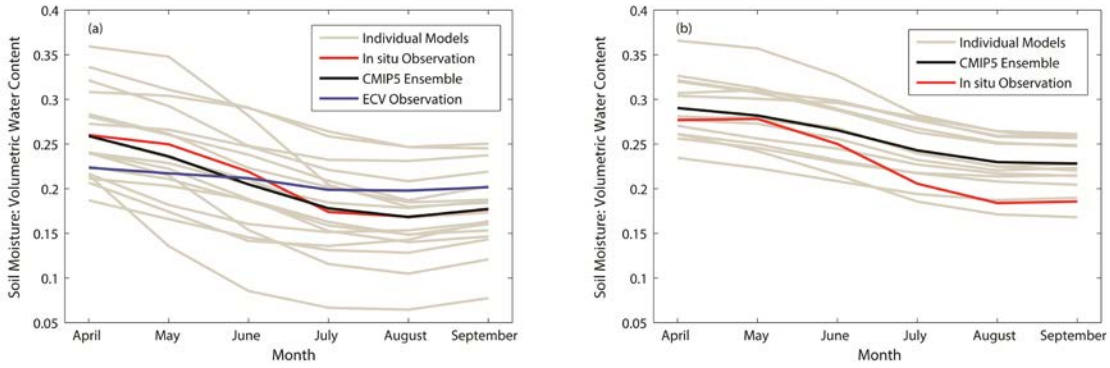

Figure 5. 3. Month to month variation of spatial averaged soil moisture in 0 – 10 cm soil layer (a) and in 0 – 1 m soil layer (b) during warm season (April to September).

We also compared the spatial pattern of the mean soil moisture (2003–2012) during the warm season (April–September) (Figure 5.4). Based on the CMIP5 ensemble, the soils with the lowest soil water content in the 0–10 cm layer are typically found in the southwestern U.S. and the soils with the highest soil water content tend to be found in the northeastern U.S. (Figure 5.4a). This pattern is also evident in the 0–100 cm soil layer, however the gradient is less pronounced (Figure 5.4b). The patterns are somewhat less spatially consistent when one examines the in situ observations because of the influence of local factors (e.g., edaphic, climatic, topographic, vegetation, etc.).

The differences between CMIP5 and the in situ observations are shown in Figure 5.4e and 5.4f. Generally, CMIP5 tends to be significantly wetter than the in situ observations in the western U.S. and it tends to be significantly drier than the in situ observations in the eastern U.S. In fact, 79.3 percent of the differences between CMIP5 and the in situ observations in the 0–10 cm layer are statistically significant. The same patterns are evident in the differences between CMIP5 and the in situ observations in the 0–100 cm layer (Figure 5.4f). However, a greater number (8.8% more) of the positive biases in western U.S. and the negative biases in the eastern U.S. are statistically significant than in the 0–10 cm layer. These results agree with previous research. Sheffield et al. (2013) concluded that the CMIP5 models tend to overestimate precipitation in west North America. Given that precipitation is a principal control of soil moisture, a positive bias in precipitation can cause soils to be too wet. Sheffield et al. (2013) also found that CMIP5 models tend to overestimate evaporation in eastern North

America. This would lead to drier soils and could help to explain the dry biases in CMIP5 that were observed in the eastern U.S.

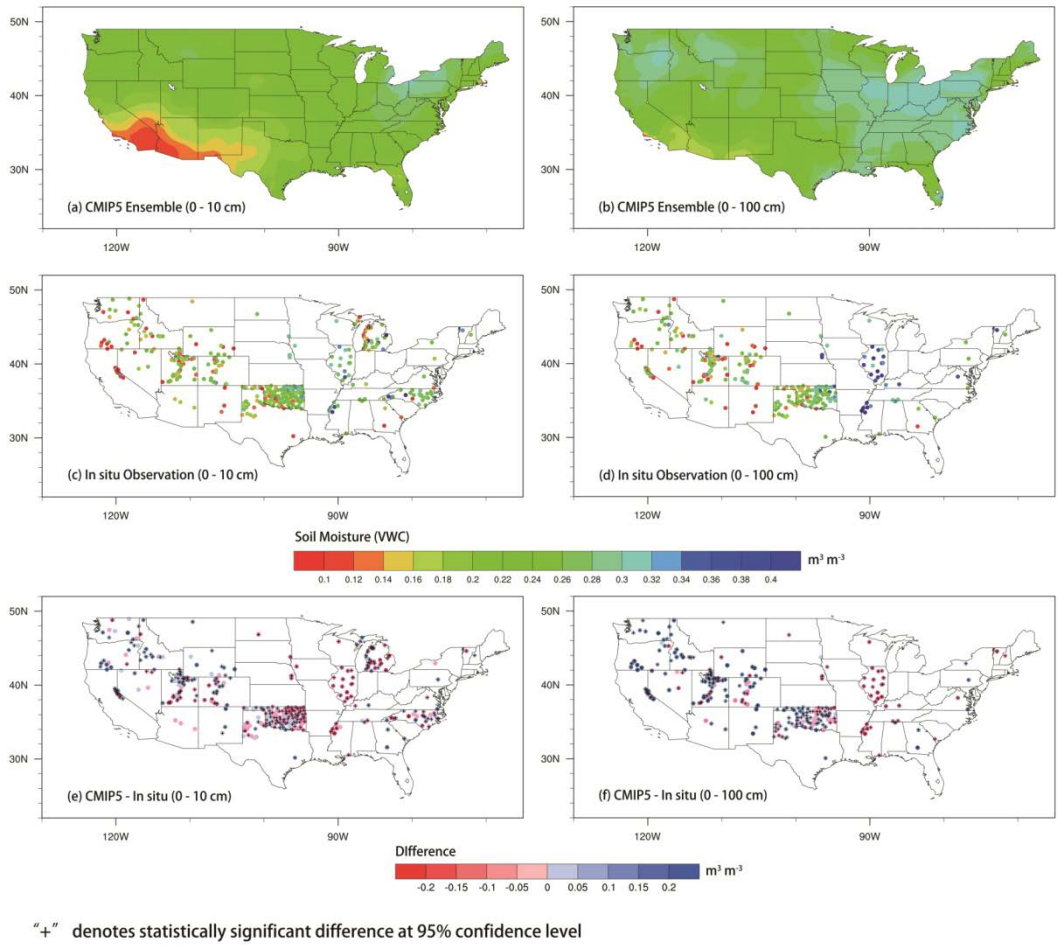

Figure 5. 4. Spatial pattern of mean (2003 – 2012) soil moisture over CONUS during warm season (April to September). 0 – 10 cm soil moisture is shown in the left panel for: CMIP5 ensemble (a), in situ observations (c) and the difference (e; CMIP5 – in situ). 0 – 100 cm soil moisture is shown in the right panel: CMIP5 ensemble (b), in situ observations (d) and the difference (f; CMIP5 – in situ).

Figure 5.5 compares the mean warm season (April–September) soil moisture (2003–2012) in 0–10 cm soil layer from the CMIP5 ensemble to the satellite-derived ECV soil moisture. The general spatial pattern of ECV is consistent with CMIP5, however ECV has much great spatial heterogeneity. This is partly due to the finer spatial resolution of the ECV data as compared to CMIP5. It is also apparent that there are significant differences in the near-surface soil water content in ECV versus CMIP5. For example, ECV shows that the regions with relatively low soil water content during the warm season (VWC < 0.2) are much more spatially extensive than in CMIP5. Similarly, the areas with relatively high soil water content (VWC > 0.3) are also more extensive with EVC. There has also been a shift in the soil water maxima in ECV into Maine and New Hampshire, with secondary maxima in Washington. The spatial pattern of the differences between ECV and CMIP5 are similar to those seen with the in situ observations. CMIP5 tends to have wet biases in the western U.S. and dry biases in the eastern U.S. The majority of statistically significant ($p < 0.05$) differences are concentrated in the places where CMIP5 is wetter than ECV (regions with a wet bias).

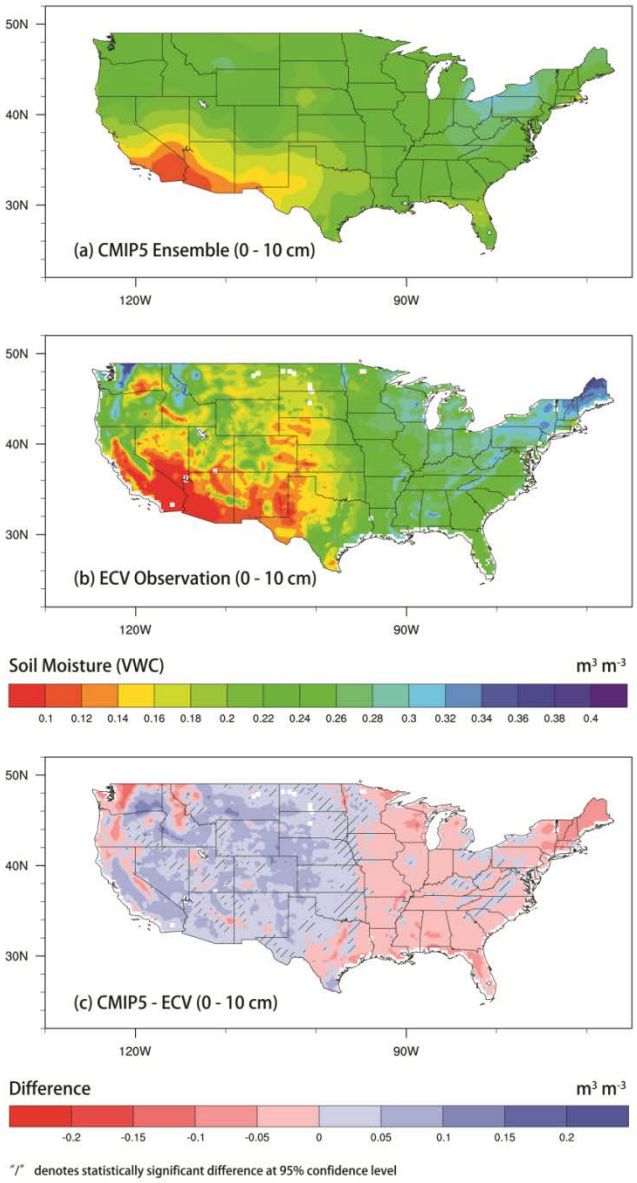

Figure 5. 5. Same as Figure 5.4, but for the CMIP5 ensemble and ECV soil moisture.

We evaluate the performance of each CMIP5 model over CONUS during the warm season using Taylor's skill score, as shown in Figure 5.6. Based on the skill score,

the individual models show a varying ability to capture the soil moisture distribution over CONUS. In the 0–10 cm soil layer, CCSM4, NorESM1-M, CESM1 and GFDL-ESM2M all perform well (when compared to in situ observations) and have higher skill scores (S = 0.89, 0.87, 0.87 and 0.85) than the CMIP5 ensemble (S = 0.84). CanESM2 (S = 0.39), INM-CM4 (S = 0.47) and HadGEM2-ES (S = 0.46) have the lowest scores.

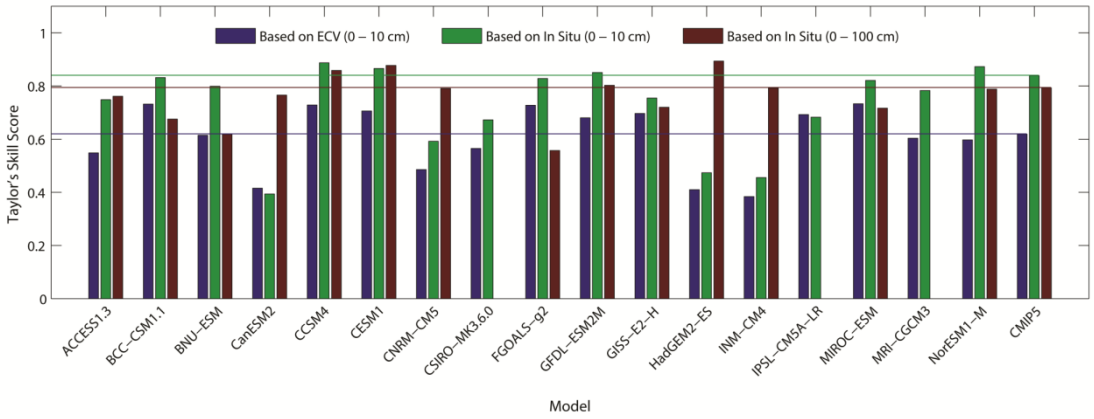

Figure 5. 6. Skill scores of CMIP5 over CONUS relative to the ECV observation (blue), in situ observation in 0 – 10 cm soil layer (green) and in 0 – 1 m soil moisture (brown). The line indicates the skill of the CMIP5 ensemble average.

When model performance is evaluated using ECV soil moisture, the skill scores decrease for all the models. Among the 17 CMIP5 models that were evaluated, 8 have higher skill scores than the CMIP5 ensemble mean (BCC-CSM1.1, CCSM4, CESM1, FGOALS-g2, GFDL-ESM2M, GISS-E2-H, IPSL-CM5A-LR and MIROC-ESM). In the 0–100 cm soil layer, CCSM4 (S = 0.86), CESM1 (S = 0.88), GFDL-ESM2M (S = 0.80) and HadGEM2-ES (S = 0.89) perform well. The performance of CanESM2, INM-CM4

and HadGEM2-ES improves in this layer as compared to the 0–10 cm layer. Generally, CCSM4, CESM1 and GFDL-ESM2M consistently perform well over CONUS in both the near-surface and deeper soil layers.

The performance of each CMIP5 model is also evaluated using correlation, RMSE and "amplitude of variations" (relative standard deviation). These metrics are represented in Figure 5.7 using a Taylor diagram (Taylor, 2001). Correlations between soil moisture simulated by CMIP5 models and ECV and in situ observations are indicated by the azimuthal position of each dot in Figure 5.7. Correlations (r) between simulated 0–10 cm soil moisture and ECV observations (Figure 5.7a) are all lower than 0.7. They tend to be clustered around 0.6, with the exception of BNU_ESM. Correlations between the CMIP5 models and the in situ soil moisture observations are more variable, as shown in Figure 5.7b. CCSM4 and CESM1 ($r = 0.79$) have the highest correlations, while IPSL-CM5A-LR ($r = 0.55$) and GISS-E2-H ($r = 0.56$) have the lowest correlations. The radial distance from the origin represents the standardized deviation of the CMIP5 models relative to the standardized deviation of the observations. When examing the performance of the CMIP5 models in the 0–10 cm soil layer, CanESM2, INM-CM4 and HadGEM2-ES are outliers showing much larger ($\sigma_{sim} / \sigma_{obs} > 2$) variations than either ECV or in situ observations. This leads to low Taylor's skill scores for these three models. All the models show larger variations than ECV soil moisture, while only 10 (out of 17) models demonstrate larger variations than in situ soil moisture. In the 0–100 cm soil layer, the models in Figure 5.7c are more clustered than in 0–10 cm soil layer. In general, the models tend to under-estimate the variability in the 0–100 cm

layer. 12 of the 14 models have standardized deviations that are lower than the observations. This indicates that most of the models cannot capture the true variability of soil moisture in this layer. INM-CM4 significantly overestimates the standardized deviation which is consistent with the results for the 0–10 cm soil layer. FGOALS-g2 (S = 0.56) has the lowest Taylor's skill score in the 0–100 cm layer. This is due to the low correlation (r = 0.69) and the model also significantly underestimates soil moisture variability ($\sigma_{sim} / \sigma_{obs} = 0.51$).

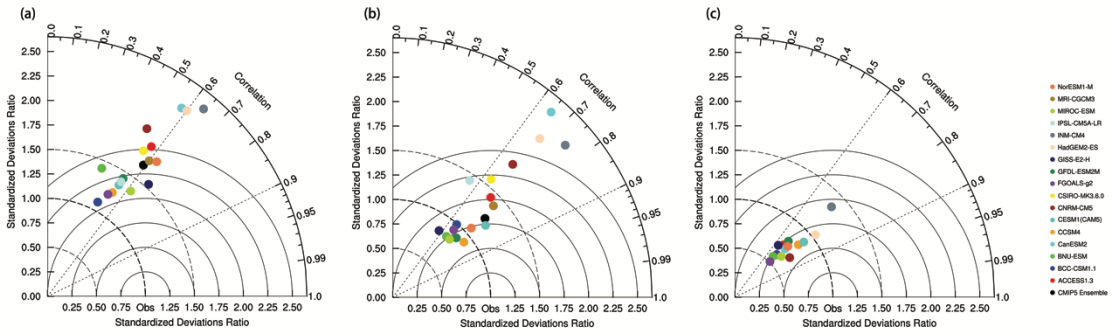

Figure 5. 7. Taylor diagrams for CMIP5 models referred to (a) ECV soil moisture (b) in situ 0 - 10 cm soil moisture and (c) in situ 0 – 1 m soil moisture. Azimuthal angle represents correlation coefficient and radial distance is the standard deviation normalized to observations.

5.3.2 Regional Evaluation

The CMIP5 models are also evaluated in eight regions in CONUS (Figure 5.8). Correlations between model-simulated and in situ surface soil moisture (green bar) are higher in all regions than the correlations (blue bar) based on ECV soil moisture, except

in the NGP region (Figure 5.8a). Focusing on the correlations between CMIP5 ensemble and in situ soil moisture, correlations for 0–100 cm soil moisture (brown bar) are similar to the correlations for 0–10 cm soil moisture. Only in the NGP region, correlation in 0–100 cm soil layer is substantially higher than in 0–10 cm soil layer. Examining the MAE gives a different perspective. In most regions, the CMIP5 ensemble has a lower MAE when compared to ECV versus the in situ observations. Only in the Northern Shrubland and Southern Shrubland regions is the MAE lower when compater to the in situ observations. Figure 5.8b indicates that MAE in the 0–100 cm soil layer is substantially higher than MAE in 0–10 cm soil layer in 7 of the 8 regions. Similarly, the coefficient of efficiency is generally higher in the 0–10 cm layer than in 0–100 cm.

Model performance varies from region to region. Based on the ECV soil moisture, the CMIP5 ensemble has relatively high correlations ($r = 0.64$ and 0.66) in the MW and NE and relatively low correlations ($r = 0.23$) in the SS region. Based on the in situ soil moisture, correlations are consistently high ($r > 0.85$) in NS, NW, SE, SGP and SS in both the near-surface and deep soil layers. The lowest correlation ($r = 0.50$) between the near-surface in situ soil moisture and CMIP5 ensemble is in the NGP. The MAE based on ECV soil moisture is relatively low in the NE, NGP and NW (MAE = 0.021, 0.021 and 0.021 $cm^3\ cm^{-3}$) and relatively high in NS and SS (MAE = 0.042 and 0.046 $cm^3\ cm^{-3}$). However, when compared to the near-surface in situ soil moisture, MAE is relatively high in the NW (MAE = 0.037 $cm^3\ cm^{-3}$).

There is substantially more regional variability in MAE for the 0–100 cm soil moisture. The MAE exceeds 0.07 $cm^3\ cm^{-3}$ in NS and NW, while in the NGP it is only

0.03 cm^3 cm^{-3}. The regional variation in coefficient of efficiency (E) is also substantial. When E is calculated based on the in situ observations it demonstrates that the CMIP5 ensemble can skillfully simulate the 0–10 cm soil moisture in the NS, NW, SE, SGP and SS regions. The results also demonstrate that CMIP5 can accurately simulate the 0–100 cm soil moisture in the NS, SE, SGP and SS regions during the warm season. However, these results do not agree with the performance assessment based on the ECV soil moisture. Based on ECV, E is best in the MW and NE regions and CMIP5 model ensemble is worse than climatology in the SS region.

Based on the results presented above, model performance differs significantly when being evaluated with in situ versus ECV soil moisture. In addition, the selection of the best performing models is dependent on which statistic is used. For example, based on the in situ soil moisture in 0–10 cm layer, the NS and NW regions have relatively high MAE (MAE = 0.037 and 0.037 cm^3 cm^{-3}) even though the correlations are also strong (r = 0.87 and 0.89). This suggests that the model is able to simulate the wetting and drying of the soil, but there is a systematic bias in the absolute magnitude of the model-simulated soil moisture.

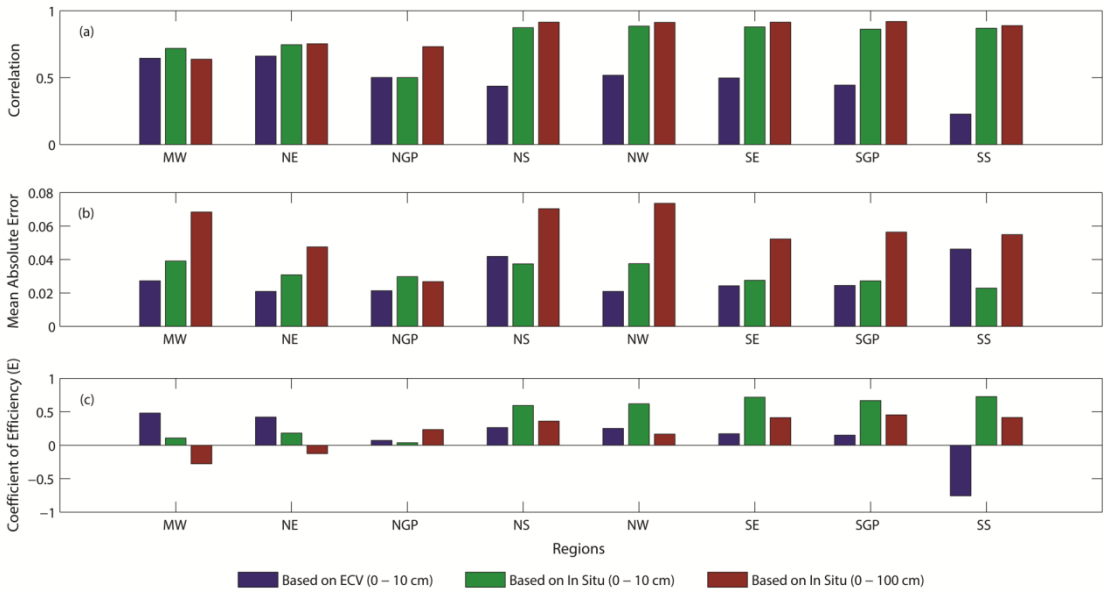

Figure 5. 8. Bar graphs of performance evaluation statistics for CMIP5 ensemble mean versus observed soil moisture (2003–2012): (a) correlation coefficient, (b) mean absolute error, and (c) coefficient of efficiency for the eight regions.

Figure 5.9 shows the skill scores of each model in the eight regions using in situ observations from the warm season as reference. There is substantial inter-model variability in performance amongst the CMIP5 models as a function of soil depth and location. CESM1 has consistently high skill in the 0–10 cm soil layer in all eight regions. MRI-CGCM3 outperforms all the other models in the MW region and it also performs well in the NE along with ACCESS1.3. CanESM2 and HadGEM2-ES do not perform well in the majority of regions (6 out of 8 regions) and GISS-E2-H does not perform well in the MW and NE. For the 0–100 cm soil layer, HadGEM2-ES performs well in all regions, especially in NGP, NS, NW, SE and SGP. The models generally perform better

in the NE, compared to other regions. FGOALS-g2 and GISS-E2-H perform relatively poorly in all regions.

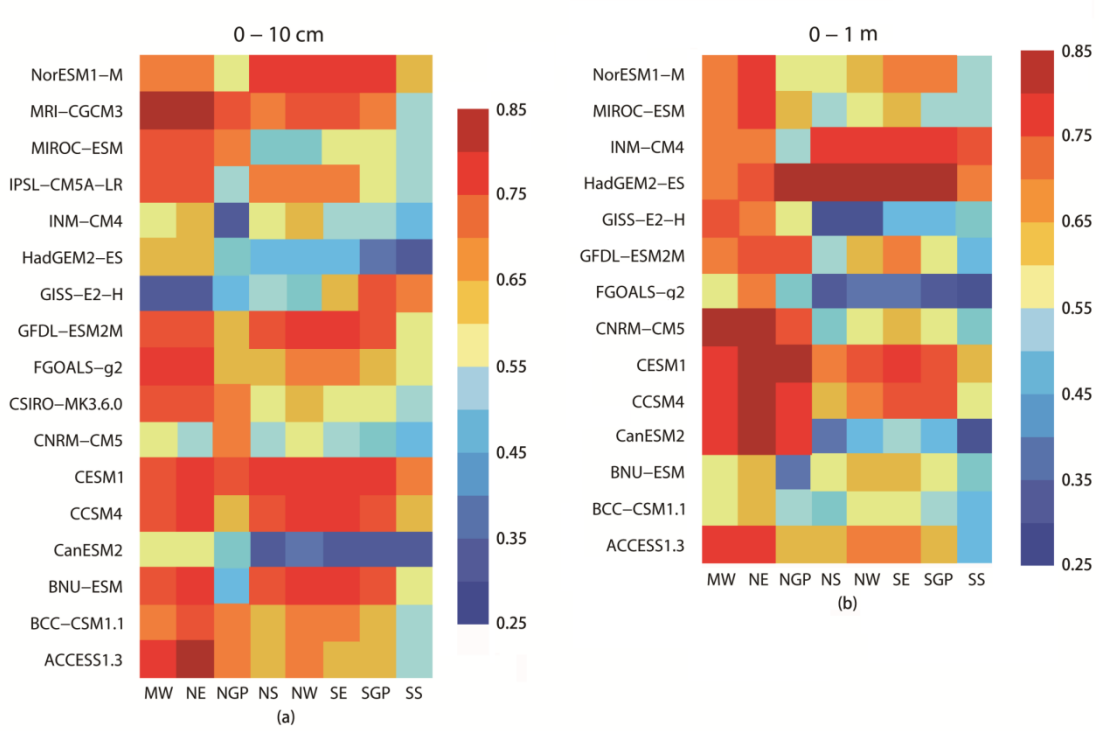

Figure 5. 9. Comparison of CMIP5 models with in situ observations over eight regions based on Taylor's skill scores: (a) 0 – 10 cm soil moisture, and (b) 0 – 1 m soil moisture.

Due to the availability of ECV data and the issues with measuring soil moisture in frozen soils, the preceding analysis focused solely on the warm season. We also evaluated model performance using data from all months in the three southern regions (SE, SGP and SS) where frozen soils are not an issue. Figure 5.10 shows the seasonal cycle of soil moisture based on the CMIP5 ensemble, in situ and ECV data in the three

southern regions. CMIP5 ensembles in the three regions consistently show that soil moisture decreases first then increases in a year. However in SE, soil moisture reaches driest condition (in September) later than soil moisture in SGP (August) and SS (July). Both the in situ and ECV show more variable seasonal patterns than the CMIP5 simulations, especially in the SGP and SS. In the SE, both the in situ and ECV soil moisture decrease starting in February and reach their lowest point in June. This is three months earlier than the CMIP5 ensemble. In situ observations are wetter than ECV soil moisture during the entire year in the SE, but they are most similar in October. In the SGP, in situ and ECV soil moisture generally decreases from April to August and then increases after August. There is good agreement between the in situ, ECV and CMIP5 in the SGP with regards to the timing of the wettest and driest months. This is the only region where the seasonal cycle is the same in all three data sources. However, the magnitude of the seasonal fluctuations differs substantially. CMIP5 is much more variable than both the in situ and ECV. While in the SS region, the ECV does not show much of a seasonal cycle. CMIP5 and the in situ observations show a similar drying of the soil from March through June, but they do not agree as well during the June to November period. Table 5.3 provides the correlation, MAE and E based on the month data from these three regions. During the warm season months the correlations and coefficient of efficiency are higher and the MAE is lower in all the cases. In terms of the surface layer, the CMIP5 ensemble is more highly correlated with in situ observations than ECV data in all three regions. However, in the SGP and SE, the MAE based on comparing the CMIP5 ensemble to the ECV is lower than the MAE based on the in situ

observations. With emphasis on in situ soil moisture in different layers, CMIP5 ensemble has higher correlation, larger MAE and lower E in 0–100 cm soil layer than in 0–10 cm soil layer in all the three regions.

Table 5. 3. Evaluation of CMIP5 ensemble over Southeast, Southern Great Plains and Southern Shrubland using all monthly soil moisture and warm season only soil moisture

		Correlation		MAE		E	
		All	Warm	All	Warm	All	Warm
SE	v.s. ECV	0.44	0.50	0.030	0.024	0.11	0.17
	v.s. In Situ (0–10 cm)	0.80	0.88	0.032	0.028	0.61	0.72
	v.s. In Situ (0–100 cm)	0.89	0.91	0.067	0.052	0.21	0.43
SGP	v.s. ECV	0.38	0.44	0.026	0.024	0.05	0.15
	v.s. In Situ (0–10 cm)	0.82	0.86	0.032	0.027	0.63	0.67
	v.s. In Situ (0–100 cm)	0.90	0.92	0.071	0.056	0.19	0.45
SS	v.s. ECV	0.21	0.23	0.051	0.046	-1.12	-0.76
	v.s. In Situ (0–10 cm)	0.81	0.87	0.028	0.023	0.66	0.73
	v.s. In Situ (0–100 cm)	0.88	0.89	0.074	0.055	0.17	0.41

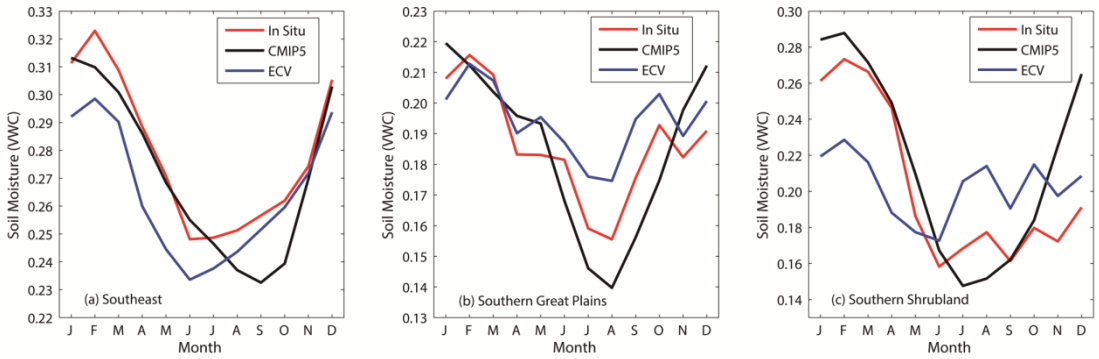

Figure 5. 10. Seasonal variation of mean monthly (2003 – 2012) soil moisture based on in situ observations (red), CMIP5 ensemble (black) and ECV observations (blue) in three regions: (a) Southeast, (b) Southern Great Plains, and (c) Southern Shrubland.

5.4 Limitations and Conclusions

5.4.1 Limitations

This study compares model-simulated soil moisture from the CMIP5 models with in situ and satellite-derived soil moisture. The in situ stations were selected based on their record length spatial coverage. However, there are relatively few stations with 10-year records. Therefore, some parts of CONUS are not well represented in this analysis. Future studies would benefit from including more in situ data to evaluate model performance. This would help to address issues with the spatial gaps in coverage and the issues related to comparing point measurements to model grid cells. Considering the in situ soil moisture come from different networks, there may also be some inconsistencies in the quality and representativeness of the soil moisture data (Dirmeyer et al., 2016). These inconsistencies can result from the use of different soil moisture sensors, calibration procedures and quality control processes. Dirmeyer et al. (2016) assessed the

random errors of 16 networks and found distinct differences between networks. Although we excluded from this study one of the networks with the largest random errors (e.g., COSMOS), more work is still needed to standardize and homogenize in situ soil moisture measurements.

Another potential limitation of this work is that we applied bilinear interpolation method to regrid all the CMIP5 model output to a uniform resolution of 0.25° × 0.25° so that it matched the resolution of the ECV data. This is a simple way of re-scaling the data. Given that we are only evaluating model performance at the regional and continental scale, we believe that this method is reasonable because the spatial variability of soil moisture at these scales is dominated by precipitation patterns (Crow et al., 2012). However, applying more advanced interpolation or downscaling methods such as the reduced optimal interpolation (ROI) method (Yuan and Quiring, 2016) may provide a better estimates of model-simulated soil moisture at this spatial scale.

5.4.2 Conclusions

We evaluated soil moisture simulations in CMIP5 experiment (17 models for 0–10 cm and 14 models for 0–100 cm) over CONUS using in situ observations and ECV satellite observations. The CONUS results show that the CMIP5 model ensemble has similar correlations with in situ observations when comparing the 0–100 cm soil layer with the 0–10 cm soil layer. However, there is evidence of a substantial wet bias in the deeper soil layer during months when the soil is dry. This wet bias is also reflected in the

multi-year mean monthly soil moisture. There is substantial variability in performance among the individual models, with the greater uncertainties in surface soil layer.

The multi-model CMIP5 ensemble mean can generally capture the spatial pattern of soil moisture. However, wet biases in the western U.S. and dry biases in the eastern U.S. are evident. Sheffield et al. (2013) found that CMIP5 models tend to overestimate precipitation in the western U.S. and this may account for the wet biases that we observed. Dry biases in the eastern U.S. may be attributed to evapotranspiration, which tends to overestimated by CMIP5 models in the eastern U.S. (Sheffield et al., 2013). Performance of the CMIP5 ensemble varies significantly from region to region. In most regions (NS, NW, SE, SGP and SS), the CMIP5 ensemble can accurately simulate warm season surface soil moisture (e.g., high correlations and low MAE). In the three southern regions, we also evaluated soil moisture simulations during the cold season and found that there is generally a decrease in model performance (e.g., higher MAE and lower E than during the warm season).

ECV soil moisture, as an independent data source, is introduced in this study to help evaluate the performance of CMIP5 soil moisture simulations. Relative to ECV soil moisture, CMIP5 ensemble shows greater month-to-month variations over CONUS. Due to this greater variance, CMIP5 models do not skillfully reproduce the ECV soil moisture. Similar with in situ soil moisture, ECV data also shows that the CMIP5 model ensemble tends to have wet biases in the western U.S. and dry biases in the eastern U.S. Additionally, in the three southern regions, the intra-annual variability shown by ECV soil moisture and in situ observations are relatively consistent. On the other hand, the

CMIP5 ensemble can only capture the general seasonal cycle, but fails to adequately capture some of the monthly variations. At the same time, there are some inconsistencies between the in situ and ECV soil moisture. For example, in the Southern Shrubland, the correlation between the CMIP5 models and ECV soil moisture ($r = 0.23$) is lower than the correlation with the in situ data ($r = 0.87$). Though comparing the two observational data is not the goal of this study, we can still point out future validation of satellite derived soil moisture is necessary.

The skill of the individual CMIP5 models also varies significantly. In the top soil layer, the Taylor skill score varies from 0.39 (CanESM2) to 0.89 (CCSM4). Generally, the skill of the models in the deeper soil layer is similar to the surface layer, but the inter-model variability in skill is greater. HadGEM2-ES has the highest skill score because it matches the variability of the in situ observations. Generally, CESM1 consistently performs well in the surface soil layer in all regions, and HadGEM2-ES performs well in the 0–100 cm soil layers in all regions. However, it is remains difficult to find a single model that consistently outperforms all others when it comes to accurately simulating soil moisture in all regions and seasons. Therefore, it is unclear whether the findings of this study will apply to other regions around the world with difference climate, soil and vegetation characteristics.

CHAPTER VI

CONCLUSIONS

6.1 Summary and Conclusions

This dissertation provided a comprehensive evaluation of the utility of soil moisture for evaluating drought conditions in the U.S. Great Plains. Four drought indices (SPI, SPEI, CMI and Z index) are compared with two soil moisture products (in situ observation and land surface model simulation) in Chapter 2. The analysis focuses on whether these drought indices are able to accurately represent the percentile, trend, variability and persistence in observed soil moisture. In the 0 – 100 cm soil layer, CMI agrees well with soil moisture observations based on all four characteristics. In the 0 – 10 cm soil layer, the results show that the best drought index depends on the goal of the application. For example, if the emphasis is on soil moisture variability, SPEI would be a good choice. In general, a more accurate representation of PET will help the drought indices to better approximate soil moisture. Except for CMI, the other three indices are more similar to soil moisture in 0 – 10 cm soil layer than in 0 – 100 cm soil layer. Therefore, we recommend using CMI as a proxy for soil moisture (0 to 100 cm) in future research.

In Chapter 3, a more realistic version of the PDSI was developed by introducing a physically-based PET model into the PDSI. The comparison with the original PDSI and Penman-Montieth approaches based PDSI show the new PDSI estimates moderate drought trend from 1980 to 2012. This comparison also indicates the PDSI is not very

sensitive to the choice of PET model because precipitation is the more important factor that influences the PDSI in the U.S. Great Plains relative to energy supply. Though the spatially-averaged PDSI is insensitive to the choice of PET model, the influence of PET on the spatial and temporal pattern of drought cannot be ignored. Significant differences of drought area are revealed during severe drought events based on different PET estimates. The spatial pattern of land cover type is also found to correspond well with the spatial pattern of differences in the trends between the three methods. This leaves an open question for future research how significant the causal link with land cover is.

Interpolation methods are used to estimate soil moisture at unsampled locations. Accurate interpolation method can provide spatially continuous drought information. Chapter 4 demonstrated the utility of the Reduced Optimal Interpolation method for soil moisture interpolation. Based on a comparison with IDW and Cokriging method, we found that ROI method significantly improves the accuracy of interpolated soil moisture at individual locations. In addition, it is not sensitive to the density and the spatial distribution of in situ measurements.

The goal of Chapter 5 was to assess the accuracy of soil moisture simulations in ESMs using measurements and satellites. ESMs are the main tool for understanding future land-atmosphere interactions and drought conditions.The performance of 17 ESMs were evaluated over CONUS relative to soil moisture observations based on 2003 to 2012. The spatially-averaged multi-model ensemble is able to accurately represent the seasonal variations in soil moisture. However, there is a substantial wet bias, especially in 0 – 100 cm soil layer. Spatially, the CMIP5 ensemble has a wet bias in the western

U.S., and a dry bias in the eastern U.S. Model performance is better in warm season than in the cool season. The results demonstrated that there is substantial variability in performance among the individual models, especially in 0 – 10 cm soil layer. In addition, model performance as varies substantially across the sub-regions. Therefore, it is difficult to find one model that consistently performs well in all regions and seasons.

6.2 Key Findings

The spatial and temporal limitations of in situ soil moisture have limited their utility in past drought studies. This knowledge gap was addressed by this dissertation research through systematically assessing different ways of extending soil moisture data back in time (through the use of drought indices), estimating soil moisture at unsampled locations (through better interpolation methods), and estimating future changes in soil moisture (through using ESMs).

First, this study identified the most appropriate soil moisture proxy based on the evaluation of four commonly-used drought indices. Although the SPI has been used in previous studies to represent soil moisture conditions, there have been very few evaluations of its ability to represent observed soil moisture conditions. Based on the results of this doctoral work, the SPI is not likely the best proxy for soil moisture. Generally, it appears that the CMI is the best index to use to represent soil moisture conditions. Therefore, the CMI should be used in studies that are interested in looking at

long term variations in soil moisture variability and land-atmosphere interactions when observed soil moisture is not available.

Second, this dissertation research developed a more physically-realistic version of the PDSI and compared it with soil moisture. We quantified how PET influences drought index variability. This new drought index has the potential to provide more accurate information on soil moisture conditions to support drought monitoring activities. It may also be useful for serving as a proxy for soil moisture conditions in times and places that do not have in situ measurements.

Third, this dissertation was the first to apply the ROI method for interpolating soil moisture. The comparison with other interpolation methods demonstrated that ROI significantly outperforms standard approaches. Therefore, ROI is a good approach to use for generating gridded soil moisture products. There are a large number of activities that are reliant on gridded soil moisture data, these include: operational drought monitoring, calibrating/validating satellites and land surface models, and documenting how soil moisture influences the climate system on seasonal to inter-annual time scales. Successfully applying the ROI method to estimate soil moisture at unsampled locations will help to address the limitations of the observing network.

Finally, this dissertation is the first to evaluate the accuracy of the soil moisture simulations in the CMIP5 ESMs using both in situ and satellite data. Future projections of drought conditions, land-atmosphere interactions and hydrological cycle are strongly dependent on these ESMs. An improved understanding of where and when these models perform well and where and when perform poorly is essential for advancing the state-of-

the-art in land-surface modeling and improving our understanding of future changes in soil moisture and hydroclimatic variability. These results can provide guidance on selecting the most appropriate model for climate assessment.

6.3 Future Research

The application of in situ soil moisture is always associated with scale problems. Comparison of point measurements with grid cells/pixels is problematic due to the scale mismatch. Future research should focus on developing methods for rescaling data (downscaling and upscaling) from point to grid cell in an optimal fashion that minimizes loss of information. Another issue related to in situ soil moisture is the uneven distribution of in situ sites. Therefore, further research is needed to improve interpolation methods and to identify the optimal resolution for gridded in situ products.

There are also opportunities to utilize the results of the ESM evaluation that was performed here to investigate future changes in land-atmosphere interactions and hydroclimatic variability. Investigating how climate response to soil moisture anomalies via running selected ESMs with more realistic soil moisture initials.

Variations in the soil moisture-climate coupling strength on decadal and multi-decadal timescales is also an important topic. This dissertation has identified the drought indices that are best suited for being proxies of long-term soil moisture conditions. This will provide the basis for evaluating how and why land-atmosphere coupling strength varies over time and space.

REFERENCES

Albergel, C., de Rosnay, P., Balsamo, G., Isaksen, L., and Muñoz-Sabater, J.: Soil moisture analyses at ECMWF: Evaluation using global ground-based in situ observations, Journal of Hydrometeorology, 13, 1442-1460, doi:10.1175/JHM-D-11-0107.1, 2012a.

Albergel, C., de Rosnay, P., Gruhier, C., Muñoz-Sabater, J., Hasenauer, S., Isaksen, L., Kerr, Y., and Wagner, W.: Evaluation of remotely sensed and modelled soil moisture products using global ground-based in situ observations, Remote Sensing of Environment, 118, 215-226, http://dx.doi.org/10.1016/j.rse.2011.11.017, 2012b.

Albergel, C., Dorigo, W., Balsamo, G., Muñoz-Sabater, J., de Rosnay, P., Isaksen, L., Brocca, L., de Jeu, R., and Wagner, W.: Monitoring multi-decadal satellite earth observation of soil moisture products through land surface reanalyses, Remote Sensing of Environment, 138, 77-89, http://dx.doi.org/10.1016/j.rse.2013.07.009, 2013a.

Albergel, C., Dorigo, W., Reichle, R. H., Balsamo, G., de Rosnay, P., Muñoz-Sabater, J., Isaksen, L., de Jeu, R., and Wagner, W.: Skill and global trend analysis of soil moisture from reanalyses and microwave remote sensing, Journal of Hydrometeorology, 14, 1259-1277, 10.1175/JHM-D-12-0161.1, 2013b.

An, R., Zhang, L., Wang, Z., Quaye-Ballard, J. A., You, J., Shen, X., Gao, W., Huang, L., Zhao, Y., and Ke, Z.: Validation of the ESA CCI soil moisture product in China, International Journal of Applied Earth Observation and Geoinformation, 48, 28-36, http://dx.doi.org/10.1016/j.jag.2015.09.009, 2016.

Anderson, W. B., Zaitchik, B. F., Hain, C. R., Anderson, M. C., Yilmaz, M. T., Mecikalski, J., and Schultz, L.: Towards an integrated soil moisture drought monitor for East Africa, Hydrol. Earth Syst. Sci., 16, 2893-2913, 10.5194/hess-16-2893-2012, 2012.

Andresen, J., Olse, L., Aichele, T., Bishop, B., Brown, J., Landis, J., Marquie, S., and Pollyea, A.: Enviro-weather:A weatherbased pest and crop management information system for Michigan., Seventh Int. Integrated Pest Management Symp, Memphis, TN, 2011.

Bárdossy, A., and Lehmann, W.: Spatial distribution of soil moisture in a small catchment. Part 1: geostatistical analysis, Journal of Hydrology, 206, 1-15, http://dx.doi.org/10.1016/S0022-1694(97)00152-2, 1998.

Baldocchi, D., Falge, E., Gu, L., Olson, R., Hollinger, D., Running, S., Anthoni, P., Bernhofer, C., Davis, K., Evans, R., Fuentes, J., Goldstein, A., Katul, G., Law, B.,

Lee, X., Malhi, Y., Meyers, T., Munger, W., Oechel, W., Paw, K. T., Pilegaard, K., Schmid, H. P., Valentini, R., Verma, S., Vesala, T., Wilson, K., and Wofsy, S.: FLUXNET: a new tool to study the temporal and spatial variability of ecosystem–scale carbon dioxide, water vapor, and energy flux densities, Bulletin of the American Meteorological Society, 82, 2415-2434, doi:10.1175/1520-0477(2001)082<2415:FANTTS>2.3.CO;2, 2001.

Baskan, O., Erpul, G., and Dengiz, O.: Comparing the efficiency of ordinary kriging and cokriging to estimate the Atterberg limits spatially using some soil physical properties, Clay Minerals, 44, 181-193, 10.1180/claymin.2009.044.2.181, 2009.

Baudena, M., D'Andrea, F., and Provenzale, A.: A model for soil-vegetation-atmosphere interactions in water-limited ecosystems, Water Resources Research, 44, W12429, 10.1029/2008WR007172, 2008.

Berg, A. A., and Mulroy, K. A.: Streamflow predictability in the Saskatchewan/Nelson River basin given macroscale estimates of the initial soil moisture status, Hydrological Sciences Journal, 51, 642-654, 10.1623/hysj.51.4.642, 2006.

Biggs, T. W., Mishra, P. K., and Turral, H.: Evapotranspiration and regional probabilities of soil moisture stress in rainfed crops, southern India, Agricultural and Forest Meteorology, 148, 1585-1597, http://dx.doi.org/10.1016/j.agrformet.2008.05.012, 2008.

Bindoff, N. L., Stott, P. A., AchutaRao, K. M., Allen, M. R., Gillett, N., Gutzler, D., Hansingo, K., Hegerl, G., Hu, Y., Jain, S., Mokhov, I. I., Overland, J., Perlwitz, J., Sebbari, R., and Zhang, X.: Detection and attribution of climate change: From global to regional. In: Climate change 2013: The physical science basis. Contribution of Working Group I to the fifth assessment report of the intergovernmental panel on climate change, Cambridge, United Kingdom and New York, NY, USA., 2013.

Bosilovich, M. G., and Sun, W.-y.: Numerical simulation of the 1993 midwestern flood: Land–atmosphere interactions, Journal of Climate, 12, 1490-1505, doi:10.1175/1520-0442(1999)012<1490:NSOTMF>2.0.CO;2, 1999.

Bosilovich, M. G., and Schubert, S. D.: Water vapor tracers as diagnostics of the regional hydrologic cycle, Journal of Hydrometeorology, 3, 149-165, doi:10.1175/1525-7541(2002)003<0149:WVTADO>2.0.CO;2, 2002.

Brabson, B. B., Lister, D. H., Jones, P. D., and Palutikof, J. P.: Soil moisture and predicted spells of extreme temperatures in Britain, Journal of Geophysical Research: Atmospheres, 110, D05104, 10.1029/2004JD005156, 2005.

Brocca, L., Hasenauer, S., Lacava, T., Melone, F., Moramarco, T., Wagner, W., Dorigo, W., Matgen, P., Martínez-Fernández, J., Llorens, P., Latron, J., Martin, C., and Bittelli, M.: Soil moisture estimation through ASCAT and AMSR-E sensors: An intercomparison and validation study across Europe, Remote Sensing of Environment, 115, 3390-3408, http://dx.doi.org/10.1016/j.rse.2011.08.003, 2011.

Brocca, L., Moramarco, T., Melone, F., and Wagner, W.: A new method for rainfall estimation through soil moisture observations, Geophysical Research Letters, 40, 853-858, 10.1002/grl.50173, 2013.

Brown, M. E., Escobar, V., Moran, S., Entekhabi, D., O'Neill, P. E., Njoku, E. G., Doorn, B., and Entin, J. K.: NASA's Soil Moisture Active Passive (SMAP) mission and opportunities for applications users, Bulletin of the American Meteorological Society, 94, 1125-1128, 10.1175/BAMS-D-11-00049.1, 2013.

Byun, H.-R., and Wilhite, D. A.: Objective quantification of drought severity and duration, Journal of Climate, 12, 2747-2756, 10.1175/1520-0442(1999)012<2747:OQODSA>2.0.CO;2, 1999.

Champagne, C., Berg, A., Belanger, J., McNairn, H., and De Jeu, R.: Evaluation of soil moisture derived from passive microwave remote sensing over agricultural sites in Canada using ground-based soil moisture monitoring networks, International Journal of Remote Sensing, 31, 3669-3690, 10.1080/01431161.2010.483485, 2010.

Collow, T. W., Robock, A., Basara, J. B., and Illston, B. G.: Evaluation of SMOS retrievals of soil moisture over the central United States with currently available in situ observations, Journal of Geophysical Research: Atmospheres, 117, D09113, 10.1029/2011JD017095, 2012.

Crow, W. T., Berg, A. A., Cosh, M. H., Loew, A., Mohanty, B. P., Panciera, R., de Rosnay, P., Ryu, D., and Walker, J. P.: Upscaling sparse ground-based soil moisture observations for the validation of coarse-resolution satellite soil moisture products, Reviews of Geophysics, 50, RG2002, 10.1029/2011RG000372, 2012.

Dai, A., Trenberth, K. E., and Qian, T.: A global dataset of Palmer Drought Severity Index for 1870–2002: Relationship with soil moisture and effects of surface warming, Journal of Hydrometeorology, 5, 1117-1130, 10.1175/JHM-386.1, 2004.

Dai, A.: Drought under global warming: A review, Wiley Interdisciplinary Reviews: Climate Change, 2, 45-65, 10.1002/wcc.81, 2011a.

Dai, A.: Characteristics and trends in various forms of the Palmer Drought Severity Index during 1900–2008, Journal of Geophysical Research: Atmospheres, 116, D12115, 10.1029/2010jd015541, 2011b.

Dai, A.: Increasing drought under global warming in observations and models, Nature Climate Change, 3, 52-58, 2012.

Damberg, L., and AghaKouchak, A.: Global trends and patterns of drought from space, Theoretical and Applied Climatology, 117, 441-448, 10.1007/s00704-013-1019-5, 2014.

de Rosnay, P., Gruhier, C., Timouk, F., Baup, F., Mougin, E., Hiernaux, P., Kergoat, L., and LeDantec, V.: Multi-scale soil moisture measurements at the Gourma meso-scale site in Mali, Journal of Hydrology, 375, 241-252, http://dx.doi.org/10.1016/j.jhydrol.2009.01.015, 2009.

Detto, M., Montaldo, N., Albertson, J. D., Mancini, M., and Katul, G.: Soil moisture and vegetation controls on evapotranspiration in a heterogeneous Mediterranean ecosystem on Sardinia, Italy, Water Resources Research, 42, n/a-n/a, 10.1029/2005WR004693, 2006.

Dirmeyer, P. A., Jin, Y., Singh, B., and Yan, X.: Trends in land–atmosphere interactions from CMIP5 simulations, Journal of Hydrometeorology, 14, 829-849, 10.1175/JHM-D-12-0107.1, 2013.

Dirmeyer, P. A., Wu, J., Norton, H. E., Dorigo, W. A., Quiring, S. M., Ford, T. W., Santanello, J. A., Bosilovich, M. G., Ek, M. B., Koster, R. D., Balsamo, G., and Lawrence, D. M.: Confronting weather and climate models with observational data from soil moisture networks over the United States, Journal of Hydrometeorology, 17, 1049-1067, 10.1175/JHM-D-15-0196.1, 2016.

Dorigo, W. A., Wagner, W., Hohensinn, R., Hahn, S., Paulik, C., Drusch, M., Mecklenburg, S., van Oevelen, P., Robock, A., and Jackson, T.: The International Soil Moisture Network: A data hosting facility for global in situ soil moisture measurements, Hydrol. Earth Syst. Sci. Discuss., 8, 1609-1663, 10.5194/hessd-8-1609-2011, 2011.

Dorigo, W. A., Gruber, A., De Jeu, R. A. M., Wagner, W., Stacke, T., Loew, A., Albergel, C., Brocca, L., Chung, D., Parinussa, R. M., and Kidd, R.: Evaluation of the ESA CCI soil moisture product using ground-based observations, Remote Sensing of Environment, 162, 380-395, http://dx.doi.org/10.1016/j.rse.2014.07.023, 2015.

Downer, C. W., and Ogden, F. L.: Prediction of runoff and soil moistures at the watershed scale: Effects of model complexity and parameter assignment, Water Resources Research, 39, 1045, 10.1029/2002WR001439, 2003.

Durre, I., Wallace, J. M., and Lettenmaier, D. P.: Dependence of extreme daily maximum temperatures on antecedent soil moisture in the contiguous United States during summer, Journal of Climate, 13, 2641-2651, doi:10.1175/1520-0442(2000)013<2641:DOEDMT>2.0.CO;2, 2000.

Ek, M. B., and Holtslag, A. A. M.: Influence of soil moisture on boundary layer cloud development, Journal of Hydrometeorology, 5, 86-99, doi:10.1175/1525-7541(2004)005<0086:IOSMOB>2.0.CO;2, 2004.

Eltahir, E. A. B.: A soil moisture–rainfall feedback mechanism: 1. theory and observations, Water Resources Research, 34, 765-776, 10.1029/97WR03499, 1998.

Falloon, P., Jones, C. D., Ades, M., and Paul, K.: Direct soil moisture controls of future global soil carbon changes: An important source of uncertainty, Global Biogeochemical Cycles, 25, GB3010, 10.1029/2010GB003938, 2011.

Famiglietti, J. S., Rudnicki, J. W., and Rodell, M.: Variability in surface moisture content along a hillslope transect: Rattlesnake Hill, Texas, Journal of Hydrology, 210, 259-281, http://dx.doi.org/10.1016/S0022-1694(98)00187-5, 1998.

Fan, Y., and van den Dool, H.: Climate Prediction Center global monthly soil moisture data set at 0.5° resolution for 1948 to present, Journal of Geophysical Research: Atmospheres, 109, n/a-n/a, 10.1029/2003JD004345, 2004.

Fang, L., Hain, C. R., Zhan, X., and Anderson, M. C.: An inter-comparison of soil moisture data products from satellite remote sensing and a land surface model, International Journal of Applied Earth Observation and Geoinformation, 48, 37-50, http://dx.doi.org/10.1016/j.jag.2015.10.006, 2016.

Fischer, E. M., Seneviratne, S. I., Lüthi, D., and Schär, C.: Contribution of land-atmosphere coupling to recent European summer heat waves, Geophysical Research Letters, 34, L06707, 10.1029/2006GL029068, 2007.

Flato, G., J. Marotzke, Abiodun, B., Braconnot, P., Chou, S. C., Collins, W., Cox, P., Driouech, F., Emori, S., Eyring, V., Forest, C., Gleckler, P., Guilyardi, E., Jakob, C., Kattsov, V., Reason, C., and Rummukainen, M.: Evaluation of climate models. In: Climate change 2013: The physical science basis. Contribution of Working Group I to the fifth assessment report of the intergovernmental panel on climate change, Cambridge University Press, Cambridge, United Kingdom and New York, NY, USA., 2013.

Ford, T. W., and Quiring, S. M.: Influence of MODIS-derived dynamic vegetation on VIC-simulated soil moisture in Oklahoma, Journal of Hydrometeorology, 14, 1910-1921, 10.1175/JHM-D-13-037.1, 2013.

Ford, T. W., and Quiring, S. M.: Comparison and application of multiple methods for temporal interpolation of daily soil moisture, International Journal of Climatology, 34, 2604-2621, 10.1002/joc.3862, 2014a.

Ford, T. W., and Quiring, S. M.: In situ soil moisture coupled with extreme temperatures: A study based on the Oklahoma Mesonet, Geophysical Research Letters, 41, 2014GL060949, 10.1002/2014GL060949, 2014b.

Ford, T. W., Wulff, C. O., and Quiring, S. M.: Assessment of observed and model-derived soil moisture-evaporative fraction relationships over the United States Southern Great Plains, Journal of Geophysical Research: Atmospheres, 119, 6279-6291, 10.1002/2014JD021490, 2014.

Ford, T. W., McRoberts, D. B., Quiring, S. M., and Hall, R. E.: On the utility of in situ soil moisture observations for flash drought early warning in Oklahoma, USA, Geophysical Research Letters, 42, 9790-9798, 10.1002/2015GL066600, 2015a.

Ford, T. W., Quiring, S. M., Frauenfeld, O. W., and Rapp, A. D.: Synoptic conditions related to soil moisture-atmosphere interactions and unorganized convection in Oklahoma, Journal of Geophysical Research: Atmospheres, 120, 11,519-511,535, 10.1002/2015JD023975, 2015b.

Ford, T. W., Rapp, A. D., and Quiring, S. M.: Does afternoon precipitation occur preferentially over dry or wet soils in Oklahoma?, Journal of Hydrometeorology, 16, 874-888, doi:10.1175/JHM-D-14-0005.1, 2015c.

Ford, T. W., Quiring, S. M., and Frauenfeld, O. W.: Multi-decadal variability of soil moisture–temperature coupling over the contiguous United States modulated by Pacific and Atlantic sea surface temperatures, International Journal of Climatology, n/a-n/a, 10.1002/joc.4785, 2016.

Guo, Z., and Dirmeyer, P. A.: Evaluation of the Second Global Soil Wetness Project soil moisture simulations: 1. Intermodel comparison, Journal of Geophysical Research: Atmospheres, 111, n/a-n/a, 10.1029/2006JD007233, 2006.

Guo, Z., Dirmeyer, P. A., and DelSole, T.: Land surface impacts on subseasonal and seasonal predictability, Geophysical Research Letters, 38, L24812, 10.1029/2011GL049945, 2011.

Guo, Z., and Dirmeyer, P. A.: Interannual variability of land–atmosphere coupling strength, Journal of Hydrometeorology, 14, 1636-1646, doi:10.1175/JHM-D-12-0171.1, 2013.

Guttman, N. B.: A sensitivity analysis of the Palmer Hydrologic Drought Index, JAWRA Journal of the American Water Resources Association, 27, 797-807, 10.1111/j.1752-1688.1991.tb01478.x, 1991.

Hao, Z., and AghaKouchak, A.: Multivariate Standardized Drought Index: A parametric multi-index model, Adv. Water Resour., 57, 12-18, 2013.

Hartmann, D. L., Klein Tank, A. M. G., Rusticucci, M., Alexander, L. V., Brönnimann, S., Charabi, Y., Dentener, F. J., Dlugokencky, E. J., Easterling, D. R., Kaplan, A., Soden, B. J., Thorne, P. W., Wild, M., and Zhai, P. M.: Observations: atmosphere and surface. In: Climate change 2013: The physical science basis. Contribution of Working Group I to the fifth assessment report of the intergovernmental panel on climate change, Cambridge University Press Cambridge, United Kingdom and New York, NY, USA., 2013.

Heim, R. R.: A review of twentieth-century drought indices used in the United States, Bulletin of the American Meteorological Society, 83, 1149-1165, 10.1175/1520-0477(2002)083<1149:AROTDI>2.3.CO;2, 2002.

Hirschi, M., Seneviratne, S. I., Alexandrov, V., Boberg, F., Boroneant, C., Christensen, O. B., Formayer, H., Orlowsky, B., and Stepanek, P.: Observational evidence for soil-moisture impact on hot extremes in southeastern Europe, Nature Geosci, 4, 17-21, http://www.nature.com/ngeo/journal/v4/n1/abs/ngeo1032.html#supplementary-information, 2011.

Hoerling, M., Eischeid, J., Kumar, A., Leung, R., Mariotti, A., Mo, K., Schubert, S., and Seager, R.: Causes and predictability of the 2012 Great Plains drought, Bulletin of the American Meteorological Society, 95, 269-282, doi:10.1175/BAMS-D-13-00055.1, 2014.

Hoerling, M. P., and Kumar, A.: Atmospheric response patterns associated with tropical forcing, Journal of Climate, 15, 2184-2203, doi:10.1175/1520-0442(2002)015<2184:ARPAWT>2.0.CO;2, 2002.

Hogg, E. H., Barr, A. G., and Black, T. A.: A simple soil moisture index for representing multi-year drought impacts on aspen productivity in the western Canadian interior, Agricultural and Forest Meteorology, 178–179, 173-182, http://dx.doi.org/10.1016/j.agrformet.2013.04.025, 2013.

Hollinger, S. E., and Isard, S. A.: A soil moisture climatology of Illinois, Journal of Climate, 7, 822-833, 10.1175/1520-0442(1994)007<0822:ASMCOI>2.0.CO;2, 1994.

Hollinger, S. E., Reinke, B. C., and Peppler, R. A.: Illinois Climate Network: Site descriptions, instrumentation, and data management., Champaign, IL 62, 1994.

Houborg, R., Rodell, M., Li, B., Reichle, R., and Zaitchik, B. F.: Drought indicators based on model-assimilated Gravity Recovery and Climate Experiment (GRACE) terrestrial water storage observations, Water Resources Research, 48, W07525, 10.1029/2011WR011291, 2012.

Huang, J., van den Dool, H. M., and Georgarakos, K. P.: Analysis of model-calculated soil moisture over the United States (1931–1993) and applications to long-range temperature forecasts, Journal of Climate, 9, 1350-1362, 10.1175/1520-0442(1996)009<1350:AOMCSM>2.0.CO;2, 1996.

Isaaks, E. H., and Srivastava, R. M.: An introduction to applied geostatistics, Oxford University Press, Oxford, New York, 400 pp., 1989.

Isham, V., Cox, D. R., Rodríguez-Iturbe, I., Porporato, A., and Manfreda, S.: Representation of space–time variability of soil moisture, 2064, 4035-4055 pp., 2005.

Jacobs, J. M., Mohanty, B. P., Hsu, E.-C., and Miller, D.: SMEX02: Field scale variability, time stability and similarity of soil moisture, Remote Sensing of Environment, 92, 436-446, http://dx.doi.org/10.1016/j.rse.2004.02.017, 2004.

Jain, V. K., Pandey, R. P., Jain, M. K., and Byun, H.-R.: Comparison of drought indices for appraisal of drought characteristics in the Ken River Basin, Weather and Climate Extremes, 8, 1-11, http://dx.doi.org/10.1016/j.wace.2015.05.002, 2015.

Jones, G. S., Stott, P. A., and Christidis, N.: Attribution of observed historical near–surface temperature variations to anthropogenic and natural causes using CMIP5 simulations, Journal of Geophysical Research: Atmospheres, 118, 4001-4024, 10.1002/jgrd.50239, 2013.

Kaplan, A., Cane, M. A., Kushnir, Y., Clement, A. C., Blumenthal, M. B., and Rajagopalan, B.: Analyses of global sea surface temperature 1856–1991, Journal of Geophysical Research: Oceans, 103, 18567-18589, 10.1029/97JC01736, 1998.

Kaplan, A., Kushnir, Y., and Cane, M. A.: Reduced space optimal interpolation of historical marine sea level pressure: 1854–1992, Journal of Climate, 13, 2987-3002, 10.1175/1520-0442(2000)013<2987:RSOIOH>2.0.CO;2, 2000.

Karl, T. R., Melillo, J. M., and Peterson, T. C.: Global climate change impacts in the United States, United States Global Change Research Program. Cambridge University Press, New York, NY, USA., 2009.

Kerr, Y. H., Waldteufel, P., Wigneron, J. P., Martinuzzi, J., Font, J., and Berger, M.: Soil moisture retrieval from space: the Soil Moisture and Ocean Salinity (SMOS) mission, Geoscience and Remote Sensing, IEEE Transactions on, 39, 1729-1735, 10.1109/36.942551, 2001.

Keyantash, J., and Dracup, J. A.: The quantification of drought: an evaluation of drought indices, Bulletin of the American Meteorological Society, 83, 1167-1180, 10.1175/1520-0477(2002)083<1191:TQODAE>2.3.CO;2, 2002.

Khong, A., Wang, J. K., Quiring, S. M., and Ford, T. W.: Soil moisture variability in Iowa, International Journal of Climatology, 35, 2837-2848, 10.1002/joc.4176, 2015.

Kim, Y., and Wang, G.: Impact of initial soil moisture anomalies on subsequent precipitation over North America in the coupled land–atmosphere model CAM3–CLM3, Journal of Hydrometeorology, 8, 513-533, 10.1175/JHM611.1, 2007.

Koster, Sud, Y. C., Guo, Z., Dirmeyer, P. A., Bonan, G., Oleson, K. W., Chan, E., Verseghy, D., Cox, P., Davies, H., Kowalczyk, E., Gordon, C. T., Kanae, S., Lawrence, D., Liu, P., Mocko, D., Lu, C.-H., Mitchell, K., Malyshev, S., McAvaney, B., Oki, T., Yamada, T., Pitman, A., Taylor, C. M., Vasic, R., and Xue, Y.: GLACE: The global land–atmosphere coupling experiment. part I: overview, Journal of Hydrometeorology, 7, 590-610, 10.1175/jhm510.1, 2006.

Koster, R. D., Dirmeyer, P. A., Guo, Z., Bonan, G., Chan, E., Cox, P., Gordon, C. T., Kanae, S., Kowalczyk, E., Lawrence, D., Liu, P., Lu, C.-H., Malyshev, S., McAvaney, B., Mitchell, K., Mocko, D., Oki, T., Oleson, K., Pitman, A., Sud, Y. C., Taylor, C. M., Verseghy, D., Vasic, R., Xue, Y., and Yamada, T.: Regions of strong coupling between soil moisture and precipitation, Science, 305, 1138-1140, 10.1126/science.1100217, 2004.

Koster, R. D., Guo, Z., Yang, R., Dirmeyer, P. A., Mitchell, K., and Puma, M. J.: On the nature of soil moisture in land surface models, Journal of Climate, 22, 4322-4335, 10.1175/2009JCLI2832.1, 2009.

Koster, R. D., Mahanama, S. P. P., Yamada, T. J., Balsamo, G., Berg, A. A., Boisserie, M., Dirmeyer, P. A., Doblas-Reyes, F. J., Drewitt, G., Gordon, C. T., Guo, Z., Jeong, J. H., Lawrence, D. M., Lee, W. S., Li, Z., Luo, L., Malyshev, S., Merryfield, W. J., Seneviratne, S. I., Stanelle, T., van den Hurk, B. J. J. M., Vitart, F., and Wood, E. F.: Contribution of land surface initialization to subseasonal forecast skill: First results from a multi-model experiment, Geophysical Research Letters, 37, L02402, 10.1029/2009GL041677, 2010.

Krishnan, P., Black, T. A., Grant, N. J., Barr, A. G., Hogg, E. H., Jassal, R. S., and Morgenstern, K.: Impact of changing soil moisture distribution on net ecosystem

productivity of a boreal aspen forest during and following drought, Agricultural and Forest Meteorology, 139, 208-223, http://dx.doi.org/10.1016/j.agrformet.2006.07.002, 2006.

Kumar, A., Chen, M., Hoerling, M., and Eischeid, J.: Do extreme climate events require extreme forcings?, Geophysical Research Letters, 40, 3440-3445, 10.1002/grl.50657, 2013.

Kutepov, A. A., Feofilov, A. G., Marshall, B. T., Gordley, L. L., Pesnell, W. D., Goldberg, R. A., and Russell, J. M.: SABER temperature observations in the summer polar mesosphere and lower thermosphere: Importance of accounting for the CO2v2 quanta V–V exchange, Geophysical Research Letters, 33, L21809, 10.1029/2006GL026591, 2006.

Latron, J., and Gallart, F.: Runoff generation processes in a small Mediterranean research catchment (Vallcebre, Eastern Pyrenees), Journal of Hydrology, 358, 206-220, http://dx.doi.org/10.1016/j.jhydrol.2008.06.014, 2008.

Lawrimore, J., Heim, R. R., Svoboda, M., Swail, V., and Englehart, P. J.: Beginning a new era of drought monitoring across North America, Bulletin of the American Meteorological Society, 83, 1191-1192, 10.1175/1520-0477(2002)083<1191:BANEOD>2.3.CO;2, 2002.

Le Vine, D. M., Lagerloef, G. S. E., Colomb, F. R., Yueh, S. H., and Pellerano, F. A.: Aquarius: An instrument to monitor sea surface salinity from space, Geoscience and Remote Sensing, IEEE Transactions on, 45, 2040-2050, 10.1109/TGRS.2007.898092, 2007.

Legates, D. R., and McCabe, G. J.: Evaluating the use of “goodness-of-fit” measures in hydrologic and hydroclimatic model validation, Water Resources Research, 35, 233-241, 10.1029/1998WR900018, 1999.

Li, H., Robock, A., and Wild, M.: Evaluation of Intergovernmental Panel on Climate Change Fourth Assessment soil moisture simulations for the second half of the twentieth century, Journal of Geophysical Research: Atmospheres, 112, 10.1029/2006JD007455, 2007.

Liang, X., Lettenmaier, D. P., Wood, E. F., and Burges, S. J.: A simple hydrologically based model of land surface water and energy fluxes for general circulation models, Journal of Geophysical Research: Atmospheres, 99, 14415-14428, 10.1029/94JD00483, 1994.

Liu, Y. Y., Parinussa, R. M., Dorigo, W. A., De Jeu, R. A. M., Wagner, W., van Dijk, A. I. J. M., McCabe, M. F., and Evans, J. P.: Developing an improved soil moisture

dataset by blending passive and active microwave satellite-based retrievals, Hydrol. Earth Syst. Sci., 15, 425-436, 10.5194/hess-15-425-2011, 2011.

Liu, Y. Y., Dorigo, W. A., Parinussa, R. M., de Jeu, R. A. M., Wagner, W., McCabe, M. F., Evans, J. P., and van Dijk, A. I. J. M.: Trend-preserving blending of passive and active microwave soil moisture retrievals, Remote Sensing of Environment, 123, 280-297, http://dx.doi.org/10.1016/j.rse.2012.03.014, 2012.

Lorenz, R., Argüeso, D., Donat, M. G., Pitman, A. J., van den Hurk, B., Berg, A., Lawrence, D. M., Chéruy, F., Ducharne, A., Hagemann, S., Meier, A., Milly, P. C. D., and Seneviratne, S. I.: Influence of land-atmosphere feedbacks on temperature and precipitation extremes in the GLACE-CMIP5 ensemble, Journal of Geophysical Research: Atmospheres, 121, 607-623, 10.1002/2015JD024053, 2016.

Loveland, T. R., Reed, B. C., Brown, J. F., Ohlen, D. O., Zhu, Z., Yang, L., and Merchant, J. W.: Development of a global land cover characteristics database and IGBP DISCover from 1 km AVHRR data, International Journal of Remote Sensing, 21, 1303-1330, 10.1080/014311600210191, 2000.

Luo, Y., Wang, Z., Liu, X., and Zhang, M.: Spatial and temporal variability of precipitation in Haihe River Basin, China: Characterization and management implications, Advances in Meteorology, 2014, 9, 10.1155/2014/143246, 2014.

Mahmood, R., Littell, A., Hubbard, K. G., and You, J.: Observed data-based assessment of relationships among soil moisture at various depths, precipitation, and temperature, Applied Geography, 34, 255-264, http://dx.doi.org/10.1016/j.apgeog.2011.11.009, 2012.

May, W., Meier, A., Rummukainen, M., Berg, A., Chéruy, F., and Hagemann, S.: Contributions of soil moisture interactions to climate change in the tropics in the GLACE–CMIP5 experiment, Clim Dyn, 45, 3275-3297, 10.1007/s00382-015-2538-9, 2015.

McEvoy, D. J., Huntington, J. L., Abatzoglou, J. T., and Edwards, L. M.: An evaluation of multiscalar drought indices in Nevada and Eastern California, Earth Interactions, 16, 1-18, 10.1175/2012EI000447.1, 2012.

McKee, T., Doesken, N., and Kleist, J.: The relationship of drought frequency and duration to time scales, Eighth Conference on Applied Climatology, Boston, 1993, 179-184,

McNally, A., Shukla, S., Arsenault, K. R., Wang, S., Peters-Lidard, C. D., and Verdin, J. P.: Evaluating ESA CCI soil moisture in East Africa, International Journal of

Applied Earth Observation and Geoinformation, 48, 96-109, http://dx.doi.org/10.1016/j.jag.2016.01.001, 2016.

McVicar, T. R., Roderick, M. L., Donohue, R. J., Li, L. T., Van Niel, T. G., Thomas, A., Grieser, J., Jhajharia, D., Himri, Y., Mahowald, N. M., Mescherskaya, A. V., Kruger, A. C., Rehman, S., and Dinpashoh, Y.: Global review and synthesis of trends in observed terrestrial near-surface wind speeds: Implications for evaporation, Journal of Hydrology, 416–417, 182-205, http://dx.doi.org/10.1016/j.jhydrol.2011.10.024, 2012.

Mei, R., and Wang, G.: Summer land–atmosphere coupling strength in the United States: comparison among observations, reanalysis data, and numerical models, Journal of Hydrometeorology, 13, 1010-1022, doi:10.1175/JHM-D-11-075.1, 2012.

Meng, L., and Quiring, S. M.: A comparison of soil moisture models using soil climate analysis network observations, Journal of Hydrometeorology, 9, 641-659, 10.1175/2008JHM916.1, 2008.

Meng, L.: Examining the relationship between antecedent soil moisture and summer precipitation in the U.S. Great Plains, Doctoral dissertation, Texas A&M University, 2009.

Meng, L., and Quiring, S. M.: Examining the influence of spring soil moisture anomalies on summer precipitation in the U.S. Great Plains using the Community Atmosphere Model version 3, Journal of Geophysical Research: Atmospheres, 115, n/a-n/a, 10.1029/2010JD014449, 2010.

Menne, M. J., Jr., C. N. W., and Vose, R. S.: The U.S. Historical Climatology Network monthly temperature data, version 2, Bulletin of the American Meteorological Society, 90, 993-1007, doi:10.1175/2008BAMS2613.1, 2009.

Miller, P. R., McConkey, B. G., Clayton, G. W., Brandt, S. A., Staricka, J. A., Johnston, A. M., Lafond, G. P., Schatz, B. G., Baltensperger, D. D., and Neill, K. E.: Pulse crop adaptation in the Northern Great Plains, Agron. J., 94, 261-272, 10.2134/agronj2002.2610, 2002.

Mo, X., Liu, S., Lin, Z., and Zhao, W.: Simulating temporal and spatial variation of evapotranspiration over the Lushi basin, Journal of Hydrology, 285, 125-142, http://dx.doi.org/10.1016/j.jhydrol.2003.08.013, 2004.

Mohanty, B. P., Famiglietti, J. S., and Skaggs, T. H.: Evolution of soil moisture spatial structure in a mixed vegetation pixel during the Southern Great Plains 1997 (SGP97) Hydrology Experiment, Water Resources Research, 36, 3675-3686, 10.1029/2000WR900258, 2000a.

Mohanty, B. P., Skaggs, T. H., and Famiglietti, J. S.: Analysis and mapping of field-scale soil moisture variability using high-resolution, ground-based data during the Southern Great Plains 1997 (SGP97) Hydrology Experiment, Water Resources Research, 36, 1023-1031, 10.1029/1999WR900360, 2000b.

Morid, S., Smakhtin, V., and Moghaddasi, M.: Comparison of seven meteorological indices for drought monitoring in Iran, International Journal of Climatology, 26, 971-985, 10.1002/joc.1264, 2006.

Mueller, B., and Seneviratne, S. I.: Hot days induced by precipitation deficits at the global scale, Proceedings of the National Academy of Sciences, 109, 12398-12403, 10.1073/pnas.1204330109, 2012.

Namias, J.: Spring and Summer 1988 Drought over the contiguous United States—causes and prediction, Journal of Climate, 4, 54-65, 10.1175/1520-0442(1991)004<0054:sasdot>2.0.co;2, 1991.

North, G. R.: Empirical orthogonal functions and normal modes, Journal of the Atmospheric Sciences, 41, 879-887, 10.1175/1520-0469(1984)041<0879:EOFANM>2.0.CO;2, 1984.

Notaro, M., Liu, Z., and Williams, J. W.: Observed vegetation–climate feedbacks in the United States, Journal of Climate, 19, 763-786, doi:10.1175/JCLI3657.1, 2006.

Oglesby, R. J., and Erickson, D. J.: Soil moisture and the persistence of North American drought, Journal of Climate, 2, 1362-1380, doi:10.1175/1520-0442(1989)002<1362:SMATPO>2.0.CO;2, 1989.

Oglesby, R. J.: Springtime soil moisture, natural climatic variability, and North American drought as simulated by the NCAR Community Climate Model 1, Journal of Climate, 4, 890-897, 10.1175/1520-0442(1991)004<0890:SSMNCV>2.0.CO;2, 1991.

Padbury, G., Waltman, S., Caprio, J., Coen, G., McGinn, S., Mortensen, D., Nielsen, G., and Sinclair, R.: Agroecosystems and land resources of the Northern Great Plains, Agron. J., 94, 251-261, 10.2134/agronj2002.2510, 2002.

Paegle, J., Mo, K. C., and Nogués-Paegle, J.: Dependence of simulated precipitation on surface evaporation during the 1993 United States summer floods, Monthly Weather Review, 124, 345-361, doi:10.1175/1520-0493(1996)124<0345:DOSPOS>2.0.CO;2, 1996.

Palmer, W. C.: Meteorological drought, US Department of Commerce, Weather Bureau Washington, DC, USA, 1965.

Pan, W., Boyles, R. P., White, J. G., and Heitman, J. L.: Characterizing soil physical properties for soil moisture monitoring with the North Carolina Environment and Climate Observing Network, Journal of Atmospheric and Oceanic Technology, 29, 933-943, doi:10.1175/JTECH-D-11-00104.1, 2012.

Pellenq, J., Kalma, J., Boulet, G., Saulnier, G. M., Wooldridge, S., Kerr, Y., and Chehbouni, A.: A disaggregation scheme for soil moisture based on topography and soil depth, Journal of Hydrology, 276, 112-127, http://dx.doi.org/10.1016/S0022-1694(03)00066-0, 2003.

Penna, D., Tromp-van Meerveld, H. J., Gobbi, A., Borga, M., and Dalla Fontana, G.: The influence of soil moisture on threshold runoff generation processes in an alpine headwater catchment, Hydrol. Earth Syst. Sci., 15, 689-702, 10.5194/hess-15-689-2011, 2011.

Perry, M. A., and Niemann, J. D.: Generation of soil moisture patterns at the catchment scale by EOF interpolation, Hydrol. Earth Syst. Sci., 12, 15, 10.5194/hess-12-39-2008, 2008.

Pratola, C., Barrett, B., Gruber, A., Kiely, G., and Dwyer, E.: Evaluation of a global soil moisture product from finer spatial resolution SAR data and ground measurements at Irish Sites, Remote Sensing, 6, 8190, 2014.

Preisendorfer, R. W., and Mobley, C. D.: Principal component analysis in meteorology and oceanography, Developments in atmospheric science, Elsevier, the University of California, 1988.

Quiring, S. M.: Monitoring Drought: An evaluation of meteorological drought indices, Geography Compass, 3, 64-88, 10.1111/j.1749-8198.2008.00207.x, 2009.

Quiring, S. M., and Ganesh, S.: Evaluating the utility of the Vegetation Condition Index (VCI) for monitoring meteorological drought in Texas, Agricultural and Forest Meteorology, 150, 330-339, http://dx.doi.org/10.1016/j.agrformet.2009.11.015, 2010.

Quiring, S. M., Ford, T. W., Wang, J. K., Khong, A., Harris, E., Lindgren, T., Goldberg, D. W., and Li, Z.: The North American Soil Moisture Database: development and applications, Bulletin of the American Meteorological Society, 10.1175/BAMS-D-13-00263.1, 2015.

Quiring, S. M., Ford, T. W., Wang, J. K., Khong, A., Harris, E., Lindgren, T., Goldberg, D. W., and Li, Z.: The North American Soil Moisture Database: development and applications, Bulletin of the American Meteorological Society, 97, 1441-1459, doi:10.1175/BAMS-D-13-00263.1, 2016.

Rötzer, K., Montzka, C., and Vereecken, H.: Spatio-temporal variability of global soil moisture products, Journal of Hydrology, 522, 187-202, http://dx.doi.org/10.1016/j.jhydrol.2014.12.038, 2015.

Renzullo, L. J., van Dijk, A. I. J. M., Perraud, J. M., Collins, D., Henderson, B., Jin, H., Smith, A. B., and McJannet, D. L.: Continental satellite soil moisture data assimilation improves root-zone moisture analysis for water resources assessment, Journal of Hydrology, 519, Part D, 2747-2762, http://dx.doi.org/10.1016/j.jhydrol.2014.08.008, 2014.

Rhee, J., Carbone, G. J., and Hussey, J.: Drought index mapping at different spatial units, Journal of Hydrometeorology, 9, 1523-1534, 10.1175/2008JHM983.1, 2008.

Robock, A., Vinnikov, K. Y., Schlosser, C. A., Speranskaya, N. A., and Xue, Y.: Use of midlatitude soil moisture and meteorological observations to validate soil moisture simulations with Biosphere and Bucket Models, Journal of Climate, 8, 15-35, doi:10.1175/1520-0442(1995)008<0015:UOMSMA>2.0.CO;2, 1995.

Robock, A., Vinnikov, K. Y., Srinivasan, G., Entin, J. K., Hollinger, S. E., Speranskaya, N. A., Liu, S., and Namkhai, A.: The global soil moisture data bank, Bulletin of the American Meteorological Society, 81, 1281-1299, 10.1175/1520-0477(2000)081<1281:TGSMDB>2.3.CO;2, 2000.

Robock, A., Luo, L., Wood, E. F., Wen, F., Mitchell, K. E., Houser, P. R., Schaake, J. C., Lohmann, D., Cosgrove, B., Sheffield, J., Duan, Q., Higgins, R. W., Pinker, R. T., Tarpley, J. D., Basara, J. B., and Crawford, K. C.: Evaluation of the North American Land Data Assimilation System over the southern Great Plains during the warm season, Journal of Geophysical Research: Atmospheres, 108, n/a-n/a, 10.1029/2002JD003245, 2003.

Roderick, M. L., and Farquhar, G. D.: The cause of decreased pan evaporation over the past 50 Years, Science, 298, 1410-1411, 10.1126/science.1075390-a, 2002.

Roderick, M. L., Rotstayn, L. D., Farquhar, G. D., and Hobbins, M. T.: On the attribution of changing pan evaporation, Geophysical Research Letters, 34, L17403, 10.1029/2007gl031166, 2007.

Rodriguez-Iturbe, I., Vogel, G. K., Rigon, R., Entekhabi, D., Castelli, F., and Rinaldo, A.: On the spatial organization of soil moisture fields, Geophysical Research Letters, 22, 2757-2760, 10.1029/95GL02779, 1995.

Sabater, J. M., Rüdiger, C., Calvet, J.-C., Fritz, N., Jarlan, L., and Kerr, Y.: Joint assimilation of surface soil moisture and LAI observations into a land surface

model, Agricultural and Forest Meteorology, 148, 1362-1373, http://dx.doi.org/10.1016/j.agrformet.2008.04.003, 2008.

Sanchez-Mejia, Z. M., Papuga, S. A., Swetish, J. B., van Leeuwen, W. J. D., Szutu, D., and Hartfield, K.: Quantifying the influence of deep soil moisture on ecosystem albedo: The role of vegetation, Water Resources Research, 50, 4038-4053, 10.1002/2013WR014150, 2014.

Schaefer, G. L., and Paetzold, R. F.: SNOTEL (SNOwpack TELemetry) and SCAN (Soil Climate Analysis Network), automated weather stations for applications in agriculture and water resources management: Current Use and Future Perspectives, Lincoln, Nebraska, USA, 2001, 187 - 194,

Schaefer, G. L., Cosh, M. H., and Jackson, T. J.: The USDA Natural Resources Conservation Service Soil Climate Analysis Network (SCAN), Journal of Atmospheric and Oceanic Technology, 24, 2073-2077, doi:10.1175/2007JTECHA930.1, 2007.

Schroeder, J. L., Burgett, W. S., Haynie, K. B., Sonmez, I., Skwira, G. D., Doggett, A. L., and Lipe, J. W.: The West Texas Mesonet: a technical overview, Journal of Atmospheric and Oceanic Technology, 22, 211-222, doi:10.1175/JTECH-1690.1, 2005.

Scott, B. L., Ochsner, T. E., Illston, B. G., Fiebrich, C. A., Basara, J. B., and Sutherland, A. J.: New soil property database improves Oklahoma Mesonet soil moisture estimates, Journal of Atmospheric and Oceanic Technology, 30, 2585-2595, 10.1175/JTECH-D-13-00084.1, 2013.

Seneviratne, S. I., Koster, R. D., Guo, Z., Dirmeyer, P. A., Kowalczyk, E., Lawrence, D., Liu, P., Mocko, D., Lu, C.-H., Oleson, K. W., and Verseghy, D.: Soil moisture memory in AGCM simulations: Analysis of Global Land–Atmosphere Coupling Experiment (GLACE) data, Journal of Hydrometeorology, 7, 1090-1112, doi:10.1175/JHM533.1, 2006.

Seneviratne, S. I., Corti, T., Davin, E. L., Hirschi, M., Jaeger, E. B., Lehner, I., Orlowsky, B., and Teuling, A. J.: Investigating soil moisture–climate interactions in a changing climate: A review, Earth-Science Reviews, 99, 125-161, http://dx.doi.org/10.1016/j.earscirev.2010.02.004, 2010.

Seneviratne, S. I., Wilhelm, M., Stanelle, T., van den Hurk, B., Hagemann, S., Berg, A., Cheruy, F., Higgins, M. E., Meier, A., Brovkin, V., Claussen, M., Ducharne, A., Dufresne, J.-L., Findell, K. L., Ghattas, J., Lawrence, D. M., Malyshev, S., Rummukainen, M., and Smith, B.: Impact of soil moisture-climate feedbacks on

CMIP5 projections: first results from the GLACE-CMIP5 experiment, Geophysical Research Letters, 40, 2013GL057153, 10.1002/grl.50956, 2013.

Sheffield, J., Wood, E. F., and Roderick, M. L.: Little change in global drought over the past 60 years, Nature, 491, 435-438, http://www.nature.com/nature/journal/v491/n7424/abs/nature11575.html#supplementary-information, 2012.

Sheffield, J., Barrett, A. P., Colle, B., Fernando, D. N., Fu, R., Geil, K. L., Hu, Q., Kinter, J., Kumar, S., Langenbrunner, B., Lombardo, K., Long, L. N., Maloney, E., Mariotti, A., Meyerson, J. E., Mo, K. C., Neelin, J. D., Nigam, S., Pan, Z., Ren, T., Ruiz-Barradas, A., Serra, Y. L., Seth, A., Thibeault, J. M., Stroeve, J. C., Yang, Z., and Yin, L.: North American climate in CMIP5 experiments. Part I: evaluation of historical simulations of continental and regional climatology, Journal of Climate, 26, 9209-9245, doi:10.1175/JCLI-D-12-00592.1, 2013.

Shepard, D.: A two-dimensional interpolation function for irregularly-spaced data, Proceedings of the 1968 23rd ACM national conference, 1968.

Srinivasan, G., Robock, A., Entin, J. K., Luo, L., Vinnikov, K. Y., and Viterbo, P.: Soil moisture simulations in revised AMIP models, Journal of Geophysical Research: Atmospheres, 105, 26635-26644, 10.1029/2000JD900443, 2000.

Stéfanon, M., Drobinski, P., D'Andrea, F., Lebeaupin-Brossier, C., and Bastin, S.: Soil moisture-temperature feedbacks at meso-scale during summer heat waves over Western Europe, Clim Dyn, 42, 1309-1324, 10.1007/s00382-013-1794-9, 2014.

Stannard, D. I.: Comparison of Penman-Monteith, Shuttleworth-Wallace, and Modified Priestley-Taylor Evapotranspiration Models for wildland vegetation in semiarid rangeland, Water Resources Research, 29, 1379-1392, 10.1029/93wr00333, 1993.

Taylor, C. M., de Jeu, R. A. M., Guichard, F., Harris, P. P., and Dorigo, W. A.: Afternoon rain more likely over drier soils, Nature, 489, 423-426, http://www.nature.com/nature/journal/v489/n7416/abs/nature11377.html#supplementary-information, 2012a.

Taylor, K. E.: Summarizing multiple aspects of model performance in a single diagram, Journal of Geophysical Research: Atmospheres, 106, 7183-7192, 10.1029/2000JD900719, 2001.

Taylor, K. E., Stouffer, R. J., and Meehl, G. A.: An overview of CMIP5 and the experiment design, Bulletin of the American Meteorological Society, 93, 485-498, doi:10.1175/BAMS-D-11-00094.1, 2012b.

Teuling, A. J., Hirschi, M., Ohmura, A., Wild, M., Reichstein, M., Ciais, P., Buchmann, N., Ammann, C., Montagnani, L., Richardson, A. D., Wohlfahrt, G., and Seneviratne, S. I.: A regional perspective on trends in continental evaporation, Geophysical Research Letters, 36, L02404, 10.1029/2008GL036584, 2009.

Teuling, A. J., Seneviratne, S. I., Stockli, R., Reichstein, M., Moors, E., Ciais, P., Luyssaert, S., van den Hurk, B., Ammann, C., Bernhofer, C., Dellwik, E., Gianelle, D., Gielen, B., Grunwald, T., Klumpp, K., Montagnani, L., Moureaux, C., Sottocornola, M., and Wohlfahrt, G.: Contrasting response of European forest and grassland energy exchange to heatwaves, Nature Geosci, 3, 722-727, http://www.nature.com/ngeo/journal/v3/n10/abs/ngeo950.html#supplementary-information, 2010.

Thomson, A., Calvin, K., Smith, S., Kyle, G. P., Volke, A., Patel, P., Delgado-Arias, S., Bond-Lamberty, B., Wise, M., Clarke, L., and Edmonds, J.: RCP4.5: a pathway for stabilization of radiative forcing by 2100, Climatic Change, 109, 77-94, 10.1007/s10584-011-0151-4, 2011.

Trenberth, K. E.: Recent observed interdecadal climate changes in the Northern Hemisphere, Bulletin of the American Meteorological Society, 71, 988-993, 10.1175/1520-0477(1990)071<0988:ROICCI>2.0.CO;2, 1990.

Trenberth, K. E., and Guillemot, C. J.: Physical processes involved in the 1988 drought and 1993 floods in North America, Journal of Climate, 9, 1288-1298, doi:10.1175/1520-0442(1996)009<1288:PPIITD>2.0.CO;2, 1996.

van den Hurk, B., Doblas-Reyes, F., Balsamo, G., Koster, R. D., Seneviratne, S. I., and Camargo, H.: Soil moisture effects on seasonal temperature and precipitation forecast scores in Europe, Clim Dyn, 38, 349-362, 10.1007/s00382-010-0956-2, 2010.

van der Schrier, G., Jones, P. D., and Briffa, K. R.: The sensitivity of the PDSI to the Thornthwaite and Penman-Monteith parameterizations for potential evapotranspiration, Journal of Geophysical Research: Atmospheres, 116, D03106, 10.1029/2010jd015001, 2011.

van der Schrier, G., Barichivich, J., Briffa, K. R., and Jones, P. D.: A scPDSI-based global data set of dry and wet spells for 1901–2009, Journal of Geophysical Research: Atmospheres, 118, 4025-4048, 10.1002/jgrd.50355, 2013.

Vereecken, H., Kamai, T., Harter, T., Kasteel, R., Hopmans, J., and Vanderborght, J.: Explaining soil moisture variability as a function of mean soil moisture: A stochastic unsaturated flow perspective, Geophysical Research Letters, 34, L22402, 10.1029/2007GL031813, 2007.

Vicente-Serrano, S. M., Beguería, S., and López-Moreno, J. I.: A multiscalar drought index sensitive to global warming: The Standardized Precipitation Evapotranspiration Index, Journal of Climate, 23, 1696-1718, 10.1175/2009JCLI2909.1, 2009.

Vicente-Serrano, S. M., Beguería, S., López-Moreno, J. I., Angulo, M., and El Kenawy, A.: A new global 0.5° gridded dataset (1901–2006) of a multiscalar drought index: comparison with current drought index datasets based on the Palmer Drought Severity Index, Journal of Hydrometeorology, 11, 1033-1043, 10.1175/2010JHM1224.1, 2010.

Vinnikov, K. Y., Robock, A., Speranskaya, N. A., and Schlosser, C. A.: Scales of temporal and spatial variability of midlatitude soil moisture, Journal of Geophysical Research: Atmospheres, 101, 7163-7174, 10.1029/95JD02753, 1996.

Vinnikov, K. Y., Robock, A., Qiu, S., and Entin, J. K.: Optimal design of surface networks for observation of soil moisture, Journal of Geophysical Research: Atmospheres, 104, 19743-19749, 10.1029/1999JD900060, 1999.

Vivoni, E. R., Moreno, H. A., Mascaro, G., Rodriguez, J. C., Watts, C. J., Garatuza-Payan, J., and Scott, R. L.: Observed relation between evapotranspiration and soil moisture in the North American monsoon region, Geophysical Research Letters, 35, n/a-n/a, 10.1029/2008GL036001, 2008.

Wanders, N., Karssenberg, D., Bierkens, M., Parinussa, R., de Jeu, R., van Dam, J., and de Jong, S.: Observation uncertainty of satellite soil moisture products determined with physically-based modeling, Remote Sensing of Environment, 127, 341-356, http://dx.doi.org/10.1016/j.rse.2012.09.004, 2012.

Wang, A., Bohn, T. J., Mahanama, S. P., Koster, R. D., and Lettenmaier, D. P.: Multimodel ensemble reconstruction of drought over the continental United States, Journal of Climate, 22, 2694-2712, 10.1175/2008JCLI2586.1, 2009.

Wang, H., Schubert, S., Koster, R., Ham, Y.-G., and Suarez, M.: On the role of SST forcing in the 2011 and 2012 extreme U.S. heat and drought: a study in contrasts, Journal of Hydrometeorology, 15, 1255-1273, 10.1175/JHM-D-13-069.1, 2014.

Wang, J. K., Ford, T. W., and Quiring, S. M.: Distinguishing between unorganized and organized convection when examining land–atmosphere relationships, Journal of Applied Meteorology and Climatology, 54, 2229-2243, doi:10.1175/JAMC-D-15-0086.1, 2015.

Wang, K., Dickinson, R. E., and Liang, S.: Global atmospheric evaporative demand over land from 1973 to 2008, Journal of Climate, 25, 8353-8361, 10.1175/JCLI-D-11-00492.1, 2012.

Wei, J., and Dirmeyer, P. A.: Dissecting soil moisture-precipitation coupling, Geophysical Research Letters, 39, n/a-n/a, 10.1029/2012GL053038, 2012.

Wetzel, P. J., and Chang, J.-T.: Concerning the relationship between evapotranspiration and soil moisture, Journal of Climate and Applied Meteorology, 26, 18-27, doi:10.1175/1520-0450(1987)026<0018:CTRBEA>2.0.CO;2, 1987.

Wu, L., and Zhang, J.: Asymmetric effects of soil moisture on mean daily maximum and minimum temperatures over eastern China, Meteorology and Atmospheric Physics, 122, 199-213, 10.1007/s00703-013-0284-2, 2013.

Wu, W., Geller, M. A., and Dickinson, R. E.: The response of soil moisture to long-term variability of precipitation, Journal of Hydrometeorology, 3, 604-613, 10.1175/1525-7541(2002)003<0604:TROSMT>2.0.CO;2, 2002.

Xia, Y., Ek, M. B., Wu, Y., Ford, T., and Quiring, S. M.: Comparison of NLDAS-2 simulated and NASMD observed daily soil moisture. part II: impact of soil texture classification and vegetation type mismatches, Journal of Hydrometeorology, 16, 1981-2000, 10.1175/JHM-D-14-0097.1, 2015a.

Xia, Y., Ek, M. B., Wu, Y., Ford, T., and Quiring, S. M.: Comparison of NLDAS-2 simulated and NASMD observed daily soil moisture. part I: comparison and analysis, Journal of Hydrometeorology, 10.1175/JHM-D-14-0096.1, 2015b.

Xia, Y., Ford, T. W., Wu, Y., Quiring, S. M., and Ek, M. B.: Automated quality control of in situ soil moisture from the North American Soil Moisture Database using NLDAS-2 products, Journal of Applied Meteorology and Climatology, 54, 1267-1282, doi:10.1175/JAMC-D-14-0275.1, 2015c.

Yao, X., Fu, B., Lü, Y., Sun, F., Wang, S., and Liu, M.: Comparison of four spatial interpolation methods for estimating soil moisture in a complex terrain catchment, PLoS ONE, 8, e54660, 10.1371/journal.pone.0054660, 2013.

Yuan, F., Ren, L., Yu, Z., and Xu, J.: Computation of potential evapotranspiration using a two-source method for the Xin'anjiang Hydrological Model, Journal of Hydrologic Engineering, 13, 305-316, doi:10.1061/(ASCE)1084-0699(2008)13:5(305), 2008.

Yuan, S., and Quiring, S. M.: Comparison of three methods of interpolating soil moisture in Oklahoma, International Journal of Climatology, n/a-n/a, 10.1002/joc.4754, 2016.

Yuan, S., Quiring, S. M., and Patil, S.: Spatial and temporal variations in the accuracy of meteorological drought indices, 2016, 42, 17, 10.18172/cig.2916, 2016.

Yue, S., Pilon, P., and Cavadias, G.: Power of the Mann–Kendall and Spearman's rho tests for detecting monotonic trends in hydrological series, Journal of Hydrology, 259, 254-271, http://dx.doi.org/10.1016/S0022-1694(01)00594-7, 2002.

Zehe, E., and Blöschl, G.: Predictability of hydrologic response at the plot and catchment scales: Role of initial conditions, Water Resources Research, 40, W10202, 10.1029/2003WR002869, 2004.

Zhang, L., Dawes, W. R., and Walker, G. R.: Response of mean annual evapotranspiration to vegetation changes at catchment scale, Water Resources Research, 37, 701-708, 10.1029/2000WR900325, 2001.

Zhou, M. C., Ishidaira, H., Hapuarachchi, H. P., Magome, J., Kiem, A. S., and Takeuchi, K.: Estimating potential evapotranspiration using Shuttleworth–Wallace model and NOAA-AVHRR NDVI data to feed a distributed hydrological model over the Mekong River basin, Journal of Hydrology, 327, 151-173, 10.1016/j.jhydrol.2005.11.013, 2006.